

STN7/8 -

A study on the regulation and function of the  
major thylakoid protein kinases



Dissertation

zur Erlangung des Doktorgrades der Fakultät für Biologie  
der Ludwig-Maximilians-Universität München

Vorgelegt von  
Tobias Wunder  
aus München

STN7/8 -  
A study on the regulation and function of the  
major thylakoid protein kinases



Dissertation  
zur Erlangung des Doktorgrades der Fakultät für Biologie  
der Ludwig-Maximilians-Universität München

Vorgelegt von  
Tobias Wunder  
aus München

20. Dezember 2012

|                             |                              |
|-----------------------------|------------------------------|
| Erstgutachter:              | Prof. Dr. Dario Leister      |
| Zweitgutachter:             | Prof. Dr. Peter Geigenberger |
| Tag der mündlichen Prüfung: | 20. März 2013                |

## Summary

Reversible phosphorylation of LHCII, the light-harvesting complex of photosystem II (PSII), controls its migration between the two photosystems (state transitions), and serves to adapt the photosynthetic machinery of plants and green algae to short-term changes in ambient light conditions. The thylakoid kinase STN7 is required for LHCII phosphorylation and state transitions in vascular plants. Here, the effects of different light conditions and chemical inhibitors on the abundance of STN7 transcripts and their products were analyzed. These analyses were performed in wild-type *Arabidopsis thaliana* plants, in several photosynthetic mutants, and in lines overexpressing STN7 (*oeSTN7*) or expressing mutant variants of STN7 carrying single or double cysteine-serine exchanges. It was found that accumulation of the STN7 protein is also controlled at the level of transcript abundance. Under certain conditions, exposure to high light or far-red light treatment, the relative decreases in LHCII phosphorylation is accompanied by a decrease in STN7 abundance. Nevertheless, inhibitor experiments showed that redox control of LHCII kinase activity persists in *oeSTN7* plants. STN7 dimers were predominantly found in *oeSTN7* plants and in lines with single cysteine-serine exchanges, indicating that dimerization involves disulphide bridges. Transient STN7 dimerization might be required for STN7 activity, and the altered dimerization behavior of *oeSTN7* plants might be responsible for the unusually high phosphorylation of LHCII in the dark found in this genotype. Furthermore, indications for a direct interaction of STN7 with thioredoxins are provided, which does not depend on the N-terminal cysteine motive.

The homologous protein kinase STN8 facilitates the phosphorylation of PSII core proteins, which was described to be involved in PSII repair cycle, supercomplex stability and macroscopic membrane folding. Here, the effect of increased PSII core phosphorylation in a line overexpressing STN8 (*oeSTN8*) was analyzed and an impact on supercomplex formation and membrane structure was observed. The STN8 protein levels in wild-type plants were shown not to vary depending on lighting conditions. Moreover, evidence for a tight association of STN7 and STN8 with large multisubunit complexes within the thylakoid membrane is given.

## Zusammenfassung

Pflanzen und Grünalgen passen ihre Photosynthese-Maschinerie kurzfristigen Änderungen der Lichtbedingungen an, indem sie einen Teil der Lichtsammelkomplexe des Photosystems II (LHCII) zwischen den Photosystemen relokalisieren (State Transitions) und dadurch deren unterschiedliche Anregung ausgleichen. Dieser Prozess wird durch reversible LHCII-Phosphorylierung gesteuert, welche in Gefäßpflanzen durch die Thylakoidkinase STN7 vermittelt wird. In dieser Arbeit wurden die Auswirkungen von unterschiedlichen Lichtbedingungen und chemischen Inhibitoren auf die Abundanz der STN7-Transkripte und deren Produkte analysiert. Hierfür wurden Wildtyp-Pflanzen von *Arabidopsis thaliana*, verschiedene Photosynthesemutanten, STN7 Überexprimierer (*oeSTN7*) und STN7-Mutanten, bei denen ein oder zwei Cystein-Reste gegen Serine ausgetauscht wurden, untersucht. Dabei wurde festgestellt, dass die Akkumulation von STN7-Proteinen auch auf Transkriptebene kontrolliert wird. Unter bestimmten Lichtbedingungen, wie starkem Licht oder Dunkelrot, wird der relative Rückgang der LHCII-Phosphorylierung von einer Abnahme der STN7-Proteinmenge begleitet. Trotzdem zeigten Experimente mit Inhibitoren, dass die LHCII-Kinaseaktivität in *oeSTN7*-Pflanzen noch immer der Redox-Kontrolle unterworfen ist. STN7-Dimere konnten besonders deutlich in *oeSTN7* und in Mutanten, bei denen ein Cystein-Rest ausgetauscht wurde, nachgewiesen werden. Dies deutet darauf hin, dass bei der Dimerisierung Disulfidbrücken involviert sind. Eine transiente STN7-Dimerisierung könnte essenziell für die Aktivität der STN7-Kinase sein und ein verändertes Dimerisationsverhalten in *oeSTN7*-Pflanzen für die übermäßig starke LHCII-Phosphorylierung im Dunklen verantwortlich sein könnte. Darüber hinaus werden Hinweise für eine direkte Wechselwirkung zwischen STN7 und Thioredoxin präsentiert, welche nicht vom N-terminalen Cysteinmotiv abhängig ist.

Die homologe Proteinkinase STN8 ermöglicht die Phosphorylierung der PSII-Kernproteine, welche vermutlich eine Rolle beim PSII-Reparaturzyklus, bei der Stabilität von Superkomplexen und bei der makroskopischen Membranfaltung spielt. Hier wurden Auswirkungen einer erhöhten PSII-Kernphosphorylierung in einer STN8 überexprimierenden Linie auf die Formation von Superkomplexen und Membranstrukturen beobachtet. Zudem wurden Hinweise auf eine Assoziierung der STN7- und STN8-Kinase mit großen Komplexen der Thylakoid-Membran gefunden.

## Index

|                                                                                                         |            |
|---------------------------------------------------------------------------------------------------------|------------|
| <b>Summary</b> .....                                                                                    | <b>II</b>  |
| <b>Zusammenfassung</b> .....                                                                            | <b>III</b> |
| <b>Index</b> .....                                                                                      | <b>IV</b>  |
| <b>List of Figures</b> .....                                                                            | <b>IX</b>  |
| <b>Abbreviations</b> .....                                                                              | <b>XI</b>  |
| <b>1 Introduction</b> .....                                                                             | <b>1</b>   |
| 1.1 Photosynthesis, the chloroplast and linear electron flow (LEF).....                                 | 1          |
| 1.2 Alternative electron pathways act beside LEF.....                                                   | 3          |
| 1.3 Involvement of cysteines in photosynthetic processes .....                                          | 4          |
| 1.4 Measurement of photosynthetic parameters .....                                                      | 5          |
| 1.5 Protein phosphorylation in chloroplasts .....                                                       | 5          |
| 1.6 Adaptation of photosynthesis to changing light conditions.....                                      | 5          |
| 1.6.1 Long term response (LTR).....                                                                     | 6          |
| 1.6.2 State transitions .....                                                                           | 7          |
| 1.6.3 The LHCII kinases STN7 and STT7.....                                                              | 11         |
| 1.6.4 Activation of the STN7/STT7 kinase by the Cyt <i>b6f</i> complex .....                            | 14         |
| 1.6.5 STN8 –the keyplayer in PSII core protein phosphorylation .....                                    | 15         |
| 1.6.6 Function of PSII core protein phosphorylation .....                                               | 17         |
| 1.7 Aims of this work .....                                                                             | 18         |
| <b>2 Materials and Methods</b> .....                                                                    | <b>19</b>  |
| 2.1 Plant material .....                                                                                | 19         |
| 2.1.1 Gateway cloning and generation of transgenic <i>A. thaliana</i> lines.....                        | 19         |
| 2.1.2 Site-directed mutagenesis and generation of cysteine exchange mutants of <i>A. thaliana</i> ..... | 20         |

|        |                                                                          |    |
|--------|--------------------------------------------------------------------------|----|
| 2.1.3  | Generation of <i>A. thaliana</i> lines expressing GFP-tagged STN7 .....  | 20 |
| 2.2    | Growth conditions and light treatments .....                             | 20 |
| 2.3    | cDNA synthesis and real-time PCR.....                                    | 21 |
| 2.4    | Isolation of total protein.....                                          | 21 |
| 2.5    | Isolation of thylakoid membranes.....                                    | 22 |
| 2.6    | Antibodies and immunoblot analysis.....                                  | 22 |
| 2.6.1  | Generation of polyclonal STN7 and STN8 antibodies.....                   | 22 |
| 2.7    | Purification of inclusion bodies .....                                   | 23 |
| 2.8    | Coomassie staining of PVDF membrane blots .....                          | 23 |
| 2.9    | PAGE analyses.....                                                       | 24 |
| 2.9.1  | BN- and 2D-PAGE .....                                                    | 24 |
| 2.9.2  | SDS-PAGE and non-reducing SDS-PAGE .....                                 | 24 |
| 2.9.3  | Diagonal-PAGE .....                                                      | 24 |
| 2.10   | Thylakoid fractionation after state 1 and 2 adaptation.....              | 25 |
| 2.11   | Sucrose gradient fractionation of thylakoid protein complexes .....      | 25 |
| 2.12   | Chloroplast isolation and fractionation into stroma and thylakoids ..... | 25 |
| 2.13   | Salt washes of thylakoid membranes.....                                  | 25 |
| 2.14   | Chlorophyll fluorescence analyses .....                                  | 26 |
| 2.14.1 | Measurement of light curves.....                                         | 26 |
| 2.14.2 | Measurement of light induction .....                                     | 26 |
| 2.14.3 | State Transition measurements via PAM fluorometry.....                   | 26 |
| 2.14.4 | PSII inactivation induced by high light.....                             | 26 |
| 2.14.5 | 77 K fluorescence emission spectroscopy.....                             | 27 |
| 2.14.6 | Determination of the PQ redox state in the dark.....                     | 27 |
| 2.15   | Non-radioactive <i>in-vitro</i> phosphorylation assays .....             | 27 |
| 2.16   | Radioactive <i>in-vitro</i> <sup>33</sup> P-phosphorylation .....        | 28 |

|          |                                                                                                                               |           |
|----------|-------------------------------------------------------------------------------------------------------------------------------|-----------|
| 2.17     | Pull-down of GFP-tagged proteins .....                                                                                        | 28        |
| 2.18     | Redox titration of STN7 protein in thylakoid membranes.....                                                                   | 28        |
| 2.19     | TRX affinity purification .....                                                                                               | 28        |
| 2.20     | Mobility shift assay of TRX .....                                                                                             | 29        |
| 2.21     | Protease treatments of thylakoids .....                                                                                       | 29        |
| 2.21.1   | Trypsin digest.....                                                                                                           | 29        |
| 2.21.2   | Thermolysin digest.....                                                                                                       | 29        |
| 2.21.3   | Protein protection assay .....                                                                                                | 30        |
| 2.22     | TEM analysis of thylakoid membranes ultrastructure.....                                                                       | 30        |
| <b>3</b> | <b>Results .....</b>                                                                                                          | <b>31</b> |
| 3.1      | Generation of STN7 and STN8 overexpressor lines.....                                                                          | 31        |
| 3.2      | Generation of polyclonal antibodies against STN7/STN8 epitopes and STN7/<br>STN8 full-length proteins .....                   | 31        |
| 3.3      | Studies on the localization and topology of the STN kinases (STN7 and STN8)                                                   | 33        |
| 3.3.1    | Both STN kinases are thylakoid integral membrane proteins.....                                                                | 33        |
| 3.3.2    | The STN kinases form part of high molecular supercomplexes .....                                                              | 34        |
| 3.3.3    | STN8 and STN7 are located in different subfractions of the thylakoid<br>membrane .....                                        | 34        |
| 3.3.4    | STN8 kinase is mainly attached to photosystem II.....                                                                         | 36        |
| 3.3.5    | Protease treatments of thylakoid membranes suggest an association of STN7<br>with other proteins.....                         | 37        |
| 3.3.6    | Trypsination patterns of STN8 allow to estimate its topology and propose a<br>potential association with other proteins ..... | 39        |
| 3.4      | Analyses on the regulation of the chloroplast protein kinase STN7.....                                                        | 40        |
| 3.4.1    | STN7 accumulation is regulated at both protein and transcript levels.....                                                     | 40        |
| 3.4.2    | Accumulation of STN7 is redox-dependent.....                                                                                  | 43        |

|        |                                                                                                                               |    |
|--------|-------------------------------------------------------------------------------------------------------------------------------|----|
| 3.4.3  | PSII and a functional cytochrome <i>b6f</i> complex are required for accumulation of STN7 .....                               | 45 |
| 3.4.4  | Elevated STN7 levels enhance LHCII phosphorylation and PSI-LHCI-pLHCII complex formation under certain light conditions ..... | 45 |
| 3.4.5  | Increased STN7 levels are compatible with state transitions and result in LHCII phosphorylation in the dark.....              | 49 |
| 3.4.6  | The PQ redox state of <i>oeSTN7</i> in the dark is not aberrant from WT .....                                                 | 52 |
| 3.4.7  | Increased STN7 levels result in a more highly oxidized PQ pool and a higher PSI quantum yield upon light induction.....       | 52 |
| 3.4.8  | LHCII phosphorylation of <i>oeSTN7</i> plants in the dark depends on stromal factors .....                                    | 57 |
| 3.4.9  | The N-terminal cysteine residues of STN7 are essential for its activity.....                                                  | 62 |
| 3.4.10 | STN7 forms redox-dependent inter- and intramolecular disulphide bridges...                                                    | 63 |
| 3.4.11 | The two N-terminal Cys residues of STN7 are involved in STN7 dimerization .<br>.....                                          | 66 |
| 3.4.12 | STN7 single cysteine mutants provide evidence for further intermolecular interaction partners .....                           | 69 |
| 3.4.13 | Redox sensitivity of STN7 beyond N-terminal cysteines .....                                                                   | 70 |
| 3.4.14 | Some indication that STN7 interacts directly with thioredoxin independent of its N-terminal cysteines.....                    | 71 |
| 3.5    | In-depth analysis of the chloroplast protein kinase STN8.....                                                                 | 73 |
| 3.5.1  | STN8 protein levels do not respond to light treatments.....                                                                   | 73 |
| 3.5.2  | STN8 overexpression increases PSII phosphorylation and decreases PSII-supercomplex formation.....                             | 73 |
| 3.5.3  | <i>oeSTN8</i> is slightly less susceptible to PSII photoinhibition.....                                                       | 76 |
| 3.5.4  | Increased STN8 protein levels result in a tendency for larger grana stacks ....                                               | 76 |
| 3.5.5  | Increased STN8 levels result in a slightly higher oxidized PQ pool.....                                                       | 78 |

|          |                                                                                                                                      |            |
|----------|--------------------------------------------------------------------------------------------------------------------------------------|------------|
| 3.6      | Substrate overlap of STN7 and STN8 .....                                                                                             | 81         |
| <b>4</b> | <b>Discussion.....</b>                                                                                                               | <b>82</b>  |
| 4.1      | STN7 and STN8 are associated with high molecular weight supercomplexes of the thylakoid membrane.....                                | 82         |
| 4.2      | Control of <i>STN7</i> transcript abundance and transient STN7 dimerization are involved in the regulation of STN7 activity .....    | 84         |
| 4.2.1    | At what level is STN7 abundance regulated? .....                                                                                     | 84         |
| 4.2.2    | At what level is STN7 activity regulated? .....                                                                                      | 85         |
| 4.2.3    | Why is LHCII phosphorylation in dark-adapted <i>oeSTN7</i> lines higher than in light-adapted ones?.....                             | 86         |
| 4.2.4    | What is the physiological significance of STN7 dimerization?.....                                                                    | 89         |
| 4.2.5    | Is STN7 regulated by thioredoxins?.....                                                                                              | 90         |
| 4.3      | Which physiological effects do variable STN8 protein levels bring about? .....                                                       | 91         |
| 4.3.1    | STN8 activity is not regulated via modulation of STN8 protein levels .....                                                           | 91         |
| 4.3.2    | STN8 protein levels affect PSII core phosphorylation, supercomplex formation and thylakoid ultrastructure.....                       | 92         |
| 4.3.3    | STN8 protein levels and PSII core phosphorylation have minor effects on photosynthetic performance .....                             | 95         |
| 4.4      | An overlap in substrate specificity of STN7 and STN8 does not correlate with a mutual influence on each other's protein levels ..... | 95         |
| <b>5</b> | <b>References .....</b>                                                                                                              | <b>96</b>  |
|          | <b>Acknowledgements.....</b>                                                                                                         | <b>104</b> |
|          | <b>Publications.....</b>                                                                                                             | <b>105</b> |
|          | <b>Eidesstattliche Erklärung.....</b>                                                                                                | <b>106</b> |

## List of Figures

|                                                                                                                                          |    |
|------------------------------------------------------------------------------------------------------------------------------------------|----|
| <b>Figure 1</b> The chloroplast.....                                                                                                     | 2  |
| <b>Figure 2</b> Simplified model of the state transition mechanism.....                                                                  | 8  |
| <b>Figure 3</b> Regulation of STN7 activity during high light exposure.....                                                              | 13 |
| <b>Figure 4</b> Two-step model for activation of the STN7 kinase by the Cyt <i>b6f</i> complex.....                                      | 15 |
| <b>Figure 5</b> Comparison of STN protein accumulation in WT and STN overexpressor plants.....                                           | 31 |
| <b>Figure 6</b> Assessment of the specificity of polyclonal antibodies raised against full-length protein sequence of STN8 and STN7..... | 32 |
| <b>Figure 7</b> Suborganellar localization of STN8 and membrane association.....                                                         | 33 |
| <b>Figure 8</b> Localization of STN kinases within the thylakoid membrane.....                                                           | 36 |
| <b>Figure 9</b> STN8 accumulation in mutants deficient in one of the major photosynthetic complexes.....                                 | 36 |
| <b>Figure 10</b> Thermolysin digest of intact and sonicated/solubilized thylakoid membranes.....                                         | 38 |
| <b>Figure 11</b> Analysis of STN8 topology by protease treatment.....                                                                    | 40 |
| <b>Figure 12</b> STN7 protein and transcript accumulation under different light conditions.....                                          | 41 |
| <b>Figure 13</b> STN7 protein and transcript accumulation in different transgenic backgrounds.....                                       | 42 |
| <b>Figure 14</b> Effects of long-term acclimation to different light qualities on STN7 protein levels in leaves.....                     | 43 |
| <b>Figure 15</b> STN7 protein and transcript accumulation in different genetic backgrounds.....                                          | 44 |
| <b>Figure 16</b> Effects of increased STN7 levels on LHCII phosphorylation and PSI-LHCI-pLHCII supercomplex formation.....               | 47 |
| <b>Figure 17</b> Response of LHCII phosphorylation in WT and <i>oeSTN7</i> plants to high light intensity.....                           | 48 |
| <b>Figure 18</b> STN7 protein levels in <i>oeSTN7</i> and WT upon a shift from FR to LL or D.....                                        | 48 |
| <b>Figure 19</b> Measurements of state transitions in <i>oeSTN7</i> , <i>tap38-1</i> , <i>stn7-1</i> and WT plants.....                  | 49 |
| <b>Figure 20</b> Time-course of LHCII phosphorylation and 77 K fluorescence emission spectra in different light conditions.....          | 51 |
| <b>Figure 21</b> Determination of the PQ pool redox state in the dark based on OJIP transients.....                                      | 53 |
| <b>Figure 22</b> Kinetics of Chl a fluorescence of WT, <i>oeSTN7</i> , <i>stn7-1</i> and <i>tap38-1</i> .....                            | 54 |
| <b>Figure 23</b> Kinetics of absorption parameters of WT, <i>oeSTN7</i> , <i>stn7-1</i> and <i>tap38-1</i> .....                         | 55 |
| <b>Figure 24</b> PSI levels in thylakoids of WT, <i>stn7-1</i> and <i>oeSTN7</i> .....                                                   | 56 |

|                                                                                                                                                                                 |    |
|---------------------------------------------------------------------------------------------------------------------------------------------------------------------------------|----|
| <b>Figure 25</b> Effects of chemical modulation of PQ redox state on LHCII phosphorylation in WT and <i>oeSTN7</i> .....                                                        | 58 |
| <b>Figure 26</b> <i>In-vitro</i> LHCII phosphorylation in WT and <i>oeSTN7</i> plants after treatment with chemicals that alter the PQ redox state or modify Cys residues. .... | 60 |
| <b>Figure 27</b> <i>In-vitro de-novo</i> phosphorylation of WT and <i>oeSTN7</i> thylakoids using <sup>33</sup> P-ATP.....                                                      | 61 |
| <b>Figure 28</b> Activity of Cys/Ser-exchange STN7 variants. ....                                                                                                               | 63 |
| <b>Figure 29</b> Elusive formation of a putative STN7 dimer in the WT. ....                                                                                                     | 65 |
| <b>Figure 30</b> Dimer formation of STN7 variants. ....                                                                                                                         | 67 |
| <b>Figure 31</b> Confirmation of STN7 homo-dimerization by STN7-GFP-tagged lines. ....                                                                                          | 69 |
| <b>Figure 32</b> Diagonal-PAGE of STN7 <sub>C→S:70</sub> thylakoids under oxidizing conditions.....                                                                             | 70 |
| <b>Figure 33</b> Redox titration of STN7 variants. ....                                                                                                                         | 71 |
| <b>Figure 34</b> Affinity chromatography and mobility shift assay indicate STN7-TRX-f interaction. ....                                                                         | 72 |
| <b>Figure 35</b> Variation of STN8 protein levels upon D, LL, FR and HL exposure. ....                                                                                          | 73 |
| <b>Figure 36</b> STN8 dosage effects on thylakoid phosphorylation and PSII supercomplex formation. ....                                                                         | 75 |
| <b>Figure 37</b> PSII photoinhibition time-course of WT, <i>stn8-1</i> and <i>oeSTN8</i> plants.....                                                                            | 76 |
| <b>Figure 38</b> Analysis of thylakoid ultrastructure of WT, <i>stn8-1</i> and <i>oeSTN8</i> plants by transmission electron microscopy (TEM).....                              | 77 |
| <b>Figure 39</b> Kinetics of Chl a fluorescence parameters of WT, <i>oeSTN8</i> , <i>stn8-1</i> and <i>stn7 stn8</i> . ....                                                     | 79 |
| <b>Figure 40</b> Light-intensity dependence of absorption parameters of WT, <i>oeSTN8</i> , <i>stn8-1</i> and <i>stn7 stn8</i> . ....                                           | 80 |
| <b>Figure 41</b> Interdependence of STN kinase accumulation.....                                                                                                                | 81 |

## Abbreviations

|                       |                                                        |                   |                                                             |
|-----------------------|--------------------------------------------------------|-------------------|-------------------------------------------------------------|
| 1-qL                  | measure for the fraction of open PSII reaction centers | FR                | far-red light                                               |
| 2D                    | 2-dimensional                                          | FRAP              | fluorescence recovery after photobleaching                  |
| <i>A. thaliana</i>    | <i>Arabidopsis thaliana</i>                            | F <sub>v</sub>    | variable fluorescence                                       |
| ATP                   | adenosine-5'-triphosphate                              | GFP               | green fluorescent protein                                   |
| ATPase                | ATP synthase                                           | Hcf164            | high chlorophyll fluorescence 164; thioredoxin-like protein |
| β-DM                  | n-dodecyl β-D-maltoside                                | HEPES             | 4-(2-hydroxyethyl)-1-piperazineethanesulfonic acid          |
| BN                    | blue-native                                            | HL                | high light                                                  |
| CaCl <sub>2</sub>     | calcium chloride                                       | IPTG              | isopropyl β-D-1-thiogalactopyranoside                       |
| CcdA                  | CcdA, cytochrome c defective A;                        | KCl               | potassium chloride                                          |
| cDNA                  | complementary DNA                                      | KOH               | potassium hydroxide                                         |
| CDS                   | coding sequence                                        | LED               | light-emitting diode                                        |
| CEF                   | cyclic electron flow                                   | LEF               | linear electron flow                                        |
| Chl a/b               | chlorophyll a/b                                        | leSTN7            | lowexpressor of STN7                                        |
| CLSM                  | confocal laser scanning microscopy                     | LHCI/II           | light harvesting complex I/II                               |
| <i>C. reinhardtii</i> | <i>Chlamydomonas reinhardtii</i>                       | LL                | low light                                                   |
| CSK                   | chloroplast sensor kinase                              | LTR               | long-term response                                          |
| Cys                   | cysteine                                               | MOPS              | 3-(N-morpholino)-propanesulfonic acid                       |
| Cyt                   | cytochrome                                             | mRNA              | messenger RNA                                               |
| Cyt <i>b6f</i>        | cytochrome <i>b6f</i> complex                          | MS                | Mass spectrometry                                           |
| D                     | dark                                                   | NaCl              | sodium chloride                                             |
| DBMIB                 | 2,5-dibromo-6-isopropyl-3-methyl-1,4-benzoquinone      | NADP <sup>+</sup> | oxidized nicotinamide adenine dinucleotide phosphate        |
| DCMU                  | 3-(3,4-dichloro- phenyl)-1,1-dimethylurea              | NADPH             | reduced nicotinamide adenine dinucleotide phosphate         |
| DNA                   | deoxyribonucleic acid                                  | NaOH              | sodium hydroxide                                            |
| DOC                   | deoxycholic acid                                       | NDH               | NADPH dehydrogenase complex                                 |
| DTT                   | dithiothreitol                                         | NEM               | N-ethylmaleimide                                            |
| EDTA                  | ethylene diamine tetraacetic acid                      | NPQ               | non-photochemical energy quenching                          |
| F <sub>m</sub> / m'   | maximum fluorescence in the dark/ light                |                   |                                                             |
| F <sub>0</sub>        | fluorescence after dark adaptation                     |                   |                                                             |

|                      |                                                           |                           |                                                                                                             |
|----------------------|-----------------------------------------------------------|---------------------------|-------------------------------------------------------------------------------------------------------------|
| oe                   | overexpressor                                             | RNA                       | ribonucleic acid                                                                                            |
| oeSTN7               | overexpressor of STN7                                     | RT-PCR                    | reverse transcriptase/ <i>real-time</i> -quantitative- PCR                                                  |
| oeTAP38              | overexpressor of TAP38                                    | SD                        | standard deviation                                                                                          |
| P680                 | PSII reaction center                                      | SDS                       | sodium dodecyl sulphate                                                                                     |
| P700                 | PSI reaction center                                       | Ser                       | serine                                                                                                      |
| pLHCII               | phosphorylated light-harvesting complex of photosystem II | SIG1                      | chloroplast sigma factor 1                                                                                  |
| P-Thr                | phosphothreonine                                          | STN7                      | thylakoid-associated Ser-Thr protein kinase State Transition 7 ( <i>A. thaliana</i> )                       |
| PSI/II               | Photosystem I/II                                          | STN7 <sub>C→S:65</sub>    | transgenic line expressing Cys 65-Ser exchange variants of STN7 ( <i>stn7-1</i> background)                 |
| PAGE                 | polyacrylamide gel electrophoresis                        | STN7 <sub>C→S:70</sub>    | transgenic line expressing Cys 70-Ser exchange variants of STN7 ( <i>stn7-1</i> background)                 |
| PAM                  | pulse amplitude modulation                                | STN7 <sub>C→S:65+70</sub> | transgenic line expressing Cys 65-Ser 65 / Cys 70-Ser exchange variants of STN7 ( <i>stn7-1</i> background) |
| PAR                  | photosynthetically active radiation                       | STN8                      | thylakoid-associated Ser-Thr protein kinase State Transition 8 ( <i>A. thaliana</i> )                       |
| PCR                  | polymerase chain reaction                                 | STR                       | short-term response                                                                                         |
| PVDF                 | polyvinylidene fluoride                                   | STT7                      | thylakoid-associated Ser-Thr protein kinase <i>C. reinhardtii</i>                                           |
| pLHCII               | phosphorylated LHCII                                      | TAP38/ PPH1               | Thylakoid-Associated Phosphatase of 38 kDa/ Protein Phosphatase 1                                           |
| PP2C                 | protein phosphatase 2 C                                   | Thr                       | threonine                                                                                                   |
| PBCP                 | Photosystem II Core Phosphatase                           | TM                        | transmembrane domain                                                                                        |
| PQ/ PQH <sub>2</sub> | plastoquinone (oxidized)/ plastoquinol (reduced)          | Tris                      | tris (hydroxymethyl) aminomethane                                                                           |
| PSI/ II              | photosystem I/ II                                         | TRX                       | thioredoxin                                                                                                 |
| PTK                  | plastid transcription kinase                              | w/o                       | without                                                                                                     |
| PVDF                 | polyvinylidene fluoride                                   | WT                        | wild type                                                                                                   |
| Φ I                  | effective quantum yield of PSI                            | <b>Units</b>              |                                                                                                             |
| Φ II                 | effective quantum yield of photosystem II                 | °C                        | degree Celcius                                                                                              |
| ΦNA                  | Acceptor side limitation of PSI                           | Da                        | Dalton                                                                                                      |
| ΦND                  | Donor side limitation of PSI                              | g                         | gram                                                                                                        |
| Q <sub>A</sub>       | the primary quinone electron acceptor of PSII             |                           |                                                                                                             |
| Q <sub>o</sub>       | the quinol oxidation site of the <i>Cyt b6f</i>           |                           |                                                                                                             |
| qL                   | photochemical quenching                                   |                           |                                                                                                             |
| qT                   | fluorescence quenching because of state transition        |                           |                                                                                                             |

|          |            |     |            |
|----------|------------|-----|------------|
| <i>g</i> | gravity    | min | minutes    |
| <i>h</i> | hour       | mL  | milliliter |
| <i>k</i> | kilo       | mM  | millimolar |
| kDa      | Kilodalton | mol | molar      |
| <i>L</i> | liter      | nm  | nanometer  |
| $\mu$    | micro      | s   | second     |
| <i>M</i> | molar      | v   | volume     |
| <i>m</i> | meter      | w   | weight     |

## 1 Introduction

### 1.1 Photosynthesis, the chloroplast and linear electron flow (LEF)

Photosynthesis is the process that enables organisms to convert sun energy into stable organic compounds, which are essential to sustain heterotrophic life. It is a reduction-oxidation (redox) process in which water (or rarely H<sub>2</sub>S) serves as electron source and carbon dioxide as electron acceptor. As side product of this elementary process free oxygen is released to the atmosphere, which is vital to all respiration-dependent life. A major challenge for photoautotrophic organisms is the coordination of the absorption of sunlight, energy conversion, transfer of electrons and multistep enzymatic pathways (Buchanan et al. 2002).

In eukaryotes the compartment for all photosynthetic processes is the chloroplast, a specialized plastid with chlorophyll-binding membrane proteins. Like mitochondria this organelle has arisen from an endosymbiotic event. Thereby, an ancestral cyanobacterium was integrated into a non-photosynthetic eukaryotic host cell. During evolution most of the genes of the endosymbiont were transferred to the nucleus of the host cell, whereas just a small set of genes was retained by the organelle. Thus, an import system had to evolve, that allowed for proteins synthesized in the cytosol to be reimported into the organelle. For the coordination of inter- and intra-organelle communication, as well as for optimization of metabolic processes, new genes, specific for eukaryotes, developed (Buchanan et al. 2002; Hohmann-Marriott and Blankenship 2011).

These processes were also accompanied by structural differentiation of the new organelle. The modern chloroplast of higher plants is surrounded by two membranes, named the outer and the inner envelope. Its internal membrane, the chlorophyll-containing thylakoid membrane, represents the site of photosynthesis (Lodish et al. 2000), which constitutes a continuum and encases an internal compartment called thylakoid lumen. Structurally the thylakoid membrane can be subdivided into grana, grana margins and stroma lamellae (**Figure 1**). Grana thylakoids are stacks of appressed membranes, whose highly curved non-appressed margins constitute an own domain (Anderson 1989). Stroma lamellae represent the unstacked membrane fraction, which is therefore in closer contact to the stroma, the semi-fluid matrix surrounding the thylakoids. This system of thylakoid membranes contains membrane proteins that incorporate light-absorbing pigments, such as chlorophylls, and large multiprotein complexes, which enable the conversion of

light energy into chemical bound energy (ATP, NADPH) in the first phase of photosynthesis (Lodish et al. 2000).

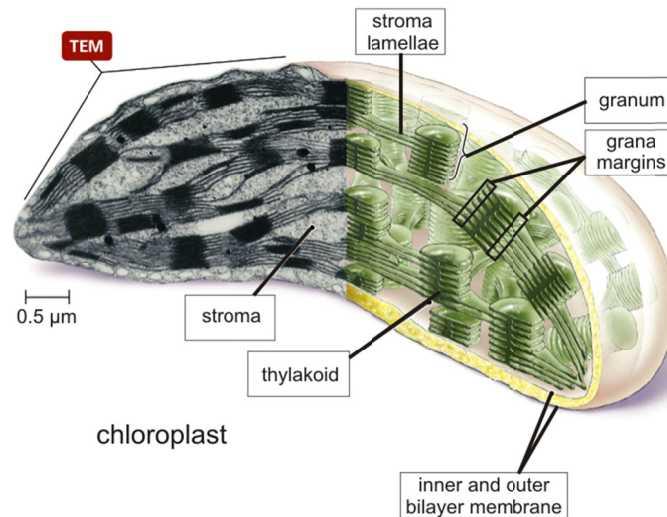


**Figure 1 The chloroplast.**

The organelle of photosynthesis is the chloroplast. It is surrounded by the inner and outer envelope (bilayer) membrane and traversed by the structured thylakoid membrane embedded in the stroma compartment. Thylakoids carry the chlorophyll-binding proteins and complexes that facilitate the light reaction. They are further subdivided in grana stacks and stroma lamellae, and enclose an additional compartment, the lumen. The border regions of the grana stacks are called the grana margins. The left side depicts a Transmission Electron Microscope (TEM) picture (adapted from Garrett 2006).

The four major complexes of the thylakoid membrane are the photosystem II (PSII) enriched in the grana, photosystem I (PSI) and ATP synthase (ATPase) in the stroma lamellae, and the rather equally distributed cytochrome *b6f* complex (Cyt *b6f*). These complexes, as well as mobile electron transporters, which act in between those complexes, facilitate the linear electron flow (LEF) of the sunlight driven light reaction, which starts at the PSII. Upon absorption of photons at the PSII the electrons of the P680 reaction center are excited to a higher level and can be transferred to a bound pheophytin a molecule, the primary electron acceptor. Consequently, the oxidized P680 is re-reduced by splitting water into oxygen and protons via the oxygen evolving complex (OEC) located in the lumen. Pheophytin a transfers its electrons to a fixed plastoquinone ( $Q_A$ ), which in turn reduces reversible bound plastoquinone ( $Q_B$ ) to plastoquinol ( $PQH_2$ ). This mobile carrier diffuses through the membrane and delivers its electrons to the Cyt *b6f* complex. The latter catalyzes the transfer of electrons from  $PQH_2$  to luminal plastocyanin, which as well

represents a mobile carrier protein and donates its electrons to the PSI reaction center (P700). Similar to PSII, this chlorophyll-containing complex uses light energy to reduce ferredoxin. In the last step of the light reaction the ferredoxin-NADP<sup>+</sup> reductase generates NADPH at the stromal side. Concomitantly to the PQH<sub>2</sub> turnover at the Cyt *b6f* complex protons are transported into the thylakoids lumen (Q-cycle) leading to its acidification. The resulting proton gradient between lumen and stroma is the energy source that is exploited for the phosphorylation of adenosine-diphosphate (ADP) to energy-rich adenosine-triphosphate (ATP) by the ATP synthase. The second phase of photosynthesis, the Calvin cycle, is taking place in the stroma. Here the high energy product ATP and the reducing compound NADPH are consumed during CO<sub>2</sub> fixation (Buchanan et al. 2002).

## 1.2 Alternative electron pathways act beside LEF

Beside the linear electron flow (LEF) outlined above (1.1), two cyclic electron pathways (CEFs) around PSI were described, which reinject electrons to the plastoquinone (PQ) pool.

The ferredoxin-dependent reduction of plastoquinone is facilitated by the PGRL1/PGR5 proteins if the preferred NADP<sup>+</sup>-reduction pathway is inhibited. Thus, this cyclic pathway is promoted under HL conditions, when the NADP<sup>+</sup>/NADPH pool is highly reduced, or after dark-acclimation, when the Calvin-Benson-cycle is not yet activated (Breyton et al. 2006; DalCorso et al. 2008; Joliot and Joliot 2005).

The second route of CEF depends on the plastidial NADPH-dehydrogenase (NDH), which enables the reduction of the PQ pool by stromal NADPH (Shikanai 2007). This NDH-dependent PQ reduction occurs also without PSI involvement, for example during heat stress in the dark (Sazanov et al. 1998). The light-independent oxidation of the PQ pool involves a plastid terminal plastoquinone oxidase (PTOX) or the PSII subunit cytochrome b559 (Bondarava et al. 2003; Casano et al. 2000; Pospisil 2011; Rumeau et al. 2007; Schwenkert et al. 2006; Shinopoulos and Brudvig 2012). These non-photochemical electron pathways contribute to the observation that up to one fourth of the PQ pool stays in a reduced state in the dark (Kruk and Karpinski 2006; Toth et al. 2007). Thereby a tight correlation with the metabolic state of the chloroplast is evident (Hou et al. 2003). Moreover, it is suggested that CEF fine-tunes the ATP/NADPH ratio by increasing ATP production (Eberhard et al. 2008).

### 1.3 Involvement of cysteines in photosynthetic processes

Many plastidic processes are regulated via the formation and reduction of disulfide bonds of cysteine-residue-containing proteins. Due to changes of the stromal redox state by varying light and metabolic conditions, the thiol-redox state and consequently the activity of those proteins are affected (Buchanan and Balmer 2005). Also a trans-thylakoid thiol-reducing pathway has been described, which is supposed to transfer redox state information of the stroma to the lumen. The two components identified of this pathway are the CcdA protein, which belongs to the DsbD/DipZ family of membrane polytopic proteins, and Hcf164, actually involved in Cyt *b6f* assembly. CcdA was proposed to play a role in the transfer of thiol-reducing equivalents from the stroma to the lumen (Page et al. 2004) and the transmembrane protein Hcf164 comprises a thioredoxin domain with disulfide-reductase activity on the luminal side of the thylakoid membrane (Lemeille and Rochaix 2010; Lennartz et al. 2001; Motohashi and Hisabori 2006).

Important mediators of redox regulation are members of the thioredoxin (TRX) family (Motohashi et al. 2001), of which at least five distinct families are described until today. In plants f- and m-types of chloroplastic TRXs were identified, which were shown to target up to 90 potential substrates (Lemaire et al. 2007). TRXs are disulfide oxidoreductases of about 12 kDa and are characterized by highly conserved cysteine (CxxC-) motives (Cain et al. 2009). These motives are involved in the thiol-disulfide interchange reaction, which is the underlying mechanism for regulation via thioredoxin (Buchanan and Balmer 2005). Enzymes of the Calvin-Benson-cycle and the pentose phosphate pathway, as well as the ATP synthase are activated by reduction via thioredoxin after onset of light (Kohzuma et al. 2012; Marri et al. 2009). Also the activity of the RuBisCo-activase (Zhang et al. 2001) and the deactivation of the LHCII kinase STN7 under strong light intensities is supposed to be regulated by the ferredoxin-thioredoxin pathway (Lemeille and Rochaix 2010; Martinsuo et al. 2003; Puthiyaveetil 2011; Rintamaki et al. 2000). However, CxxC motives are also known to be ligands of metal ions in metalloproteins like transcription factors or iron-storage proteins (Frauer et al. 2011; Leon et al. 2003). Also photosynthesis involves indispensable thiol-redox regulation and coordination of co-factors by cysteines. For example iron-sulfur-clusters can be found in ferredoxin, photosystem I or the Rieske-protein of the Cyt *b6f* complex (Droux et al. 1987; Jagannathan and Golbeck 2009; Yang et al. 2012). Cysteines that are not arranged in an obvious motive within the amino acid sequence can as well play a decisive role in thiol-dependent processes.

#### **1.4 Measurement of photosynthetic parameters**

Light energy absorbed by the plant is used for photochemical processes in the thylakoid membrane; however, generally not all of it is consumed by conversion into electron transport. Depending on the light condition and the operation state of the photosynthetic machinery, light energy is partially converted to heat or quenched by fluorescence emission. This chlorophyll *a* fluorescence can be measured by a pulse-amplitude-modulation (PAM) fluorometer, which provides information about the state of PSII, including the effective photosynthesis rate, the reduction state of electron acceptors, and the extent of heat dissipation (Schreiber 2004). In contrast, the state of PSI can be assessed via its absorbance behavior in the near-infrared (peaking at 810-840 nm), which is changing with the redox state of the P700 reaction center (Klughammer and Schreiber 2008).

#### **1.5 Protein phosphorylation in chloroplasts**

Reversible phosphorylation is a major post-translational modification and occurs on more than 30 % of all eukaryotic proteins (Olsen et al. 2006), modulating their conformation, activity, stability and localization. In eukaryotes mainly serine (Ser), threonine (Thr) or tyrosine (Tyr) residues become phosphorylated (Laugesen et al. 2004); however, in the course of the two-component signaling pathway also histidine and aspartate residues are involved (Saito 2001). For chloroplastidic proteins predominantly reversible phosphorylation of serine and threonine residues was detected regulating several cellular reactions, like starch metabolism (Tetlow et al. 2004), plastidic transcription (Baginsky et al. 1997; Kleffmann et al. 2007), thylakoid ultrastructure formation (Fristedt et al. 2009), NDH complex activity (Lascano et al. 2003), photosynthetic light reaction and LHCII mobility (Haldrup et al. 1999; Vener et al. 1998; Wollman 2001).

#### **1.6 Adaptation of photosynthesis to changing light conditions**

Land plants are sessile organisms that are bound to their habitat. They therefore have to cope with changing environmental conditions. Thus, in order to survive and remain competitive, photosynthetic organisms have developed a suite of mechanisms to deal with changes in water and nutrient supply, and variations in light and temperature. The incidence of sunlight is subject to fluctuations in quality and quantity to which plants react with acclimation responses including modulation of thylakoid ultrastructure (Fristedt et al. 2009, Pfeiffer and Krupinska 2005) and reorganization of photosynthetic complexes (Kanervo et al. 2005; Walters 2005). Within minutes

photosynthetic organisms are able to respond to changing light conditions by reorganization of reversible association of the reaction centers of the photosystems with a fraction of the light harvesting complexes of PSII (LHCII). This short-term light acclimation response involves phosphorylation of the LHCII proteins and is called state transitions, which facilitate the adjustment of photosystem I and II excitation (Kanervo et al. 2005; Walters 2005). By comparison, long-term changes in light quality are compensated by stoichiometric changes of PSII and PSI based on adjustment of gene expression (Pfannschmidt et al. 2003). However, for both mechanisms the redox state of the PQ pool was shown to be relevant (Puthiyaveetil et al. 2012).

If the photosynthetic machinery is excited above its capacity under high light (HL) intensities, the plant is unable to transform its excess of energy into controlled photochemical operation, which increases the generation of harmful reactive oxygen species (ROS). The plant is able to respond with mechanisms promoting the non-photochemical quenching (NPQ) of the incident light energy (Puthiyaveetil et al. 2012). This NPQ comprises the enhanced turnover of PSII reaction centers D1 (photoinhibition) (Aro et al. 2005; Fristedt et al. 2009; Tikkanen et al. 2008a), the qE mechanism (Ruban et al. 2012), and as a minor component state transitions (qT) (Tikkanen and Aro 2012). The fast damage and repair of D1 protein prevents the generation of uncontrolled electron transmission and thus the photodamage of further components by lowering excitation pressure on PSII (Aro et al. 2005). The qE mechanism is regulated by luminal pH affecting PSBS protonation, which triggers the binding of xanthophylls to chlorophyll antenna resulting in heat dissipation instead of photoreduction at the PSII (Ruban et al. 2012). Finally, part of the spectrum of possibilities is as well a long-term acclimation of the photosynthetic machinery to HL intensities (Tikkanen et al. 2006).

### **1.6.1 Long term response (LTR)**

Preferential excitation of PSI or PSII for a longer time period is answered by photosynthetic organisms with stoichiometric changes of the amounts of their photosystems to escape imbalances in energy distribution within hours or days. In this long-term acclimation process the abundance of reaction centers and light-harvesting proteins is adjusted on the transcriptional level, which is reflected by changes in the chlorophyll a and b ratio and changes in grana stack formation (Dietzel et al. 2008; Fujita 1997; Melis 1991; Pfannschmidt et al. 2001). Thereby, the redox state of the PQ pool serves as the ultimate signal for LTR initiation, which is directly affected by

unequal excitation of the reaction centers. Continuous oxidation of the PQ pool due to preferential PSI stimulation leads to transcriptional down-regulation of the *psaAB* operon coding for the PSI reaction center core proteins (Dietzel et al. 2008; Fey et al. 2005). Bonardi et al. (2005) revealed for the LHCII protein kinase STN7 a function as key sensor or signal transducer for both state transitions and the LTR. The assumption of a regulatory coupling of both processes (Allen 1995; Allen and Pfannschmidt 2000; Pursiheimo et al. 2001) was supported by analysis of a *STN7* knock-out mutant of *A. thaliana* (*stn7*), which was shown to be deficient in both pathways (Bonardi et al. 2005). However, Pesaresi et al. (2009) could show that state transitions per se are not essential for the LTR. Recently, an alternative model was suggested based on the chloroplast sensor kinase (CSK), and its partners the plastid transcription kinase (PTK) and the chloroplast sigma factor 1 (SIG1) (Puthiyaveetil et al. 2012). CSK is a modified two-component sensor kinase of endosymbiotic origin, which would similar to STN7 sense the redox state of the PQ pool in order to adjust photosystem stoichiometry. In this case, oxidized PQ would serve as the signaling trigger. This pathway would proceed distinctly from the state transition mechanism, because the latter depends on the presence of reduced plastoquinone (PQH<sub>2</sub>) (Puthiyaveetil et al. 2012).

### 1.6.2 State transitions

PSII is organized in large super- and megacomplexes containing several PSII cores with a variable number of LHCII being attached. In plants dimeric PSII is surrounded by two to four LHCII trimers composed of combinations of LHCB1, LHCB2 and LHCB3. Those are connected to PSII via the monomeric minor antenna proteins LHCB4, LHCB5 and LHCB6, also called CP29, CP26, CP24, respectively (Caffarri et al. 2004; Dekker and Boekema 2005; van Oort et al. 2010; Yakushevskaya et al. 2003). The short-term response (state transitions) describes the reversible translocation of a mobile fraction of LHCII between PSII and PSI in order to balance excitation energy by modulating the antennae cross-sections of the two photosystems (**Figure 2**) (Allen 1992; Wollman 2001). This process proceeds within minutes and is controlled by reversible phosphorylation of the LHCII proteins LHCB1, LHCB2 and CP29 (Tokutsu et al. 2009), which depends on the presence of the protein kinase STT7 in *C. reinhardtii* (Depege et al. 2003; Lemeille et al. 2009). With a mobile LHCII fraction up to 80 % *Chlamydomonas reinhardtii* (*C. reinhardtii*) is an ideal model system for studying state transitions (Delosme et al. 1996; Finazzi et al. 2002). In flowering plants the fraction of mobile antenna proteins that are

transferred constitute only 15 % of the overall LHCII pool (Allen 1992; Delosme et al. 1994). However, also here the process is accompanied by substantial remodeling of the thylakoid structure, including fission and fusion events at the edges of grana lamellae (Chuartzman et al. 2008). In *Arabidopsis thaliana* (*A. thaliana*) the phosphorylation and the corresponding dephosphorylation of LHCII are catalyzed by the protein kinase STN7 and the thylakoid associated protein phosphatase of 38 kDa named TAP38/PPH1, respectively (Bellafiore et al. 2005; Bonardi et al. 2005; Pribil et al. 2010; Shapiguzov et al. 2010; Vainonen et al. 2005).

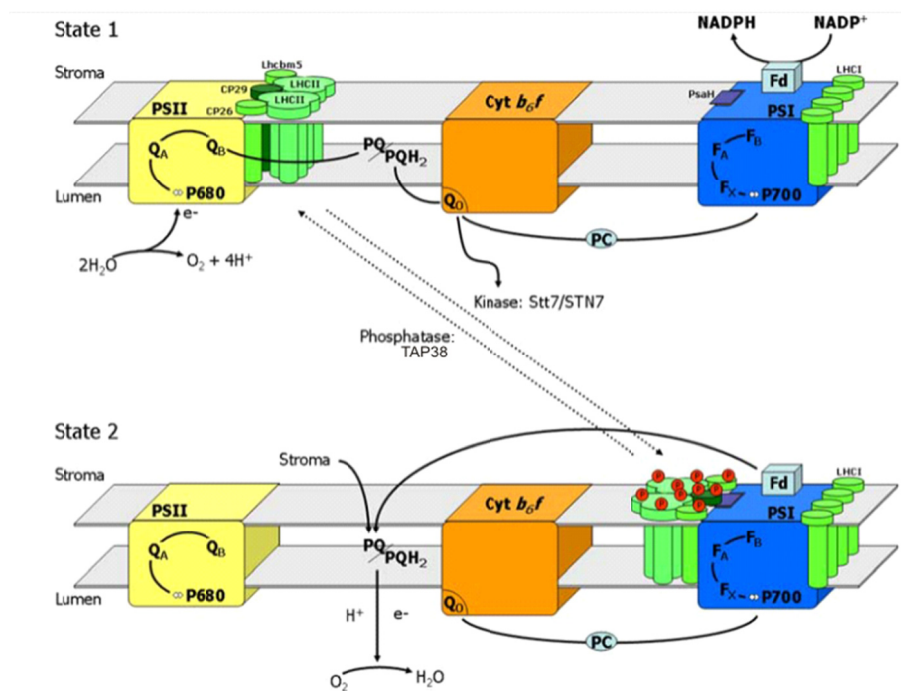


**Figure 2 Simplified model of the state transition mechanism.**

State transitions are a short-term response to changing light conditions. If one of the photosystems (PSII or PI) is preferentially excited, the equal electron transport of the light reaction is disturbed. I.e. overstimulation of PSII leads to a significant reduction of the PQ pool. Sensing the PQ/PQH<sub>2</sub> ratio the chloroplast tries to balance the excitation of PSII and PSI by adjusting the respective antenna surfaces of the photosystems. Upon phosphorylation a mobile fraction of LHCII dissociates from PSII and binds to PSI. The kinases STN7 (higher plants) or STT7 (*Chlamydomonas reinhardtii*) enable the phosphorylation of LHCII. Contrarily, the LHCII phosphatase TAP38/PPH1 (higher plants) facilitates the dephosphorylation of pLHCII and its movement back to PSII. A prerequisite for STN7/STT7 activity is the presence of PQH<sub>2</sub> at the Q<sub>o</sub> site of the Cyt b<sub>6</sub>/f complex, whose occupancy in turn depends on the redox state of the PQ pool (Lemeille and Rochaix 2010).

The major regulatory signals are supposed to originate from the redox state of the PQ pool, which directly affects the binding of plastoquinol to the Q<sub>o</sub> site of the Cyt *b6f* complex and thereby activates the LHCII kinase. That is to say, a chemical reduction of the PQ by moderate PSII specific light (state 2 conditions) promotes LHCII phosphorylation and therefore its dissociation from PSII and transfer to PSI in the stroma lamellae (Bonardi et al. 2005). On the contrary, oxidation of the PQ pool by PSI specific light (state 1 conditions), like far-red light, results in dephosphorylation of LHCII and its detachment from PSI and binding to PSII in the grana (**Figure 2**).

This simplified traditional model was challenged by results from thylakoid sub-fractionation experiments, chlorophyll fluorescence measurements and phosphorylation assays, which helped to elaborate a revised state transition model (Tikkanen et al. 2008b). It is generally accepted, that phosphorylation of LHCII leads to repulsion effects between proteins complexes due to the additional negative charges of the phosphate groups. The tightly appressed thylakoid layers in the grana stacks visible in state 1 relax during state 2 conditions and thereby facilitate the movement of protein complexes. Possibly, these repulsion forces also mediate the movement of pLHCII-PSII complexes towards stroma lamellae, where they participate in heat dissipation. However, substantial amounts of pLHCII-PSII stay in central regions of the grana stacks. Furthermore, phosphorylation of LHCII seems to attract PSI-LHCI complexes towards grana stacks, which enables the energy transfer from LHCII to PSI upon formation of PSII-pLHCII-PSI complexes in the grana margins (Tikkanen et al. 2008b).

The regulation of state transitions is not only limited to changes in light quality, but also light quantity affects LHCII phosphorylation. In dark-adapted plants, a state-1-like situation is restored, owing to their predominantly oxidized PQ pool. Contrarily, state 2 is promoted in plants exposed to white light intensities below the growth light level, to which they were acclimated (Bonardi et al. 2005). Remarkably, already at growth light conditions plants exhibit a substantial amount of pLHCII bound to PSI. However, an increase in light intensity to high light (HL) leads to a displacement of LHCII from PSI, which represents a relatively fast way to remove excitation pressure from PSI in order to balance the system (Grieco et al. 2012; Hou et al. 2003; Tikkanen et al. 2010; Tikkanen et al. 2006). In this way, state transitions represent a protective mechanism against over-excitation of PSI and concomitantly against the generation of deleterious reactive oxygen species (ROS) at PSI under fluctuating light intensities (Grieco et al. 2012). Although HL intensities actually cause a strong reduction of the PQ pool, the dephosphorylation of pLHCII is

promoted, which reveals a mechanism for feedback down-regulation of STN7 activity, overriding the stimulating effect of PQ reduction. In this case, the deactivation mechanism most likely depends on the redox state of the stromal ferredoxin-thioredoxin system, which becomes strongly reduced under HL (Lemeille and Rochaix 2010; Martinsuo et al. 2003; Puthiyaveetil 2011; Rintamaki et al. 2000). Aberrant from far-red light (FR), low light (LL) or dark (D) conditions an energy transfer from dephosphorylated LHCII to the PSII reaction centers would be counterproductive under HL since down-regulation of PSII activity is triggered upon light excess. Consequently, it was shown that LHCII can form aggregates in the thylakoid membrane that allow quenching of excess light energy via heat dissipation (Iwai et al. 2010; Tikkanen et al. 2011; Tikkanen et al. 2010).

Not only changes in light but also temperature conditions (Nellaepalli et al. 2012; Nellaepalli et al. 2011) and the cellular metabolism affect state transitions in *A. thaliana* (Hou et al. 2003; Tikkanen et al. 2010). Furthermore, feeding experiments with NADPH or glucose in the dark could trigger LHCII phosphorylation, implying a feedback effect of the metabolic state of the chloroplasts stroma on state transitions (Hou et al. 2003; Tikkanen et al. 2010). This tight connection suggests that state transitions are not restricted to balance the excitation of PSII and PSI but could as well play a role in obtaining a suitable NADPH/ATP ratio for CO<sub>2</sub> fixation by coordinating the light reactions with carbon metabolism (Burrows et al. 1998; Tikkanen et al. 2006). In *C. reinhardtii*, state transitions were even supposed to be primarily responsible for ATP homeostasis by regulating the CEF/LEF ratio which clearly increases upon state-2 transition (Finazzi et al. 2002). Low levels of ATP or anaerobiosis combined with dark conditions lead to the influx of electrons from the NADPH to the PQ pool, promoting LHCII phosphorylation, whereupon cyclic electron flow generates a proton gradient which drives ATP production (Bulté et al. 1990; Burrows et al. 1998; Endo et al. 1999). Hence, whereas STT7 mutants exhibit no growth defect, the lack of state transitions was shown to become critical in respiration-deficient mutants of *C. reinhardtii* (Cardol et al. 2009; Fleischmann et al. 1999).

*A. thaliana* mutants deficient in state transitions do not exhibit obvious defects in fitness and development under normal controlled growth conditions (Bonardi et al. 2005; Lunde et al. 2000; Tikkanen et al. 2006), even though the knock-out of *STN7* leads to severe changes in gene expression (Bonardi et al. 2005; Pesaresi et al. 2009; Pfanschmidt et al. 2003) and accumulation of various thylakoid proteins (Tikkanen et al. 2006). Pesaresi et al. could show in 2009 that state transitions play a significant physiological role in flowering plants that suffer from a disturbance

in LEF. A severe growth phenotype of *stn7* mutants could as well be provoked by exposure to fluctuating light intensities, which was explained by a disturbance in the redox homeostasis of the PQ pool (Bellafiore et al. 2005; Tikkanen et al. 2010). Furthermore, in field trials under natural environmental conditions a true fitness relevance of STN7 could be demonstrated. Despite the lack of a visible growth phenotype, *A. thaliana stn7* and *stn7 stn8* double mutants showed reduced seed production compared to wild type (WT) plants (Frenkel et al. 2007). Surprisingly, a knock-out mutant of the LHCII phosphatase, *tap38-1*, constantly trapped in state 2, rather shows an increased growth rate under continuous LL conditions (Pribil et al. 2010).

### 1.6.3 The LHCII kinases STN7 and STT7

Fluorescence yield changes during state transitions in *C. reinhardtii* served for the screening of mutants deficient in this LHCII antenna dislocation. This approach allowed for the identification of STT7, the Ser-Thr protein kinase responsible for LHCII phosphorylation. In *A. thaliana* two homologs of STT7 exist, the Ser-Thr protein kinases STN7 and STN8. Immunological analyses of the respective single and double mutants revealed a partial substrate overlap of STN7 and STN8 protein kinases (Bonardi et al. 2005), with LHCII phosphorylation being almost exclusively performed by STN7. *stn8* mutant plants are not affected in state transitions but show a significant reduction in light induced PSII core protein (CP43, D1, D2) phosphorylation (see 1.6.6), although a considerable level of phosphorylation of the PSII core proteins D1 und CP43 is still detectable (Bonardi et al. 2005; Tikkanen et al. 2010; Tikkanen et al. 2008a). This residual phosphorylation was ascribed to STN7 activity as no thylakoid phosphorylation was detected in the *stn7 stn8* double mutant (Bellafiore et al. 2005; Bonardi et al. 2005; Vainonen et al. 2005). Lemeille et al. (2010) proposed a consensus motif for STT7/STN7 target sites upon which further potential target proteins were identified. Putative substrate candidates like ATP-synthase subunits, proteins involved in chlorophyll biosynthesis and in synthesis of photosynthetic proteins, like PSBB and PSAB, have to be independently verified (Lemeille et al. 2010).

For both STN7 and STT7 it was not yet unequivocally clarified whether LHCII is the direct substrate or is phosphorylated by means of a kinase cascade. Co-immunoprecipitation experiments with HA-tagged STT7 suggested an association of STT7 with LHCII antenna; however, no difference could be observed between state 1 and 2 conditions for most interactions (Lemeille et al. 2009). Thus, STT7 and LHCII could interact directly or be part of a multiprotein

complex including further kinases. In *C. reinhardtii*, the state-2-dependent phosphorylation of a homologous protein kinase of STT7 named STL1 requires STT7. This suggests the existence of a protein kinase cascade; however, despite a significant homology to STN8, the function of STL1 is largely unknown (Depege et al. 2003; Lemeille et al. 2010). STT7 itself becomes phosphorylated under state 2 conditions at serine residue 533 (Ser 553). The adjacent amino acid residues of this phosphorylation site differ from the consensus motif of proteins phosphorylated in a STT7-dependent manner, supporting the idea of a kinase cascade. Interestingly, the exchange of the respective phosphorylation site did not affect STT7 kinase activity (Lemeille et al. 2010). Although the amino acid sequence around Ser 533 is not conserved between STT7 and STN7, STN7 becomes equally phosphorylated at its C-terminus. Recently it was shown that the phosphorylation of STN7 itself is also not affecting its activity but affects its turnover on protein level. Mimicking a permanent phosphorylation of STN7 at 4 potential phosphorylation sites prevented a decrease of STN7 protein level under state 1 conditions, which was observed for the wild type (Willig et al. 2011). Whether STN7 regulates its turnover by autophosphorylation remains to be clarified (Willig et al. 2011). Also in *C. reinhardtii* the protein levels of STT7 directly correlate with LHClI phosphorylation activity and were suggested to be controlled on the post-translational level (Lemeille et al. 2009; Willig et al. 2011).

Topology studies on STT7 in *C. reinhardtii* propose a local separation of the C-terminal stroma-exposed catalytic kinase domain from its lumen-located N-terminus by a single alpha-helical transmembrane domain (Lemeille et al. 2009). The N-terminus contains two conserved cysteine residues that are essential for STT7 activity, and was shown to be relevant for the interaction of STT7 with the Rieske protein PETC (Lemeille et al. 2009). A homologous N-terminal cysteine motive (Cys 65 and Cys 70) is present in STN7 of *A. thaliana* (Lemeille et al. 2009; Puthiyaveetil 2011). The latter possesses a further stromal cysteine motive (Cys 187 and Cys 191) in the ATP-binding domain, which is widely conserved beyond land plants and even appears in the STT7 homolog of *Ostreococcus*, a genus of the green algae. However this motive is missing in *C. reinhardtii* STT7, which in turn contains further cysteine residues within the kinase domain (Puthiyaveetil 2011). It was proposed that the luminal cysteine motif could be the site of PQH<sub>2</sub>-dependent activation, whereas the conserved stromal CxxxC motif might account for the thioredoxin-dependent feedback down-regulation of STN7 activity in flowering plants under HL conditions (Martinsuo et al. 2003; Puthiyaveetil 2011; Rintamaki et al. 2000). This implies that the redox signal of the ferredoxin-thioredoxin pathway is not transferred to the lumen via the

putative CcdA/Hcf164 pathway as suggested by Lemeille and Rochaix (2010), but that rather thioredoxin directly deactivates STN7 by reducing the stroma located disulfide bridge in the ATP catalyzing domain (Puthiyaveetil 2011) (**Figure 3**).

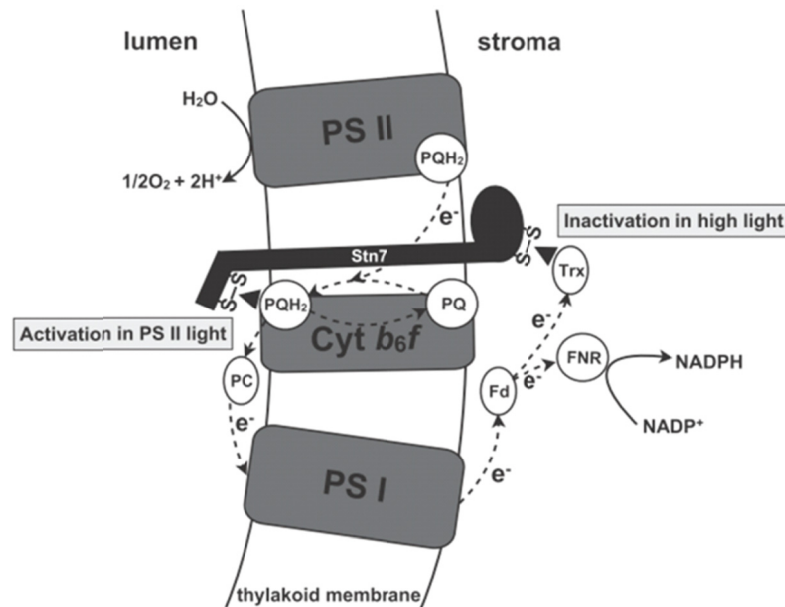


**Figure 3 Regulation of STN7 activity during high light exposure.**

A topology model of STN7 locates a short N-terminal sequence into the lumen and the C-terminal ATP binding domain to the stromal side. The N-terminus comprises a conserved thioredoxin-like cysteine motif and is potentially relevant for activation of the kinase via the Cyt *b6f* complex. Thereby, STN7 activity depends on the binding of PQH<sub>2</sub> at the Q<sub>o</sub> site of the Cyt *b6f* complex upon PQ pool reduction. At the stromal side the kinase domain contains a putative cysteine motive that could be directly targeted by the ferredoxin-thioredoxin pathway to enable the inactivation of the STN7 kinase under high light intensities (Puthiyaveetil 2011).

The regulation of the STN7 kinase is thought to be more relevant than the one of the LHCII phosphatase TAP38, which was proposed to exhibit constant but low activity. Eventually LHCII phosphorylation equilibrates on a level depending on the activity ratio of both antagonistic enzymes STN7 and TAP38 (Puthiyaveetil et al. 2012). Based on early biochemical data, light- or redox-dependent regulation of TAP38 is considered to be less likely (Elich et al. 1997; Puthiyaveetil et al. 2012; Silverstein et al. 1993), and TAP38 protein levels were shown to accumulate equally under state 1 and 2 conditions (Pribil et al. 2010). Contrarily, there is evidence that light or reducing agents do modulate LHCII phosphatase activity (Hammer et al. 1995). Also a regulatory interaction of the LHCII phosphatase with the immunophilin-like protein TLP40 was suggested but could not be confirmed so far (Fulgosi et al. 1998).

#### 1.6.4 Activation of the STN7/STT7 kinase by the Cyt *b6f* complex

The Cyt *b6f* complex was identified as the sensor and signal transducer for the redox state of the PQ pool and thus is responsible for the control of LHCII phosphorylation. Consequently, state transitions are not triggered in the absence of a functional Cyt *b6f* complex even if the PQ pool is strongly reduced due to a block in LEF, as shown for *C. reinhardtii* (Lemaire et al. 1986; Wollman and Lemaire 1988) and higher plants (Bennett et al. 1988; Coughlan 1988; Gal et al. 1987). For both, the state of the plastoquinone-binding site Qo of the Cyt *b6f* complex could be determined as being crucial for the regulation of LHCII kinase activity (Vener et al. 1997; Zito et al. 1999). Despite the plethora of data, the exact mechanism of STN7/STT7 activation is still under debate. It was proposed that the iron-sulfur-containing Rieske protein of the Cyt *b6f* complex located in the lumen plays a decisive role. This protein was shown to undergo conformational changes depending on the ligand-binding situation at the Qo site, which are thought to involve a reorganization of the Cyt *b6f* complex (Breyton 2000; Finazzi et al. 2001). This, together with the observation that subunit V (PETO) of the Cyt *b6f* complex is phosphorylated under state 2 conditions even if *C. reinhardtii* is blocked in state 1, gave rise to a two-step model, which suggests how phosphorylation of LHCII at the stromal side of the thylakoid membrane can be activated by the binding of PQH<sub>2</sub> at the rather luminal Qo site (**Figure 4**) (Finazzi et al. 2001; Hamel et al. 2000; Wollman 2001). In the first step of the model, binding of PQH<sub>2</sub> to the Qo pocket shifts the Rieske protein towards the Qo site in the membrane (proximal position) and thereby activates the LHCII kinase to phosphorylate subunit V of the Cyt *b6f* complex. The subsequent oxidation of PQH<sub>2</sub> leads to the transition of the Rieske protein to its distal position away from the membrane, leading to the release of STT7/STN7 from Cyt *b6f* complex and its interaction with LHCII. This model suggests the necessity of at least a transient interaction of the LHCII kinase with the Cyt *b6f* complex in order to “read” the activation mode of the complex. Two decades ago direct physical interaction between the LHCII kinase and the Cyt *b6f* complex was proven based on detection of kinase activity in purified Cyt *b6f* fractions of higher plants (Gal et al. 1990). Interestingly, similar indications for this interaction were obtained for *C. reinhardtii* by co-immunoprecipitation of STT7 with the Rieske protein of the Cyt *b6f* complex, which prevailed under both state 1 and state 2 conditions (Lemeille et al. 2009).

The turnover rate of PQH<sub>2</sub> in the Qo site should not be a limiting factor for kinase activation since mutants with decreased rate of electron transfer activity displayed no phenotype in LHCII phosphorylation (de Vitry et al. 2004; Yan and Cramer 2003). Moreover, de Lacroix de

Lavalette et al. (2008) provided evidence for an involvement of a chlorophyll molecule bound by the Cyt *b6f* complex (subunit IV, PETD) in kinase activation, which has to be further investigated.

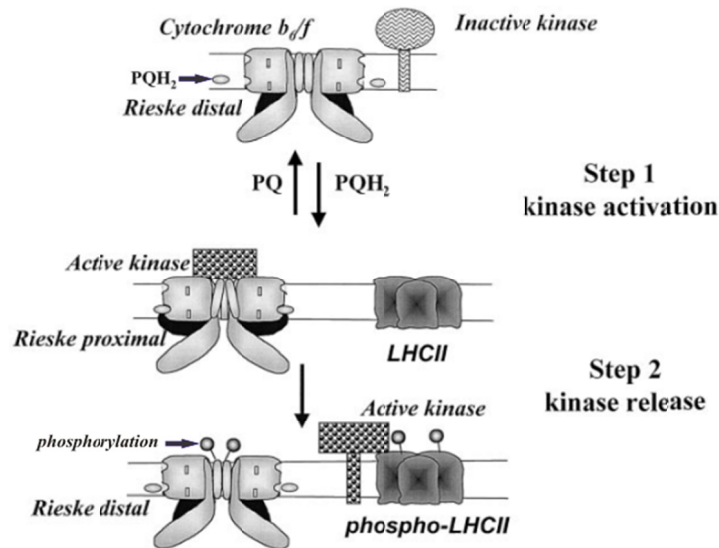


**Figure 4 Two-step model for activation of the STN7 kinase by the Cyt *b6f* complex.**

Dimeric Cyt *b6f* conducts membrane spanning reorganization upon conformational changes of the Rieske protein (*in black*). Depending on PQH<sub>2</sub> turnover the Rieske protein moves between a proximal and a distal position in respect to the Qo site of the Cyt *b6f* complex. These conformational changes help to transfer the state of the rather luminal Qo site to the stromal located kinase domain of STN7. In step 1 the proximal Rieske enables interaction with and activation of the STN7 kinase resulting in the phosphorylation of subunit V of the Cyt *b6f* complex. In step 2 the movement of Rieske to its distal position releases the activated STN7 kinase, allowing LHCII phosphorylation (Wollman 2001).

### 1.6.5 STN8 –the keyplayer in PSII core protein phosphorylation

In *A. thaliana stn8* mutant lines the level of LHCII phosphorylation, the functionality of state transitions (Bonardi et al. 2005; Vainonen et al. 2005) and the long-term response are not affected (Bonardi et al. 2005). The STN8 kinase is rather required for the quantitative phosphorylation of PSII core proteins (CP43, D1, D2 and PSBH), particularly under high light conditions (Bonardi et al. 2005; Tikkanen et al. 2010; Vainonen et al. 2005). However, inactivation of *STN8* alone does not completely abolish PSII core protein phosphorylation. Especially in the dark and under LL conditions, STN7 significantly contributes to PSII phosphorylation (Bonardi et al. 2005; Tikkanen et al. 2008a). The lack of STN8 decreases D1 and D2 protein phosphorylation only to about 50-60 % and 35 % of the wild-type level, respectively

(Vainonen et al. 2005). There are contradictory reports on reduced phosphorylation of CP43 in the *stn8* mutant except for the clear decrease after exposure to high light, thus under conditions that lead to inhibition of STN7 (Bonardi et al. 2005; Tikkanen et al. 2008a; Vainonen et al. 2005). The STN8-dependent phosphorylation of PSBH at residue Thr-4 was shown to require both, light and preceding phosphorylation at residue Thr-2, whereas the latter is also light-independently phosphorylated in *stn7 stn8* plants (Fristedt et al. 2009; Vainonen et al. 2005; Vener et al. 2001). A simultaneous knock-out of *STN7* and *STN8* leads to a loss of thylakoid phosphorylation on the level of Western blot detection (Bonardi et al. 2005; Tikkanen et al. 2008a). However, via MS and immunoblot analyses, Fristedt et al. (2009) were able to detect residual light-independent D2 phosphorylation at residue Thr-1 in *stn7 stn8* plants corresponding to less than 10 % of the wild-type level. Contrarily, the N-terminal phosphorylation of the D1 and CP43 proteins of PSII was confirmed to be completely absent in *stn7 stn8* mutants (Bonardi et al. 2005; Fristedt et al. 2009; Tikkanen et al. 2008a).

These results demonstrate that STN7 and STN8 seem to show a certain degree of overlap regarding their substrate specificities, while having distinct main substrates. With the double knock-out of *STN7/STN8* showing an overadditive effect on thylakoid phosphorylation, a parallel rather than a serial action of STN7 and STN8 can be assumed (Bonardi et al. 2005).

Lately, the chloroplast PP2C-type protein phosphatase, PHOTOSYSTEM II CORE PHOSPHATASE (PBCP), was shown to be essential for efficient PSII core protein dephosphorylation. Plants lacking PBCP exhibit an altered phenotype in thylakoid folding, while its overexpression affects state transitions (Samol et al. 2012). Thus, there is indication for substrate overlap with the LHCII phosphatase TAP38, similar to the kinases STN7 and STN8. Interestingly, the calcium-sensing receptor CaS was shown to be phosphorylated by STN8, but to be dephosphorylated by TAP38. This again illustrates the complex interplay of the major thylakoid protein kinases and phosphatases (Pribil et al. 2010; Vainonen et al. 2008).

Furthermore, Reiland et al. (2011) identified additional substrates of STN8 by an approach combining affinity chromatography and mass spectrometry. This extended substrate set of STN8 includes the calcium-sensing receptor CaS, the large subunit of RuBisCo (LSU), the minor PSII antenna protein CP29, an ATP synthase family protein and the PGR5-like protein 1 A (PGRL1-A), a protein essential of CEF (DalCorso et al. 2008; Reiland et al. 2011). The differential phosphorylation of PGRL1-A in *stn8* mutant plants was demonstrated to result in a faster switch between CEF and LEF during dark-light transitions (Reiland et al. 2011).

### 1.6.6 Function of PSII core protein phosphorylation

Compared to LHCII phosphorylation, the function of reversible PSII core protein phosphorylation is less clear. Since an increase of the number of damaged PSII reaction centers (D1) upon a rise in light intensity is accompanied by the phosphorylation of PSII core proteins, an involvement in D1 turnover during photo-inhibition of PSII was proposed (Baena-Gonzalez et al. 1999). An early model on D1 turnover stated, that the phosphorylated version of damaged D1 is resistant to proteolysis (Koivuniemi et al. 1995). However, it is able to move laterally from grana to stroma lamellae, where it becomes dephosphorylated, degraded and replaced by newly synthesized D1 (Rintamaki et al. 1996). A successive study of Bonardi et al. in 2005, making use of the *stn* mutant collection in *A. thaliana*, indicated that STN8-mediated phosphorylation of D1 *per se* is not crucial for D1 turnover and PSII repair. Here, PSII inactivation under high light intensities ( $2000 \mu\text{mol photons m}^{-2}\text{s}^{-1}$ ) was just slightly increased in *stn8* and *stn7 stn8* and was also not reflected in changes in the rate of HL-induced D1 degradation, which remained at wild-type level during pulse-chase experiments (Bonardi et al. 2005). These findings challenged the previous view of the physiological significance of D1 phosphorylation (Baena-Gonzalez et al. 1999).

However, later studies in rice again provided evidence for a higher susceptibility to photoinhibition due to a lack of *STN8* (Nath et al. 2007). Moreover, Tikkanen et al. (2008a) revealed a retardation of D1 degradation in the *stn8* and *stn7 stn8* mutants by applying less intense high light. It was claimed that a photon fluence rate of  $1000 \mu\text{mol m}^{-2}\text{s}^{-1}$  allows WT plants to balance PSII operation on a steady state level, while under these light conditions PSII repair in the *stn7 stn8* mutant is too slow to keep up with the occurring inhibition rate (Tikkanen et al. 2008a). Tikkanen et al. (2008a) explain this discrepancy between WT and *stn8* and *stn7 stn8* mutants by difficulties in the disassembly of PSII supercomplexes, leading to a less efficient exchange of damaged D1 between grana and stroma lamella due to changes in its migration behavior.

In a more recent study by Fristedt et al. (2009) the observed delay of D1 degradation in *stn8* and *stn7 stn8* plants was confirmed, even at  $2000 \mu\text{mol m}^{-2}\text{s}^{-1}$ . However, differences in the distribution of PSII monomers, dimers or supercomplexes could not be detected by Blue-native gel electrophoresis (Fristedt et al. 2009). Instead, gravity-driven sedimentation of isolated thylakoids and transmission electron microscopy demonstrated an enhancement in the size and density of stacked thylakoid membranes (grana) in *stn7 stn8* and *stn8*, which is supposed to influence the lateral diffusion of proteins including photo-damaged D1 and the bulky FtsH

complex (Fristedt et al. 2009). The latter is responsible for D1 degradation (Adam et al. 2006; Nixon et al. 2005) and was reported to be spatially kept away from PSII in STN8-deficient mutants by its relocation from the dense grana to the stroma lamella and grana margins (Fristedt et al. 2009). In summary, phosphorylation of PSII core proteins modulates macroscopic rearrangements of the entire network of thylakoid membranes and affects lateral movement of proteins in the membrane. But is the reduced PSII core phosphorylation in *stn8* mutants fitness-relevant for *A. thaliana* plants? Photosynthetic electron flow, measured on the basis of chlorophyll fluorescence, was not altered in *stn8* mutants (Bonardi et al. 2005). Also the growth rate and timing of seed germination in the greenhouse of all *stn* mutants was equal to wild type (Bonardi et al. 2005) and introducing the *stn8* mutation into *pete2-1.1*, *psad1-1* and *psae1-3* did not exacerbate the phenotype of the single mutants (Pesaresi et al. 2009). Merely the seed production of the double mutant *stn7 stn8* under natural field conditions was more strongly affected than for *stn7* single mutants, whereas seed yields of *stn8* mutants were similar to wild-type plants (Frenkel et al. 2007).

### 1.7 Aims of this work

Apart from Willig et al. (2011) using STN7 antibodies, this work is the first study applying specific antibodies against STN7 and STN8 of higher plants (*A. thaliana*). By means of immunoblotting, information about the topology and exact localization of STN7 and STN8 was obtained, as well as about the light and redox dependency of their accumulation on protein level. A correlation between the latter and *STN7* transcription was addressed by real-time PCR. Furthermore, this work is an approach to gain insights into the regulatory redox-dependent mechanisms acting on STN7. To this end, STN7 mutants expressing Cys-Ser exchange variants were examined with respect to their activity and dimerization behavior. Moreover, overexpressor lines of STN7 and STN8 were generated to examine the effect of increased thylakoid phosphorylation on associated processes and photosynthetic properties.

## 2 Materials and Methods

### 2.1 Plant material

The *Arabidopsis thaliana* L. (*A. thaliana*) ecotype Columbia-0, used in this study as wild type (WT), was obtained from NASC (Nottingham Arabidopsis Stock Centre; accession number N1092). Previously described mutant lines employed in this study were *stn7-1*, *stn8-1*, *stn7 stn8* (Bonardi et al. 2005), *hcf136* (Meurer et al. 1998), *psad1-1* (Ihnatowicz et al. 2004), *psad1-1 psad2-1* (Ihnatowicz et al. 2004), *atpd-1* (Maiwald et al. 2003), *petc-1* (Maiwald et al. 2003), *psae1-3* (Ihnatowicz et al. 2007), *psal-1* (Pesaresi et al. 2009) and *tap38-1* (Pribil et al. 2010).

#### 2.1.1 Gateway cloning and generation of transgenic *A. thaliana* lines

Transgenic lines generated in this study included the overexpressor (oe*STN7*) and low-expressor (le*STN7*) of STN7. To generate oe*STN7* and le*STN7*, full-length *STN7* CDS was cloned into the plant vector pLeela, which is a derivative of pJawohl3-RNAi (GenBank Accession No. AF404854) containing a GATEWAY cassette introduced into the HpaI site, using the primers *Stn7\_attB1\_forward* (5'-GGGGACAAGTTTGTACAAAAAAGCAGGCTCTATGGCTACAAT ATCTCCGGG) and *Stn7\_attB2\_reverse\_stop* (5'-GGGGACCACTTTGTACAAGAAAGCTGG GTTTCACCTCTCTCTGGGGATCCAT). The *STN7*-pLeela construct containing a double Cauliflower Mosaic Virus (CMV) 35S promoter was introduced into *stn7-1* via the floral-dip method (Clough and Bent 1998). Plants were selected based on their BASTA resistance, segregation analysis was performed, and independent lines carrying a single T-DNA insertion locus were identified. Single representative lines either overexpressing the STN7 kinase (oe*STN7*) or expressing about 30 % of the WT amount (le*STN7*) were identified by Western analysis employing a STN7-specific antibody (epitope antibodies described in 2.6). The STN8 overexpressing lines (oe*STN8*) were generated analogous to oe*STN7* by applying the primers *Stn8\_attB1\_ACC\_f* (GGGGACAAGTTTGTACAAAAAAGCAGGCTCTACCATGGCCTCTCT TCTCTCTC) and *Stn8\_attB2\_Stop\_r* (GGGGACCACTTTGTACAAGAAAGCTGGGTTTCAC TTGCTGAAACTGAGCTT) in order to clone full-length CDS of *STN8* into the vector pLeela.

#### 2.1.2 Site-directed mutagenesis and generation of cysteine exchange mutants of *A. thaliana*

To generate lines expressing STN7<sub>C→S:65</sub>, STN7<sub>C→S:70</sub> or STN7<sub>C→S:65+70</sub>, point mutations leading to the replacement of Cys 65 and/or of Cys 70 by Ser were introduced by site-directed

mutagenesis (QuikChange II Site-Directed Mutagenesis Kit) into the *STN7*-pLeela construct mentioned in paragraph 2.1.1. Transformation of *stn7-1* plants, selection, segregation and insertion analysis were performed as described in paragraph 2.1.1. Furthermore *STN7*<sub>C→S:65</sub> and *STN7*<sub>C→S:70</sub> were crossed to obtain lines expressing both *STN7* variants (65 x 70 and 70 x 65).

### 2.1.3 Generation of *A. thaliana* lines expressing GFP-tagged *STN7*

In order to obtain plants expressing WT or Cys-Ser exchange variants of *STN7* fused C-terminal to the green fluorescent protein (GFP), the coding sequences of the corresponding mutant *STN7* variants (without stop codon) were cloned into the plant expression vector pB7FWG2, placing them under the control of the CMV 35S promoter. To this end, the Gateway Cloning strategy was applied using the primer combination *Stn7\_attB1\_forward* (as above) and *Stn7\_attB2\_reverse* (5'-GGGGACCACTTTGTACAAGAAAGCTGGGTACTCCTCTCTGGGGATCCAT). Transformation of the pB7FWG2 vector into WT (Col-0) and *stn7-1* plants, selection, segregation and insertion analysis were performed as described in paragraph 2.1.1.

## 2.2 Growth conditions and light treatments

If not stated otherwise, plants were grown under controlled conditions in a growth chamber on an 8 h/16 h day-night regime providing 100  $\mu\text{mol photons m}^{-2}\text{s}^{-1}$  during the light phase (standard lighting conditions) and in all experiments, 6-week-old plants were used. For experiments with the mutants *hcf136*, *petc-1*, *psad1-1* *psad2-1*, *atpd-1*, *psal-1*, *psad1-1* and *psae1-3*, plants were grown on 1 x MS medium including vitamins (Duchefa®) at 50  $\mu\text{mol photons m}^{-2}\text{s}^{-1}$ . To study the effects of altered light conditions, plants were adapted to different light conditions specified as follows: 18 h dark adaptation (D), adaptation to low light at 60-80  $\mu\text{mol photons m}^{-2}\text{s}^{-1}$  (LL), high light at 800-1,200  $\mu\text{mol photons m}^{-2}\text{s}^{-1}$  (HL) or very high light at 1,800  $\mu\text{mol photons m}^{-2}\text{s}^{-1}$  (VHL). HL and VHL conditions were generated by an Osram Powerstar HQIBT-D/400W lamp. Far-red light (FR) was emitted by LEDs at a wavelength of 740 nm at an intensity of 3.0  $\mu\text{mol photons m}^{-2}\text{s}^{-1}$ . Alternating long-term light adaptations to PSI- and PSII-light were performed essentially as described previously (Wagner et al. 2008). In brief, 3-week-old plants were transferred from climate chamber conditions to one of the PS specific lights. Plants were kept for 6 days under the same light or were switch after 4 days to the other light for further 2 days until material was snap frozen in liquid nitrogen. PSI light (15  $\mu\text{mol m}^{-2}\text{s}^{-1}$ ) was generated by a medium red foil (Lee Filters, 027 Medium Red, transmittance 50 % at 650 nm) clamped over red fluorescent lamps of Osram, 39 W. PSII light (15  $\mu\text{mol m}^{-2}\text{s}^{-1}$ ) was generated by

an orange foil (Lee Filters, 405 Orange, transmittance 50 % at 560 nm) clamped over white fluorescent lamps of Osram, 39 W.

### 2.3 cDNA synthesis and real-time PCR

Total leaf RNA was extracted following the protocol of the RNeasy Plant Mini Kit (QIAGEN). 2 mg of total RNA was used to prepare cDNA by applying the iScript cDNA Synthesis kit (Bio-Rad) according to the manufacturer's instructions. cDNA was diluted 1:20 with water and 4 µl of the dilution were employed for 20 µl reactions with iQ SYBR Green Supermix (Bio-Rad) in real-time PCR analysis. An initial denaturation step at 95 °C for 3 min preceded the cycling. Furthermore, the PCR program comprised 40 cycles with denaturation at 95 °C for 10 s, annealing at 55 °C for 30 s, and elongation 72 °C for 10 s. Subsequently a melting curve was performed. The iQ5 Multi-Color Real-Time pPCR Detection System (Bio-Rad) was used for monitoring the reactions. For the amplification of *STN7*, the primers *Stn7\_forward* (5'-CTGATTTGAGAGTGGGAATTA ACTAC) and *Stn7\_reverse* (5'-GGAAGATGAGGCCAATGCTATAG) were employed. *UBIQUITIN* and *CYTOCHROME B5* were amplified as internal controls, using *Ubiquitin\_forward* (5'-GGAAAAAGGTCTGACCGACA), *Ubiquitin reverse* (5'-CTGTTACACGGAACCCAATTC), *Cytochrome\_B5\_forward* (5'-CGACACTGCAAGGGACATGA) and *Cytochrome\_B5\_reverse* (5'-ACGTATGTCCTAGTTGCTGGAACA) as primer pairs. All reactions were performed in triplicate with at least two biological replicates.

### 2.4 Isolation of total protein

Total protein extracts were prepared from 6-week-old leaves according to Haldrup et al. (1999). About 0.1 g of leaf material was homogenized in 200 µl solubilization buffer (100 mM Tris pH 8.0, 50 mM EDTA pH 8.0, 0.25 M NaCl, 1 mM DTT, 0.7 % SDS) and heated to 65 °C for 10 min. Samples were centrifuged for 10 min at 10,000 g to remove insoluble debris and protein concentration in the supernatant was determined by the amido black assay as described by Schaffner and Weissmann (1973). The ubiquitous protein ACTIN was used as a loading control.

### 2.5 Isolation of thylakoid membranes

Thylakoids were isolated in a modified procedure based on Bassi et al. (1995). In brief, leaf material of *A. thaliana* plants was homogenized in ice cold isolation buffer (0.4 M sorbitol, 0.1 M Tricine-KOH pH 7.8, 0.5 % milk powder, 20 mM NaF), filtered through 2 layers of Miracloth (Calbiochem) and centrifuged at 1,500 g for 10 min at 4 °C. The membrane pellet was

resuspended in ice cold resuspension buffer (20 mM HEPES-KOH pH 7.5, 10 mM EDTA, 20 mM NaF) followed by a centrifugation step at 10,000 *g* for 10 min at 4 °C after 10 min of incubation on ice. Thylakoids were resuspended in TMK buffer (10 mM Tris-HCl pH 6.8, 10 mM MgCl<sub>2</sub>, 20 mM KCl, 20 mM NaF). The chlorophyll concentration was determined in aqueous 80 % acetone according to Porra (2002).

## 2.6 Antibodies and immunoblot analysis

If not state otherwise, antibodies raised against specific epitopes of STN7 and STN8 were used for western blot analysis in this study. The peptides CKKVKVGVRGAEFG of STN8 and LQELREKEPRKKANAQ, located at the C-terminus of STN7, served as antigens during the immunization process of the antibody production in rabbit (BioGenes GmbH, Berlin, Germany). Antibodies against the mature full-length of STN7 and STN8 were generated as described below (see 2.6.1). Immunoblot (Western blot) analyses with these antibodies as well as phosphothreonine-specific antibodies (Cell Signaling Technology, Inc., Boston, USA) and polyclonal antibodies raised against ACTIN (Dianova, Germany), GFP (Chromotek, Germany), LSU, PSAC, PSAB, PSBO, PSAE, LHCB2, LHCA3 (all Agrisera, Sweden) were performed as described (Ihnatowicz et al. 2008).

### 2.6.1 Generation of polyclonal STN7 and STN8 antibodies

The coding sequences of *STN7* and *STN8* without predicted cTP were cloned into the pProExHTa vector (Invitrogen) using the primers mSTN7\_ EcoRI \_ATG\_f (5'-AAAGAATTCATGGCTCAATTGATCGAT-3') and Stn7\_Sph1\_Stop\_r (5'-AAAGCATGCCC TAGAGCTCCTCTCTGGGGATC-3') or mStn8\_BamHI\_ATG\_f (5'-CCAGGATCCGATGAGATGCAGTTTTTCTCCG-3') and Stn8\_PstI\_stop\_r (5'-ATGCTGCAGTCACTTGCTGAAACTGAGCTTTG-3'), respectively, providing a N-terminal His-Tag for both kinases. These constructs were used to transform the *E.coli* strain BL21-CodonPlus® (DE3)-RIPL (Stratagene) in order to express large amounts of the recombinant proteins. Heterologous expression was induced with 1 mM IPTG and bacterial cells were harvested after 3 h incubation at 37 °C. Proteins were identified in the inclusion bodies fraction, which could be purified by an appropriate protocol described in 2.7. GuanidinHCL was used to denature purified inclusion bodies and His-tagged STN7 and STN8 protein was purified via Ni-NTA columns according to a batch purification protocol under denaturing conditions (Expressionist, Qiagen). The purified STN7 and STN8 proteins were loaded on SDS-PAGE, cut from the gel and sent to Prof. Dr. Roberto Barbato

(Alessandria, Italy) and Dr. Paolo Pesaresi (Milan, Italy), who kindly took over the injections and maintenance of rabbits to generate polyclonal antibodies.

## **2.7 Purification of inclusion bodies**

500 ml of *E. coli* cells expressing either recombinant STN7 or STN8 in inclusion bodies were harvested by centrifugation at 3,000 g for 20 min. The cell pellet was resuspended in 30 ml resuspension buffer (50 mM HEPES pH 7.5, 50 mM NaCl), cells were broken open using a French press and the insoluble fraction was again pelleted (50,000 g, 10 min). The inclusion bodies pellet was washed in subsequent steps with 200 ml detergent buffer 1 (20 mM Tris-HCl pH 7.5, 1 mM DTT, 0.5 % Triton X-100, 200 mM NaCl), 300 ml detergent buffer 2 (20 mM-Tris HCl pH 7.5, 1 mM DTT, 0.5 % Triton X-100) and 300 ml Tris buffer (50 mM Tris-HCl pH 8.0, 1 mM DTT). After each resuspension step including 5 min incubation in the respective buffer, the inclusion bodies were collected by centrifugation (50,000 g, 10 min). Finally the inclusion bodies were pelleted and snap frozen in liquid nitrogen to be stored at - 80 °C or directly used for further purification via Ni-NTA according to the batch purification protocol under denaturing conditions mentioned above (chapter 2.6.1).

## **2.8 Coomassie staining of PVDF membrane blots**

Proteins on PVDF membranes were stained for 2 min with 0.1 % Coomassie brilliant blue R-250 dissolved in 50 % methanol before or after immunoblot analysis. Blots were washed with 50 % methanol until background staining disappeared and protein bands became clearly visible. Complete destaining was achieved by washing several times with 100 % methanol.

## **2.9 PAGE analyses**

### **2.9.1 BN- and 2D-PAGE**

For Blue-native polyacrylamide gel electrophoresis (BN-PAGE), samples of freshly isolated thylakoids corresponding to 50 µg Chl were resuspended in solubilization buffer (750 mM  $\epsilon$ -aminocaproic acid, 50 mM Bis-Tris pH 7.0, 5 mM EDTA pH 7.0, 50 mM NaCl) and were solubilized for 60 min with 1.5 % (w/v) digitonin or for 10 min with n-dodecyl- $\beta$ -D-maltoside ( $\beta$ -DM) (Sigma) on ice (Pribil et al. 2010). Solubilized thylakoids were separated from the insoluble material by centrifuging at 13,100 g and 4 °C at either 70 min or 10 min, respectively. After supplementing with 5 % Coomassie brilliant blue G-250 in 750 mM  $\epsilon$ -aminocaproic acid, the solubilized material was fractionated by non-denaturing BN-PAGE (4-12 %) at 4 °C as outlined

in Heinemeyer et al. (2004). For the second dimension, a single lane of the BN gel was incubated in 2x Laemmli buffer with 100 mM DTT for 30 min and then placed on top of a SDS gel followed by electrophoresis (two-dimensional (2D) BN/SDS-PAGE) (Schottkowski et al. 2009a; Schottkowski et al. 2009b).

### **2.9.2 SDS-PAGE and non-reducing SDS-PAGE**

Standard 12 % SDS-PAGE was performed according to Laemmli (1970) if not indicated otherwise. To run a non-reducing SDS-PAGE, reducing agents (like DTT) were omitted in the loading dye and samples were not cooked if not stated otherwise.

### **2.9.3 Diagonal-PAGE**

For diagonal SDS-PAGE, thylakoid samples were divided into two aliquots, and either 200 mM diamide or 100 mM DTT was added for 30 min at room temperature. Afterwards thylakoids were collected by centrifugation (10,000 g; 10 min) and supplemented with Laemmli buffer without reducing agents. Protein amounts corresponding to 20 µg Chl were separated on non-reducing 12 % acrylamide gels as described (Laemmli 1970). For the second dimension of the diagonal-PAGE, these lanes were excised and incubated in Laemmli buffer in the presence of 100 mM DTT for 30 min at room temperature. Electrophoresis in the second dimension was performed on denaturing SDS-PA gels as described before (Pesaresi et al. 2001).

## **2.10 Thylakoid fractionation after state 1 and 2 adaptation**

Plants were acclimated to either state 1 or state 2 light (Pribil et al. 2010) and thylakoid fractionation was performed as previously described (Shapiguzov et al. 2010). Briefly, isolated thylakoids at a concentration of 0,6 mg of chlorophyll/mL were solubilized with 1 % digitonin for 5 min followed by stepwise centrifugation of supernatants. Pellets collected after centrifugation at 10,000 g, 40,000 g and 150,000 g represent fractions of enriched grana, margins and stroma lamellae, respectively. The protein samples were analysed by SDS-PAGE and Western blotting.

## **2.11 Sucrose gradient fractionation of thylakoid protein complexes**

To prepare sucrose gradients 11 ml of 0.4 M sucrose, 20 mM Tricine-NaOH (pH 7.5), 0.06 %  $\beta$ -DM were three times frozen and subsequently thawed at 4 °C. The gradient was underlayered with a cushion of 1 ml of 60 % (w/v) sucrose. Thylakoids, prepared from LL exposed plants were washed twice with 5 mM EDTA (pH 7.8) and diluted to a final chlorophyll concentration of 2 mg/mL. Solubilization with  $\beta$ -DM at a final concentration of 1 % was performed on ice for 10

min and followed by centrifugation (16,000 g, 5 min, 4 °C). The supernatant was loaded on sucrose gradients and centrifuged at 132,000 g for 21 h at 4 °C in a swing-out rotor (Beckman SW 40). Gradients were divided into 16 fractions, separated on a 15 % SDS-PAGE and analysed by Western blot.

## **2.12 Chloroplast isolation and fractionation into stroma and thylakoids**

Chloroplasts were isolated from *A. thaliana* leaves as described (Aronsson and Jarvis 2002). To obtain thylakoid and stroma fractions, chloroplasts were ruptured by adding 10 volumes of lysis buffer (20 mM HEPES-KOH pH 7.5, 10 mM EDTA) incubated on ice for 30 min. After centrifugation for 30 min at 42,000 g and 4 °C the collected supernatant and pellet represented the stroma and thylakoid fractions, respectively.

## **2.13 Salt washes of thylakoid membranes**

Salt washes of thylakoid membranes were basically performed according to Karnaukhov et al. (1997). To this end, freshly isolated thylakoids at a chlorophyll concentration of 0.5 mg/mL were incubated for 30 min on ice in HS buffer (0.1 M sucrose, 10 mM HEPES-NaOH pH 8.0) or HS buffer containing 2 mM NaCl, 2 M NaBr, 2 M NaSCN, 0.1 M Na<sub>2</sub>CO<sub>3</sub> or 0.1 M NaOH, respectively. After addition of two volumes of HS buffer the samples were centrifuged at 13,100 g for 15 min at 4 °C. Subsequently, proteins of the pellet fraction were directly solubilized in Laemmli buffer, whereas the supernatant was first precipitated in 80 % acetone.

## **2.14 Chlorophyll fluorescence analyses**

### **2.14.1 Measurement of light curves**

Steady-state photosynthetic parameters were measured under increasing light intensities of actinic red light (22, 37, 53, 95, 216, 513, 825, 1,287 and 1,952  $\mu\text{mol photons m}^{-2}\text{s}^{-1}$ ) with the Dual-PAM 100 system (Walz GmbH, Effeltrich, Germany) in the Dual PAM mode, according to the manufacturer's instructions and using standard settings. Plants were dark-adapted for 10 min prior to measurements and allowed to adapt for 5 min to the respective light intensities. Five plants of each genotype were analysed for each measurement.

### **2.14.2 Measurement of light induction**

Effects of varying light intensities on photosynthetic parameters during light induction were monitored using different levels of actinic light (22, 94 and 339  $\mu\text{mol photons m}^{-2}\text{s}^{-1}$ ). Plants were

dark-adapted for 10 min prior to measurements, and subsequently exposed for 5 or 6 min 40 s to actinic light and if indicated followed by 100 s of dark-relaxation as reported before (Munekage et al. 2002). Saturating light flashes ( $5,000 \mu\text{mol photons m}^{-2}\text{s}^{-1}$ ; 800 ms) were applied at 20-s intervals during the light-dark phases. Five plants of each genotype were analysed for each measurement, and three independent measurements were performed.

#### **2.14.3 State Transition measurements via PAM fluorometry**

State transitions were measured by pulse-amplitude modulation fluorometry (PAM) as described (Pribil et al. 2010; Ruban and Johnson 2009). The quenching of Chl fluorescence due to state transitions (qT) was calculated using the equation  $qT = (Fm1 - Fm2)/Fm2$  (Jensen et al. 2000).

#### **2.14.4 PSII inactivation induced by high light**

Photoinhibition of photosystem II (PSII) was induced over a period of 10 h by means of the Imaging PAM System (Heinz Walz GmbH) exposing leaves to blue light alternating every two minutes between HL ( $1,250 \mu\text{mol photons m}^{-2}\text{s}^{-1}$ ) and LL ( $10 \mu\text{mol photons m}^{-2}\text{s}^{-1}$ ). Maximal PSII quantum yield,  $Fv/Fm = (Fm - Fo)/Fm$ , was determined every 60 min after the LL phase and additional 5 min dark-adaptation.

#### **2.14.5 77 K fluorescence emission spectroscopy**

Leaves adapted to different light conditions were snap frozen in liquid nitrogen and grinded in buffer containing 50 mM HEPES-KOH pH 7.5, 100 mM sorbitol, 10 mM  $\text{MgCl}_2$ , and 20 mM NaF. Samples were filtrated through a nylon mesh, centrifuged 10 min at 3,000 g and resuspended to a final chlorophyll concentration of  $10 \mu\text{g/mL}$  (Tikkanen et al. 2006). Thylakoid suspensions were transferred to small glass tubes and frozen with liquid nitrogen. Pigments were excited at 475 nm and 77 K fluorescence emission spectra between 600 and 800 nm were recorded using a Spex Fluorolog mod.1 fluorometer (Spex Industries, Texas, USA). Spectra were normalized relative to the PSII peak around 685 nm. Of each genotype and light condition more than 5 independent measurements were conducted.

#### **2.14.6 Determination of the PQ redox state in the dark**

In order to determine the redox state of the PQ pool in dark-adapted plants, two OJIP transients were recorded for each leaf with the Dual-PAM 100 system (Walz GmbH, Effeltrich, Germany), basically as described (Toth et al. 2007). Briefly, after 3 h of dark adaptation plant

leaves were directly exposed for 300 ms to a saturating red-light flash of  $3000 \mu\text{mol photons m}^{-2}\text{s}^{-1}$ . The measured transient provides the fluorescence values for a fully reduced PQ pool,  $F_m$ , and for the current PQ redox state in dark-adapted plants,  $F_J$ , as a plateau after about 3 ms. In order to obtain the minimal  $F_J$  value of a completely oxidized PQ-pool ( $F_{J\text{-ox}}$ ), a second transient was recorded 5 min after the first one. This time a 10 s FR saturation pulse (intensity level 20) was applied until 10 ms before the measurement. The fraction of reduced PQ is equivalent to  $(F_J - F_{J\text{-ox}})/(F_m - F_{J\text{-ox}})$ .

### 2.15 Non-radioactive *in-vitro* phosphorylation assays

Thylakoids were isolated from plants pre-treated with far-red light, and resuspended in phosphorylation buffer (20 mM Tris-HCl pH 7.5; 5 mM  $\text{MgCl}_2$ ; 1 mM  $\text{MnCl}_2$  and 20 mM NaF) to a concentration of 0.4 mg/mL Chl. Subsequently 3-(3,4-dichlorophenyl)-1,1-dimethylurea (DCMU), 2,5-dibromo-6-methyl-3-isopropyl-1,4-benzoquinone (DBMIB), dithiothreitol (DTT), N-ethylmaleimide (NEM), tetramethyl-*p*-benzoquinone (duroquinone) or tetramethyl-*p*-hydroquinone (duroquinol) was added to the samples on ice. Prior to addition, DTT was dissolved in  $\text{H}_2\text{O}$ , DCMU, DBMIB and NEM in ethanol and duroquinone in an 1:1 mixture of ethanol-ethylene glycol. Duroquinol was prepared from duroquinone according to Izawa and Pan (1978). *In-vitro* phosphorylation was started by addition of 25  $\mu\text{M}$  ATP and the samples were transferred to LL ( $60 \mu\text{mol photons m}^{-2}\text{s}^{-1}$ ) or darkness for 30 min. Reactions were stopped by adding 120  $\mu\text{l}$  of reducing Laemmli buffer. Protein separation and immunodetection were performed as described above.

### 2.16 Radioactive *in-vitro* $^{33}\text{P}$ -phosphorylation

Thylakoids of dark-adapted wild-type and *oeSTN7* plants were isolated and resuspended in phosphorylation buffer (20 mM Tris-HCl 7.5, 5 mM  $\text{MgCl}_2$ , 1 mM  $\text{MnCl}_2$ , 25  $\mu\text{M}$  ATP and 10 mM NaF). *In-vitro* phosphorylation in thylakoids corresponding to 1  $\mu\text{g}$  chlorophyll per sample was determined in the presence of  $^{33}\text{P}$ -labeled ATP (10  $\mu\text{Ci}$ ) in the time-course of 30 min. The reaction was performed in the dark with or without 20 mM Na-dithionite and under  $20 \mu\text{mol m}^{-2}\text{s}^{-1}$  white light. Samples were taken at time points of 0 min (right after  $^{33}\text{P}$ -ATP was added), 5 min, 15 min and 30 min, supplemented with Laemmli-buffer, separated on SDS-PAGE and analysed with a phosphor-imager (Typhoon). Coomassie staining was performed to verify equal loading.

### 2.17 Pull-down of GFP-tagged proteins

GFP-tagged proteins were pulled down using the GFP-Trap<sup>®</sup>-A (Chromotek) according to manufacturer's instructions. Thylakoids were resuspended in dilution buffer (20 mM Tris-HCl pH 7.5; 150 mM NaCl; 0.5 mM EDTA) to a Chl concentration of 100 µg/µl, and solubilized for 10 min on ice in the presence of 1 % (w/v) β-DM. After centrifugation (13,100 g, 20 min, 4 °C) the supernatant was applied to 100 µl of equilibrated GFP-Trap<sup>®</sup> beads and topped up to 500 µl with dilution buffer. After 2 h of incubation at 4 °C, three washes with 500 µl dilution buffer (incl. 0.22 % [w/v] β-DM) each were performed, followed by the elution of proteins with 100 µl Laemmli buffer.

### 2.18 Redox titration of STN7 protein in thylakoid membranes

Thylakoid proteins were isolated and equilibrated on ice for 3 h with various [DTTred]/[DTTox] ratios of redox buffers (100 mM MOPS pH 7.0, 330 mM sorbitol). Reactions were solubilized with 2 % SDS and subsequently separated by non-reducing 15 % SDS-PAGE. After transfer of proteins to PVDF membrane, reduced and oxidized forms of STN7 were detected by immunoblot analysis.

### 2.19 TRX affinity purification

The affinity purification was basically performed as described by Motohashi et al. (2001). His-tagged recΔTRX-f (-m) was expressed in *E. coli* and purified by Ni-NTA resin according to the Qiagen protocol for native protein purification (Expressionist, Qiagen), without eluting resin-bound proteins. 1 mg Chl of isolated thylakoid membranes was solubilized with 1.5 % digitonin in 50 mM Tris-HCl pH 8.0 for 60 min. After centrifugation at 16,100 g for 70 min the supernatant was incubated with the TRX-coupled resin (~5 mg TRX/ml) for 60 min at RT. The column was washed three times with washing buffer (50 mM Tris-HCl pH 8.0, 200 mM NaCl, 0.2 % digitonin) and proteins trapped by thioredoxin were eluted by applying 10 mM DTT. Samples were analyzed by Western blot, using STN7 specific antibodies.

### 2.20 Mobility shift assay of TRX

For the TRX mobility shift assay, 10 µg thylakoids were solubilized with 0.2 % deoxycholic acid (DOC) incubated with 25 µg of recombinant TRX-f (recΔTRX-f) for 30 min in 100 mM MOPS pH 7.0 and 330 mM sorbitol at RT. Untreated thylakoids (in 0.2 % DOC buffer) served as

a control. Subsequently, protein mixtures were subjected to non-reducing SDS-PAGE and immunoblotting.

## **2.21 Protease treatments of thylakoids**

### **2.21.1 Trypsin digest**

Intact isolated thylakoids were resuspended in trypsin buffer (0.1 M sucrose, 10 mM HEPES pH 8.0). Prior to trypsination thylakoid membranes were either sonicated for 6 times 30 s on ice (Branson Sonifier B12, Danbury, USA) or left untreated. Trypsin was applied for 10 min on ice at a final concentration of 10 µg/mL. The reaction was stopped after 10 min on ice by adding trypsin inhibitors (Sigma, United states). Prior to separation on SDS-PAGE proteins were cooked for 2 min at 95 °C.

### **2.21.2 Thermolysin digest**

Intact isolated thylakoids were resuspended in thermolysin buffer (0.1 M sorbitol, 5 mM MgCl<sub>2</sub>, 10 mM NaCl, 20 mM KCl, 30 mM Tricine-KOH pH 8.0, 5 mM CaCl<sub>2</sub>). In order to rupture thylakoids an aliquot of thylakoid membranes was solubilized for 10 min with 1.5 % β-DM. Digestion with 0.1 mg/mL thermolysin was stopped after 30 min incubation on ice by adding 50 mM EDTA. Proteins were precipitated with acetone (7 times the sample volume) for 15 min at 20 °C and washed twice with ice-cold acetone. Prior to separation on SDS-PAGE proteins were cooked for 2 min at 95 °C.

### **2.21.3 Protein protection assay**

Intact thylakoids were prepared and resuspended in 0.1 M sorbitol, 5 mM MgCl<sub>2</sub>, 10 mM NaCl, 20 mM KCl, 30 mM Tricine-KOH (pH 8.0) and 5 mM CaCl<sub>2</sub>. Thylakoid membranes were either sonicated for 6 times 30 sec on ice (Branson Sonifier B12, Danbury, USA) or left untreated. Both thylakoid preparations (chlorophyll concentration 50 µg/ml) were incubated with 0.1 mg/mL thermolysin at room temperature. After 0, 1, 2, 5, 10, 15 and 20 min of incubation volumes corresponding to 5 µg of chlorophyll were withdrawn from the assay and proteolysis was stopped by adding 50 mM EDTA (pH 8.0). Membranes were precipitated with acetone (7 times the sample volume) for 15 min at -20 °C and washed two more times with ice-cold acetone. The protein samples were analyzed by SDS-PAGE and Western blotting (DalCorso et al. 2008).

## **2.22 TEM analysis of thylakoid membranes ultrastructure**

In order to observe effects of differential phosphorylation on thylakoid ultrastructure transmission electron microscopy was performed in cooperation with AG Wanner (LMU Munich). Plants were grown for 4 weeks in the climate chamber under a 12 h/12 h day/night regime. 1.5 h after the initiation of the light phase the sixth real rosette leaf was sliced and fixed for 1 h with 2.5 % glutaraldehyde (1,5-pentandial) in fixation buffer (75 mM cacodylic acid, 2 mM MgCl<sub>2</sub> pH 7.0). The material was washed with buffer, incubated for 2 h with 1 % osmium tetroxide in fixation buffer and again washed with fixation buffer and finally with distilled water. Samples were dehydrated by stepwise increase of acetone concentration, embedded in resin and cut with a microtome after complete polymerisation. Micrographs of the sections were taken with an EM-912 electron microscope (Zeiss) equipped with an integrated OMEGA energy filter operated in the zero-loss mode.

### 3 Results

#### 3.1 Generation of STN7 and STN8 overexpressor lines

Like described in chapter 2.1.1 *Arabidopsis* plants overexpressing STN7 and STN8 were generated by transformation of a construct containing the CDS of *STN7* or *STN8* under 35S promoter control into the *stn7-1* or *stn8-1* mutant background, respectively. One representative STN7 and STN8 overexpressor line was chosen for further studies and designated in the following as *oeSTN7* and *oeSTN8*. As determined by immunoblot analysis of thylakoid membranes the constitutive expression of *STN7* transcripts (**Figure 13 b**) in *oeSTN7* plants results in a 5-fold increase in STN7 protein levels relative to wild type (WT) (**Figure 5 a**). *oeSTN8* plants accumulated 16 times more STN8 protein as WT plants (**Figure 5 b**).

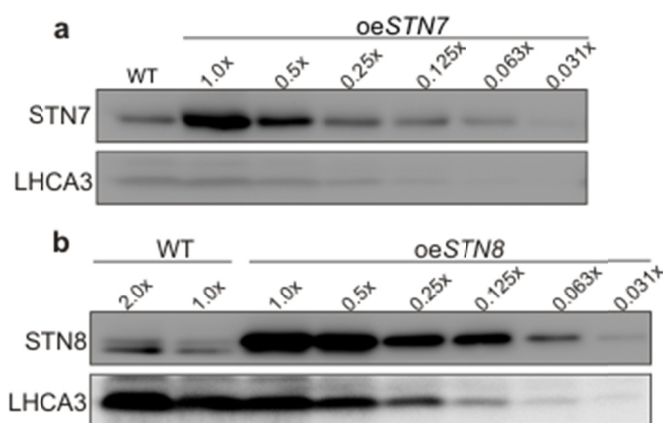


**Figure 5 Comparison of STN protein accumulation in WT and STN overexpressor plants.**

**a** Thylakoid proteins of WT and *oeSTN7* plants corresponding to 5  $\mu\text{g}$  Chl (1.0x), together with the indicated dilutions of the *oeSTN7* sample, were loaded to determine the level of STN7 protein accumulation in *oeSTN7* plants. Proteins were subjected to SDS-PAGE and Western blot analysis using STN7- and LHCA3-specific antibodies. **b** Thylakoid proteins of WT and *oeSTN8* plants, corresponding to 10  $\mu\text{g}$  (2x) and 5  $\mu\text{g}$  Chl (1.0x) and decreasing amounts of *oeSTN8* thylakoid proteins, were loaded to estimate the STN8 protein level in *oeSTN8* plants. Proteins were subjected to SDS-PAGE and Western blot analysis using STN8- and LHCA3-specific antibodies.

#### 3.2 Generation of polyclonal antibodies against STN7/STN8 epitopes and STN7/STN8 full-length proteins

In addition to the predominantly applied epitope antibodies in this study, antibodies against the full-length protein sequences of STN7 and STN8 were raised. For this purpose mature STN7 and STN8 was heterologously expressed in *E. coli*. After purification the protein preparations

were used to immunize rabbits. The obtained sera containing the polyclonal antibodies were tested by probing PVDF membranes loaded with separated thylakoid proteins of WT, *stn7-1*, *stn8-1*, *stn7 stn8*, *oeSTN7* and *oeSTN8* plants (**Figure 6**). Like the STN7/STN8 epitope antibodies (**Figure 6 a**) also the antibodies generated against the full-length protein sequences of STN7/STN8 recognized the kinases with only moderate unspecific signals (**Figure 6 b**). Unspecific binding of these antibodies occurred far less prominent when applied to samples of the respective overexpressor lines. Note, if not stated otherwise, epitope specific antibodies were used in this study.

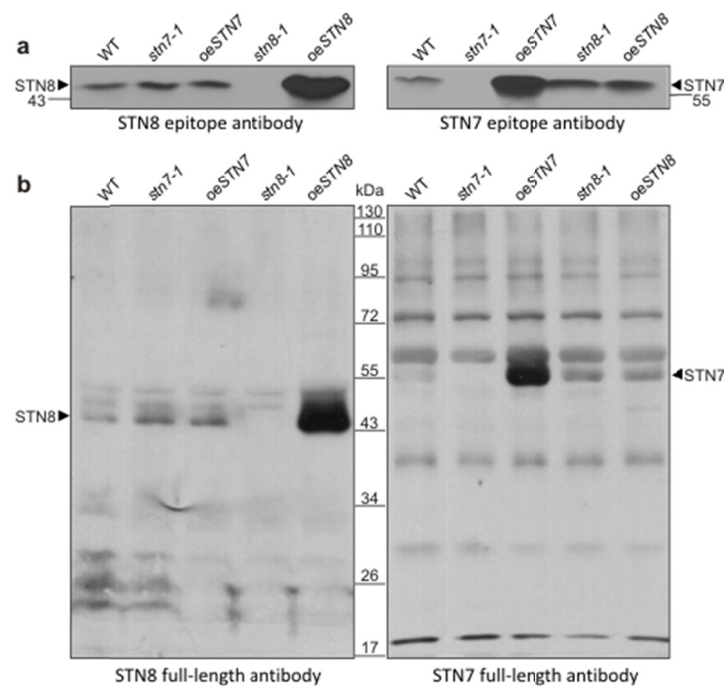


**Figure 6 Assessment of the specificity of polyclonal antibodies raised against full-length protein sequence of STN8 and STN7.**

Thylakoids of WT, *stn8-1*, *stn7-1*, *oeSTN8* and *oeSTN7* plants were isolated and membranes corresponding to 5  $\mu$ g of chlorophyll were analyzed by Western blot, applying either epitope-specific antibodies (dilution 1 : 500) (**a**) or sera (dilution 1 : 2,000) with antibodies against the full-length of mature STN8 (left) or STN7 (right), respectively (**b**). Molecular weight bands are indicated beside the blots. Specific signals are marked by *black arrowheads*.

### 3.3 Studies on the localization and topology of the STN kinases (STN7 and STN8)

#### 3.3.1 Both STN kinases are thylakoid integral membrane proteins

In previous studies STN7 and STN8 have already been localized to the thylakoid membrane by *in-vitro* import into pea chloroplasts (Bonardi et al. 2005). Since then, this localization of

STN8 was not confirmed by means of immunodetection. For this purpose, WT chloroplasts of *A. thaliana* were fractionated into stroma and membrane fractions and subjected to immunoblot analysis using antibodies specifically raised against a STN8 epitope (**Figure 7 a**). To validate the purity of the respective fractions, antibodies against the soluble large subunit of RuBisCo (LSU) and the thylakoid membrane-integral LHCB2 were used. STN8 was detected exclusively in the membrane fraction, which excludes the existence of a soluble form (**Figure 7 a**).

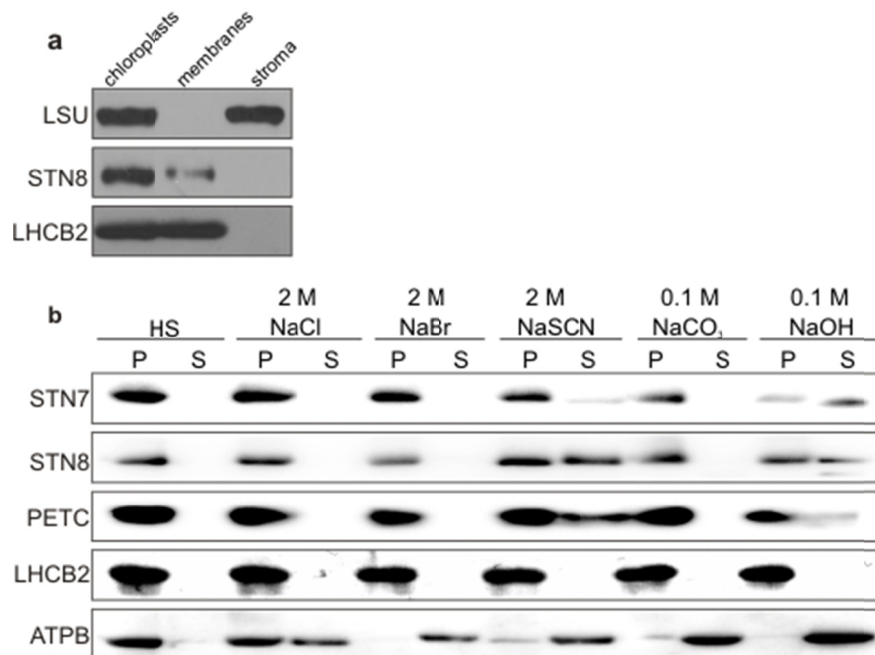


**Figure 7 Suborganellar localization of STN8 and membrane association.**

**a** Fractionation of chloroplasts. Chloroplasts were isolated from *A. thaliana* WT plants and subsequently divided into stroma and membrane fractions. Fractions were separated by SDS-PAGE, transferred to PVDF membrane, and STN8, LSU (stromal protein indicator) and LHCB2 (thylakoid protein indicator) were detected using specific antibodies. **b** Extraction of membrane-associated proteins with alkaline buffers or chaotropic salt solutions. Thylakoid membranes from WT plants were resuspended at 0.5 mg chlorophyll/ml in 10 mM HEPES-KOH, pH 7.5, containing either 2 M NaCl, 0.1 M Na<sub>2</sub>CO<sub>3</sub>, 2 M NaSCN, 0.1 M NaCO<sub>3</sub>, 0.1 M NaOH, or no additive. Samples were incubated for 30 min on ice and divided by centrifugation into supernatant containing extracted proteins (S) and membrane fraction (P). Proteins were separated by SDS-PAGE, transferred to PVDF membrane and immunolabeled with antibodies that were raised against STN7, STN8, ATPB (representative of a peripheral membrane protein), PETC (representative of a membrane protein with a single hydrophobic domain predominantly anchored by electrostatic interactions), or LHCB2 (representative of an integral membrane protein with three transmembrane helices).

To clarify whether the predicted transmembrane domains (TMDs) of the STN kinases (Vainonen et al. 2005) truly represent TMDs or the kinases are just extrinsically attached to the thylakoid membrane, WT thylakoids were washed with alkaline buffers or chaotropic agents. In this assay both kinases, STN7 and STN8, showed an extraction behavior similar to PETC (**Figure 7 b**), which contains a single hydrophobic domain and associates to the membrane predominantly via electrostatic interactions (Karnauchov et al. 1997). This result indicates that the STN kinases constitute integral membrane proteins as suggested before (Lemeille et al. 2009; Vainonen et al. 2005).

### **3.3.2 The STN kinases form part of high molecular supercomplexes**

To define the localization of the kinases more precisely, WT thylakoids were solubilized with  $\beta$ -DM, separated on BN-PAGE and subsequently resolved in a second dimension via SDS-PAGE. Both STN7 and STN8 specific antibodies gave signals across the entire molecular weight range, from high molecular supercomplexes down to the free protein fraction (**Figure 8 a**). This suggests that the STN kinases associate rather stably with various protein complexes of varying molecular weight.

In a further approach thylakoid proteins were separated by ultracentrifugation on a linear sucrose gradient after  $\beta$ -DM solubilization. Gradient fractions were collected and subjected to immunoblot analysis. Again, STN7 and STN8 were both identified in the fractions of high molecular weight complexes (**Figure 8 b**). These results are in line with Lemeille et al. (2009), who showed that STT7 associates with a large molecular weight complex, indicating that none of the kinases occurs as a monomeric polypeptide but rather in association with other proteins.

### **3.3.3 STN8 and STN7 are located in different subfractions of the thylakoid membrane**

Fractionations of thylakoids isolated after PSI-specific light (PSI light) or PSII-specific light (PSII light) exposure by slight digitonin solubilization and differential centrifugation revealed an enrichment of STN8 in the fraction containing grana lamellae, whereas STN7 was mainly present in the stroma lamellae fraction (**Figure 8 c**). The observed distribution pattern under state 1 and state 2 conditions was basically unaltered for both kinases (**Figure 8 c**). These data indicate that the main fraction of STN8 kinase resides close to its substrate, the subunits of photosystem II in the grana stacks. For a large proportion of STN7 the localization coincided with TAP38/PPH1 in the stroma lamellae like shown by Shapiguzov et al. in (2010).

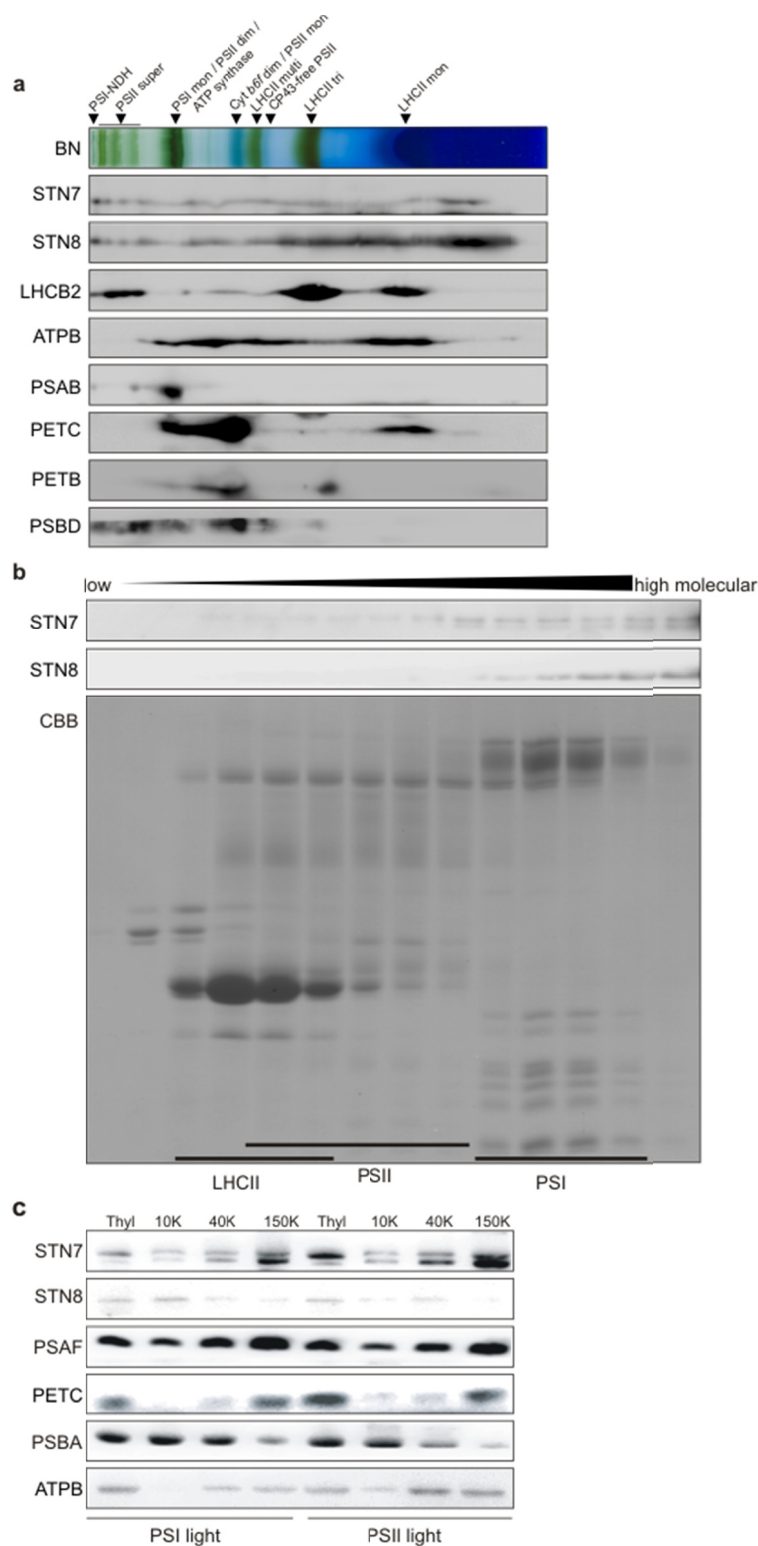


**Figure 8 Localization of STN kinases within the thylakoid membrane.**

**a** 2D BN/SDS-PAGE analysis of STN7 and STN8. Thylakoid membranes of WT equivalent to 50  $\mu\text{g}$  of chlorophyll were solubilized with  $\beta$ -DM, subjected to 2D BN/SDS-PAGE and blotted onto a PVDF membrane. The proteins

ATPB, LHCB2, PSAB, PETC, PETB and PSBD were detected by specific antibodies. *Black arrowheads* above indicate the PSI-NDH supercomplex (PSI-NDH), PSII supercomplexes (PSII super), PSI monomer (PSI mon), PSII dimer (PSII dim), ATP synthase, Cyt *b6f* dimer (Cyt *b6f* dim), PSII monomer (PSII mon), LHCII multimer (LHCII multi), CP43-free PSII monomer (CP43-free PSII), LHCII trimer (LHCII tri), LHCII monomer (LHCII mon) **b** Analysis of STN7 and STN8 by sucrose gradient centrifugation. WT thylakoids at a concentration of 2 mg chlorophyll/mL were solubilized with 1 % (w/v)  $\beta$ -DM and separated by centrifugation in a linear sucrose gradient. Fractions were collected, loaded according to an ascending density of the fractions, separated by SDS-PAGE, blotted onto PVDF membranes and specific antibodies for STN7 and STN8 were applied. As loading control a Coomassie stain was performed (CBB). **c** Analysis of STN7 and STN8 by thylakoid membrane sub-fractionation. WT plants were adapted to PSII- or PSI-specific light. Isolated thylakoids (Thyl; 0.6 mg of chlorophyll/mL) were treated with 1 % digitonin for 5 min. By differential centrifugation of the supernatant, fractions enriched in grana lamellae (10K), margins (40K) and stroma lamellae (150K) were collected. Proteins were separated by SDS-PAGE and analyzed by immunoblots with antibodies against STN7, STN8, PSAF, PETC, PSBA and ATPB.

Since state transition processes were described to take place mainly at the transition section between grana and stroma lamellae, the so called grana margins, the observed predominant stroma localization of STN7 is not contradictory to its potential site of operation. The different migration forms of STN7 in the gel could represent different redox or degradation states of the kinase (**Figure 8 c**).

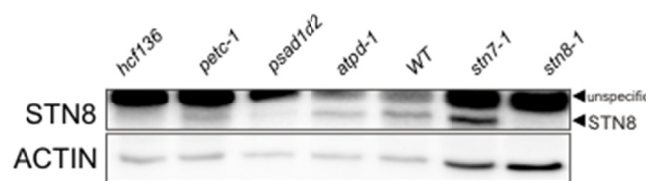


**Figure 9 STN8 accumulation in mutants deficient in one of the major photosynthetic complexes.**

Total proteins were extracted from WT, *stn7-1*, *stn8-1* and from mutant plants devoid of PSII (*hcf136*), functional Cyt *b6f* (*petc-1*), PSI (*psad1-1 psad2-1 = psad1d2*) and ATP synthase (*atpd-1*). STN8 levels were analyzed by Western blot applying antibodies raised against STN8 and ACTIN (as loading control). STN8 specific signals are marked by *black arrowheads*.

### 3.3.4 STN8 kinase is mainly attached to photosystem II.

The abundance of STN8 was analyzed in mutant plants defective in one of the major complexes of the photosynthetic machinery, like PSII (*hcf136*; Meurer et al. 1998), Cyt *b6f* (*petc-1*; Maiwald et al. 2003), PSI (*psad1-1 psad2-1 = psad1d2*; Ihnatowicz et al. 2004) or ATP synthase (*atpd-1*; Maiwald et al. 2003) (**Figure 9**). A lack of PSII prevented STN8 detection which is in accordance to its co-localization with PSII in the grana lamellae. Thus, the presence of the STN8 substrate

seems to be a prerequisite for STN8 accumulation in the thylakoid membrane potentially due to a scaffold function of PSII for STN8 (**Figure 9**). Moreover, a strong decrease in STN8 levels was also observed in *psad1-1 psad2-1* plants.

### 3.3.5 Protease treatments of thylakoid membranes suggest an association of STN7 with other proteins

For the single transmembrane helix protein STN7, the N-terminus comprising a potential redox-sensitive cysteine motive was reported to be located in the lumen, while its C-terminus containing the ATP-binding domain is directed to the stromal side (Lemeille et al. 2009). To unravel the orientation of STN7 in the thylakoid membrane of *A. thaliana* a protease protection assay was performed. To this end, isolated WT thylakoids were either left untreated or sonicated to partially destroy the membrane integrity and generate about 50 % inside-out vesicles. Subsequently, a thermolysin treatment time-course was performed and protein digestion patterns of STN7, PSBO and PSAE were monitored by Western blot analysis (**Figure 10 a**). PSAE served as a representative of stromal exposed proteins. While rapidly digested in intact thylakoids, extrinsic stroma proteins are partially protected from thermolysin after sonication due to inside-out vesicle formation (DalCorso et al. 2008). In contrast, luminal thylakoid proteins, like PSBO, are more rapidly degraded by proteases after sonication. According to these expectations the tryptic digest patterns of the very C-terminal domain of STN7, specifically recognized by the STN7 antibody, behaved rather contradictory (**Figure 10 a**). In intact thylakoid membranes STN7 seemed to be protected from quantitative degradation. More precisely, the major part of STN7 (except for ~ 5 kDa), including the antibody- and ATP-binding site, was retained despite 165 predicted thermolysin cleavage sites. However, sonication led to a higher susceptibility of STN7 (respectively its antibody binding site) to proteolytic degradation (**Figure 10 a**).

Proteolytic assays were further performed on thylakoids of WT, *stn7-1* and lines expressing STN7 fused C-terminal to GFP in the *stn7-1* mutant background. STN7-GFP showed the same thermolysin-dependent degradation pattern as native STN7 (**Figure 10 b**). These results support the idea that STN7 is degraded starting from its very C-terminus. Preceding solubilization of thylakoids with 2 %  $\beta$ -DM facilitates digestion of the whole protein (**Figure 10 b**).

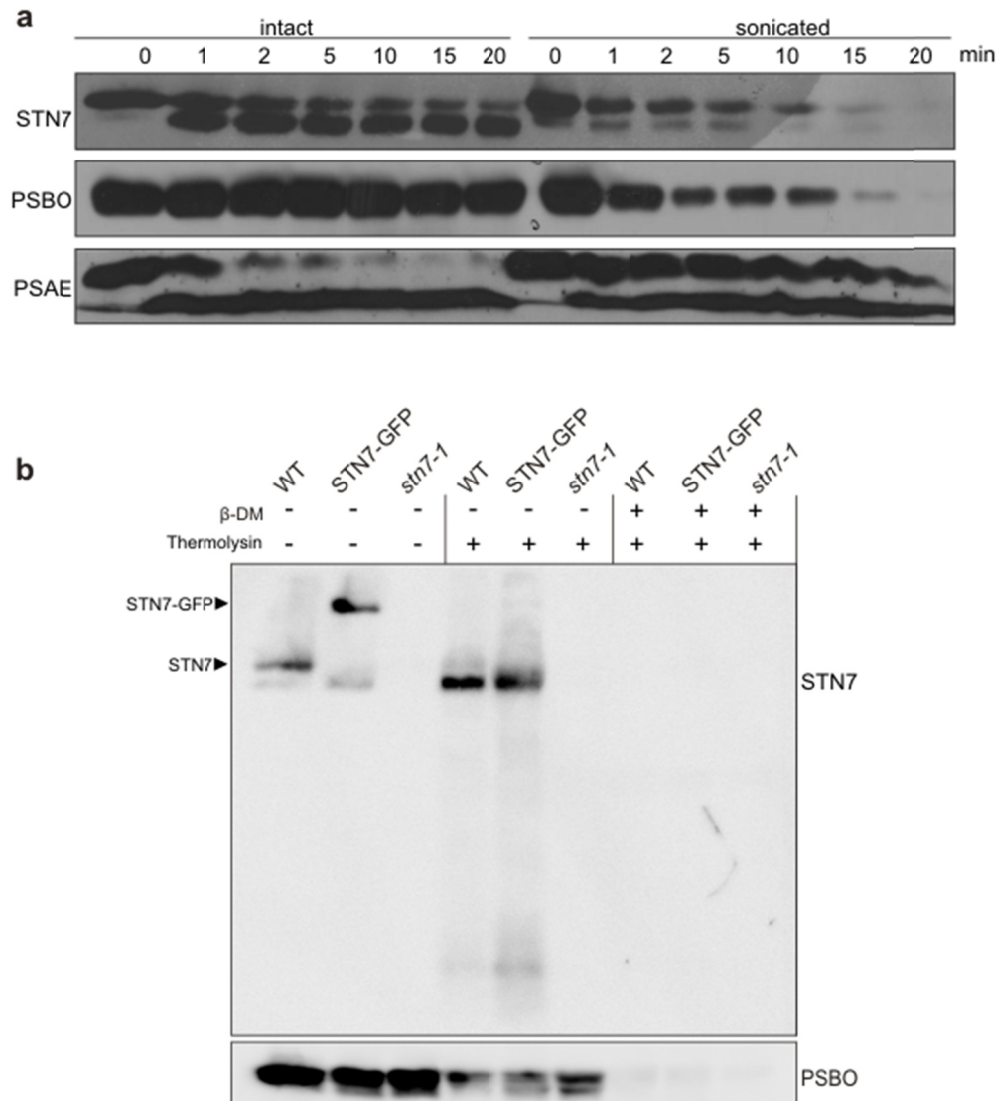


**Figure 10 Thermolysin digest of intact and sonicated/solubilized thylakoid membranes.**

**a** Protease protection assay. Intact (left) and sonicated (right) thylakoid membranes were treated with thermolysin (final concentration 0.1 mg/mL). The proteolytic degradation was stopped after the indicated time points by addition of 50 mM EDTA. Samples were analyzed by Western blot using antibodies specifically raised against STN7, PSAE and PSBO. Sonication of thylakoid membranes produced about 50 % inside-out vesicles. **b** Thylakoids of WT, STN7-GFP (in *stn7-1* background) and *stn7-1* were isolated and either treated with 1.5 %  $\beta$ -DM or left intact. After proteolytic digest with 0.1 mg/mL thermolysin for 30 min the reaction was stopped by addition of 50 mM EDTA and samples were analyzed by Western blot applying antibodies specific for STN7 and PSBO.

This could be interpreted by the main part of STN7 being imbedded in a sonication- and detergent-sensitive complex, whose components shield STN7 against digestion by thermolysin, whereas a short C-terminal part of STN7 remains unprotected and is rapidly degraded (<1 min)

(**Figure 10 a**). A loss of the protective complex subunits led to a faster proteolytic digest of at least the epitope containing part of STN7.

### **3.3.6 Trypsination patterns of STN8 allow to estimate its topology and propose a potential association with other proteins**

Similar to STN7, the STN8 kinase contains a predicted single transmembrane domain close to its N-terminus (Vainonen et al. 2005). To elucidate the topology of STN8, thylakoids of *oeSTN8* plants were treated with trypsin and analyzed by Western blot using STN8-specific antibodies recognizing either a specific epitope or the full-length protein (**Figure 11**). After tryptic digest of intact thylakoids a stable STN8 fragment of ~ 34 kDa was detected with both STN8-specific antibodies, while the signal of the mature STN8 protein (49.9 kDa) disappeared. This STN8 fragment, as well as an additional fragment of ~16.5 kDa, seemed to be firmly associated with the thylakoid membrane, suggesting that both fragments contain the predicted transmembrane helix (**Figure 11**). The antibody raised against the mature STN8 protein allowed for the detection of additional small fragments below 16.5 kDa, which most likely represent N-terminal fragments excluding the epitope region of the peptide-specific antibody. This allows the assumption that tryptic degradation occurs predominantly at the very C-terminus of STN8. Thus, the very C-terminal part of STN8 of about 15 kDa seems to be most sensitive to tryptic cleavage, while the remaining sequence appears to be protected from degradation. Similar to STN7 this could be explained by STN8 being shielded by putative interaction partners against proteolytic degradation (see **Figure 10**). Sonication of the thylakoid membranes prior to trypsin treatment partially protected the mature STN8 protein from degradation by the formation of inside-out vesicles (**Figure 11**). These data support the favored model of a stroma exposed C-terminus containing the ATP-binding domain. At the same time the relatively stable 34 kDa fragment was more prone to degradation after sonication, possibly due to the disruption of a potential protein complex protecting STN8 from being digested.

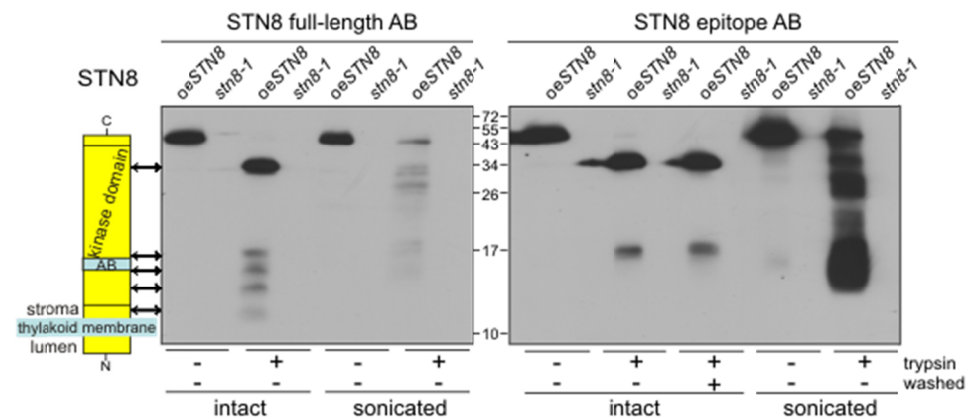


**Figure 11 Analysis of STN8 topology by protease treatment.**

Isolated intact thylakoids of *oeSTN8* and *stn8-1* plants were sonicated or left untreated. Subsequently membranes were treated with trypsin (conc. 10  $\mu\text{g}/\text{mL}$ ) for 10 min and washed twice with 0.1 M sucrose, 50 mM HEPES pH 7.6 where indicated. Samples were separated on SDS-PAGE and immunodecorated with STN8 full-length (left panel) or epitope (right panel) -specific antibodies after transfer to PVDF membrane. On the very left a simplified topology model of STN8 is depicted, showing the recognition site of the epitope antibody and the main trypsin cleavage sites. Note that the mature STN8 size is  $\sim 49.9$  kDa. The sequence comprising the N-terminus, the TM domain and the AB binding site counts 16.5 kDa. AB, antibody.

### 3.4 Analyses on the regulation of the chloroplast protein kinase STN7

#### 3.4.1 STN7 accumulation is regulated at both protein and transcript levels

To investigate the light-dependence of STN7 accumulation, WT plants were exposed to different light conditions known to oxidize (D or FR) or reduce (LL) the plastoquinone (PQ) pool. After transfer from D to LL, the level of the STN7 protein clearly increased, while subsequent exposure to FR caused a decrease in STN7 accumulation (**Figure 12 a**). To clarify whether the post-translational down-regulation observed for STN7 protein levels after high light (HL) exposure (Lemeille et al. 2009) also applies to STN7, a HL time-course experiment was performed (**Figure 12 b**). To this end, WT plants were exposed to LL for 3 h, and then to HL (800  $\mu\text{mol photons m}^{-2}\text{s}^{-1}$ ) for up to 240 min. With increasing duration of HL, a progressive decrease in levels of STN7 was observed (**Figure 12 b**). Further evidence for the regulation of STN7 at the post-translational level comes from an analysis of the kinetics of the response to HL, performed with STN7 overexpressor lines (*oeSTN7*). The constitutive expression of *STN7* transcripts at levels that are 16-fold higher than those seen in the WT results in a 5-fold increase in STN7 protein levels relative to WT (**Figure 5 a, 13 a, b**).

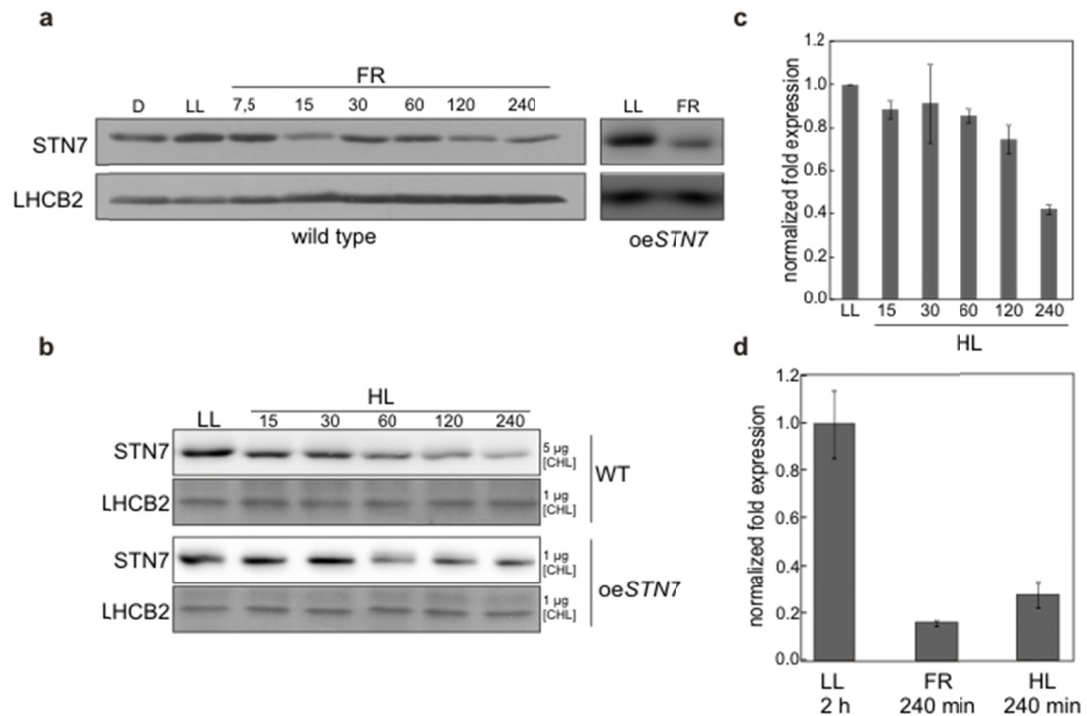


**Figure 12 STN7 protein and transcript accumulation under different light conditions.**

**a** *Left side*: time-course of changes in STN7 protein levels upon transfer from dark (D) to low light (LL;  $80 \mu\text{mol photons m}^{-2}\text{s}^{-1}$ ) and then to far-red light (FR). WT plants were dark-adapted for 18 h, transferred to LL for 2 h and then to FR for 4 h. *Right side*: reduction of STN7 levels in *oeSTN7* plants upon 120 min of FR treatment. Leaf samples were collected at different times and thylakoids were isolated. Thylakoid proteins were fractionated by SDS-PAGE and transferred to PVDF membrane. The filters were then probed with antibodies raised against STN7 and LHCb2 (as loading control). **b** Time-course of changes in STN7 protein levels in WT and STN7 overexpressor (*oeSTN7*) plants upon transfer from low light (LL;  $80 \mu\text{mol photons m}^{-2}\text{s}^{-1}$ ) to high light (HL;  $800 \mu\text{mol photons m}^{-2}\text{s}^{-1}$ ). Plants were exposed to 2 h of LL and then transferred to HL for up to 240 min. The indicated amounts of thylakoid proteins were analyzed applying antibodies specific for STN7 and LHCb2, as described in panel **a**. **c** The relative amount of *STN7* mRNA in WT leaves exposed to the same conditions as in panel **a** was determined by real-time PCR. After isolation of mRNA from leaves, cDNA was synthesized by reverse-transcription, and *STN7* transcript levels were quantified by real-time PCR using primers specific for *STN7*, as well as primers for *UBIQUITIN* and *CYTOCHROME B5* as internal controls. **d** Quantification by real-time PCR of *STN7* transcript levels in WT leaves exposed to LL ( $80 \mu\text{mol photons m}^{-2}\text{s}^{-1}$ ), HL ( $800 \mu\text{mol photons m}^{-2}\text{s}^{-1}$ ) or FR. Real-time PCR was performed as in panel **c**.

Upon exposure of the *oeSTN7* lines to HL, amounts of STN7 protein also declined substantially but remained significantly higher than the levels seen in WT plants at the end of the

experiment (**Figure 12 b**). Moreover, the level of STN7 in *oeSTN7* plants also fell after a shift from LL to FR (**Figure 12 a**).

To study whether the control of STN7 abundance might also involve changes in the accumulation of the corresponding transcripts, the level of *STN7* mRNA was studied in WT plants during the same HL time-course as in **Figure 12 b**. Strikingly, a continuous decrease in *STN7* transcripts was observed during HL treatment, which correlated well with the decrease in STN7 protein amounts noted above (**Figure 12 c**). Analogous observations were made under FR conditions (**Figure 12 d**). In order to extend this analysis, lines that express less *STN7* than WT (*leSTN7* for low expression of *STN7*) were generated and analysed. And indeed, the comparison of *leSTN7*, WT and *oeSTN7* plants after exposure to LL showed a clear correlation between *STN7* transcript abundance (**Figure 13 b**) and amounts of STN7 protein (**Figure 13 a**). Conversely, lines expressing an inactive cysteine-exchange version of STN7 (*STN7<sub>C→S:70</sub>*) under control of the 35S promoter accumulated less STN7 protein than WT, although levels of *STN7* mRNA were higher than in WT (**Figure 13 a, b**).

Taken together, these data indicate that STN7 levels are regulated not only at the post-translational level as described before (Lemeille et al. 2009; Willig et al. 2011), but also at the mRNA level.

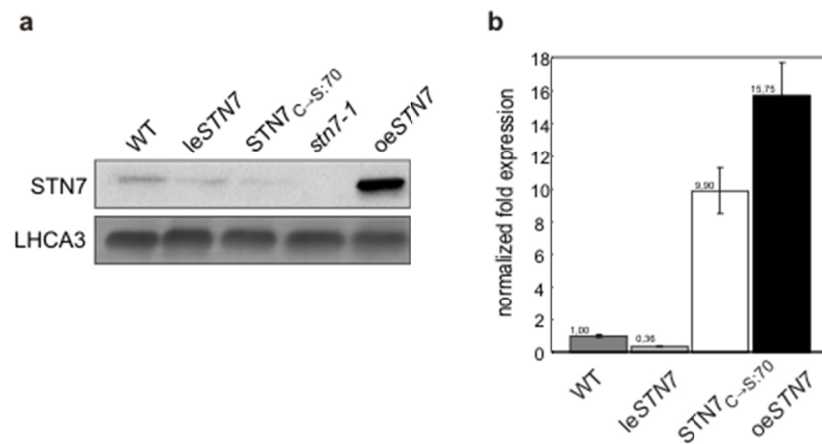


**Figure 13 STN7 protein and transcript accumulation in different transgenic backgrounds.**

**a** Comparison of STN7 amounts in leaves of WT, *leSTN7*, *STN7<sub>C→S:70</sub>* *stn7-1* (*STN7<sub>C→S:70</sub>*), *stn7-1* and *oeSTN7* plants under standard lighting conditions. Thylakoids were fractionated by SDS-PAGE and subjected to Western analysis using STN7- and LHCA3-specific antibodies. **b** Quantification by real-time PCR of *STN7* transcript levels in leaves from the plants analyzed in panel **a**. mRNA isolation, cDNA synthesis and real-time PCR were performed as in **Figure 12 c**.

### 3.4.2 Accumulation of STN7 is redox-dependent

Given that different light qualities cause changes in the redox state of the PQ pool (Wagner et al. 2008), the impact of changes in the PQ redox state on STN7 protein accumulation was investigated. Two approaches were followed: (i) transient induction of altered PQ redox states by illumination with light of different wavelengths, and (ii) analysis of genotypes with altered photosynthesis. When plants were exposed to long-term changes in light quality, the STN7 protein level in WT plants adapted to light that specifically excited PSII light was clearly higher than that in plants adapted to PSI light (**Figure 14**). This is in line with previous results (Wagner et al. 2008) showing that both the reduced fraction of the PQ pool and the degree of phosphorylation of LHCII were increased in PSII light-adapted plants relative to plants acclimated to PSI light.

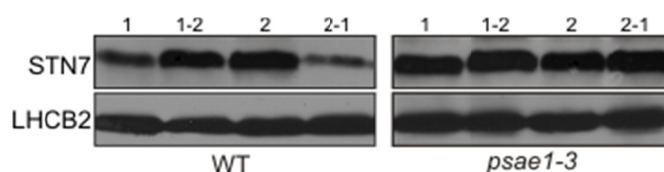


**Figure 14** Effects of long-term acclimation to different light qualities on STN7 protein levels in leaves.

WT and *psae1-3* mutant plants were grown for three weeks under controlled climate-chamber conditions and then transferred to PSI light and/or PSII light. 1, six days PSI light; 1-2, four days PSI light/ two days PSII light; 2, six days PSII light; 2-1, four days PSII light/ two days PSI light. Leaf samples were collected after each treatment and thylakoids were isolated. Thylakoid proteins were fractionated by SDS-PAGE, and analyzed with antibodies specific for STN7 and LHCB2 (loading control).

Next it was tested whether constitutive alterations in the PQ redox state induced by photosynthetic mutations have similar effects. Indeed, in the mutants *psae1-3*, *psad1-1* and *psal-1*, in which the PQ pool is constitutively over-reduced (Ihnatowicz et al. 2008; Ihnatowicz et al. 2004; Lunde et al. 2000), STN7 levels were increased compared to WT (**Figure 15 a**). As an example of a line with a more highly oxidized PQ pool under moderate light conditions, we chose the *tap38-1* mutant, which is defective in the recently identified protein phosphatase TAP38/PPH1 (Pribil et al. 2010; Shapiguzov et al. 2010). TAP38 is responsible for the dephosphorylation of pLHCII and counteracts the action of the STN7 kinase. Under standard lighting conditions (see Materials and Methods 2.2), STN7 protein levels were clearly reduced in *tap38-1* mutant plants, whereas in TAP38-overexpressing lines (*oeTAP38*), whose PQ pools are only slightly more

reduced than those of WT plants, amounts of STN7 were similar to WT (**Figure 15 b upper panel**).

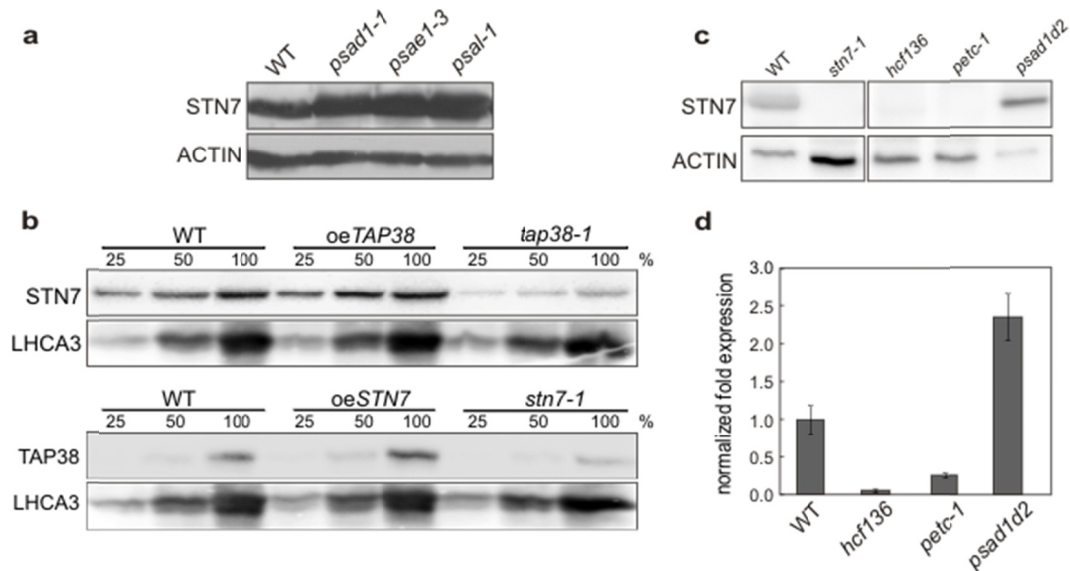


**Figure 15 STN7 protein and transcript accumulation in different genetic backgrounds.**

**a** Accumulation of STN7 protein in mutant plants (*psad1-1*, *psae1-3* and *psal-1*) in which the PQ pool is reduced to a greater degree than in WT. Immunoblot analysis of total protein extracts (30  $\mu\text{g}$  per lane) was performed after fractionation by SDS-PAGE. Antibodies specific for STN7 or ACTIN (as loading control) were used. **b Upper panel:** Accumulation of the STN7 protein in thylakoids of WT, TAP38 overexpressor (*oeTAP38*) and *tap38-1* mutant plants. Thylakoids were isolated from LL-adapted plants and amounts of thylakoid proteins corresponding to 8  $\mu\text{g}$  (100 %), 4  $\mu\text{g}$  (50 %) and 2  $\mu\text{g}$  (25 %) of Chl were loaded for Western blot analysis. STN7 and LHCA3 (as loading control) were detected with specific antibodies. **Lower panel:** Accumulation of the TAP38 protein in thylakoids of WT, *oeSTN7* and *stn7-1* mutant plants analyzed as in the upper panel using antibodies specific for TAP38. **c** STN7 protein accumulation in mutants that lack specific photosynthetic complexes. WT and mutants devoid of PSII (*hcf136*), functional Cyt *b6f* (*petc-1*) or PSI (*psad1-1 psad2-1 = psad1d2*) were grown under 30  $\mu\text{mol photons m}^{-2}\text{s}^{-1}$ . For immunoblot analysis of thylakoid proteins (corresponding to 30  $\mu\text{g}$  of total protein) of WT and mutant plants, grown under a flux of 30  $\mu\text{mol photons m}^{-2}\text{s}^{-1}$ , STN7 and ACTIN (as loading control) were detected with specific antibodies as described in panel **a**. **d** Relative amounts of STN7 mRNA in *hcf136*, *petc-1* and *psad1d2*, as determined by real-time PCR as in **Figure 12 c**.

Taken together, by employing different T- DNA mutant lines we could independently confirm that the level of the STN7 protein, as well as the extent of LHCII phosphorylation depends on the redox state of the PQ pool (reviewed in: Rochaix 2007) and that amounts of STN7

are regulated at the post-translational level in a manner that is dependent on light quality (Willig et al. 2011).

It should be noted, that the protein level of TAP38 in *stn7-1* was as well significantly reduced, while *oeSTN7* showed at the most a slight upregulation of TAP38 (**Figure 15 b lower panel**). These observations allow to consider also a direct mutual influence of the counterplayers STN7 and TAP38 on protein level. As well changes in the protein phosphorylation state in *tap38-1* might account for the observed differences in STN7 protein levels in addition to the changes of the PQ redox state.

### **3.4.3 PSII and a functional cytochrome *b6f* complex are required for accumulation of STN7**

In the *stn7-1* mutant the stability of the major thylakoid multiprotein complexes was not noticeably affected (Bonardi et al. 2005). To test the converse - whether STN7 accumulation depends on the presence of any of the major thylakoid protein complexes - immunoblot analyses were performed on total leaf proteins from photosynthetic mutants lacking either PSII (*hcf136*) or PSI (*psad1-1 psad2-1*) or devoid of a functional Cyt *b6f* (*petc-1*). While *psad1-1 psad2-1* plants accumulated more STN7 than WT, only minuscule amounts of STN7 were detected in the *hcf136* and *petc-1* mutants (**Figure 15 c**). Because this depletion at the protein level could result either from destabilization and increased degradation of the STN7 protein or from down-regulation of the expression of the *STN7* gene, levels of *STN7* mRNA were quantified by real-time RT-PCR. A strong reduction in *STN7* transcript accumulation was detected in both *hcf136* and *petc-1* plants (**Figure 15 d**), indicating that, in the absence of either PSII or a functional Cyt *b6f*, a signal is sent to the nucleus that down-regulates expression of the *STN7* gene. This, for the first time identified correlation of decrease in *STN7* transcript and STN7 protein levels in *hcf136* and *petc-1* plants, together with the observation that *STN7* transcript and STN7 protein levels increase in *psad1-1 psad2-1* lines (**Figure 15 c, d**) and decrease during exposure to HL (**Figure 12 b, c**), strongly suggests for the first time that the expression of STN7 might be additionally regulated at the level of transcript abundance.

### **3.4.4 Elevated STN7 levels enhance LHCII phosphorylation and PSI-LHCI-pLHCII complex formation under certain light conditions**

To compare the STN7 activities of WT, *stn7-1*, *tap38-1* and *oeSTN7* lines, plants were kept in darkness for 18 h, then exposed for 2 h to LL, followed by either 60 min of HL (800  $\mu\text{mol}$

photons  $\text{m}^{-2}\text{s}^{-1}$ ) or 20 min of FR treatment. Subsequently, thylakoid preparations were fractionated by SDS-PAGE and the phosphorylation pattern of thylakoid proteins was analyzed by immunolabeling with phosphothreonine-specific antibodies. Phosphorylated LHCII (pLHCII) was detected in LL-adapted WT and *oeSTN7* plants, as well as in D- and HL-adapted *oeSTN7* plants (**Figure 16 a**). The persistently higher STN7 levels seen in *oeSTN7* plants during the HL time-course experiment (see **Figure 12 b**) were accompanied by greater residual LHCII phosphorylation relative to WT plants (**Figure 17 a**). However, by exposure to very intense light (VHL;  $1800 \mu\text{mol m}^{-2}\text{s}^{-1}$ ), LHCII phosphorylation could be almost completely suppressed even in *oeSTN7* plants (**Figure 17 b**). In *tap38-1*, which served as control, LHCII phosphorylation was detected under all light conditions as described before (Pribil et al. 2010).

To exclude that the strongly enhanced LHCII phosphorylation of *oeSTN7* plants in the dark compared to LL is solely due to increased STN7 protein levels, thylakoids of WT and *oeSTN7* were treated with FR and then exposed to LL or D for 30 min. The protein levels in *oeSTN7* were not elevated in the dark compared to LL (**Figure 18**). Moreover, the STN7 protein levels in both WT and *oeSTN7* lines increased immediately upon transfer from FR to LL and D.

To assess the effect of enhanced LHCII phosphorylation on the extent of formation of the PSI-LHCI-pLHCII supercomplex (Pesaresi et al. 2009; Pribil et al. 2010), thylakoid samples were solubilized with digitonin, and then analysed by BN-PAGE. The PSI-LHCI-pLHCII supercomplex was detectable in *tap38-1* mutant plants under all conditions as described (Pribil et al. 2010) - in LL-adapted WT and *oeSTN7* plants, and also in D- and HL-adapted *oeSTN7* plants (**Figure 16 b**). This indicates that, in *oeSTN7* plants, LHCII phosphorylation persists in the dark, and to a somewhat reduced extent also under HL conditions, which results in the formation of the PSI-LHCI-pLHCII supercomplex under these conditions. However, treatment with VHL (**Figure 17 b**) or FR light (**Figure 16 a**) could dephosphorylate LHCII almost completely and, in turn, cause dissociation of the PSI-LHCI-pLHCII supercomplex even in *oeSTN7* plants.

The observation of strongly increased PSI-LHCI-pLHCII supercomplex formation in *oeSTN7* compared to WT in the dark was additionally confirmed by 77 K measurements (**Figure 16 c**). Moreover, the extent of state 2 in dark-adapted *oeSTN7* plants seemed to be significantly increased compared to *oeSTN7* plants in the middle of the light phase.

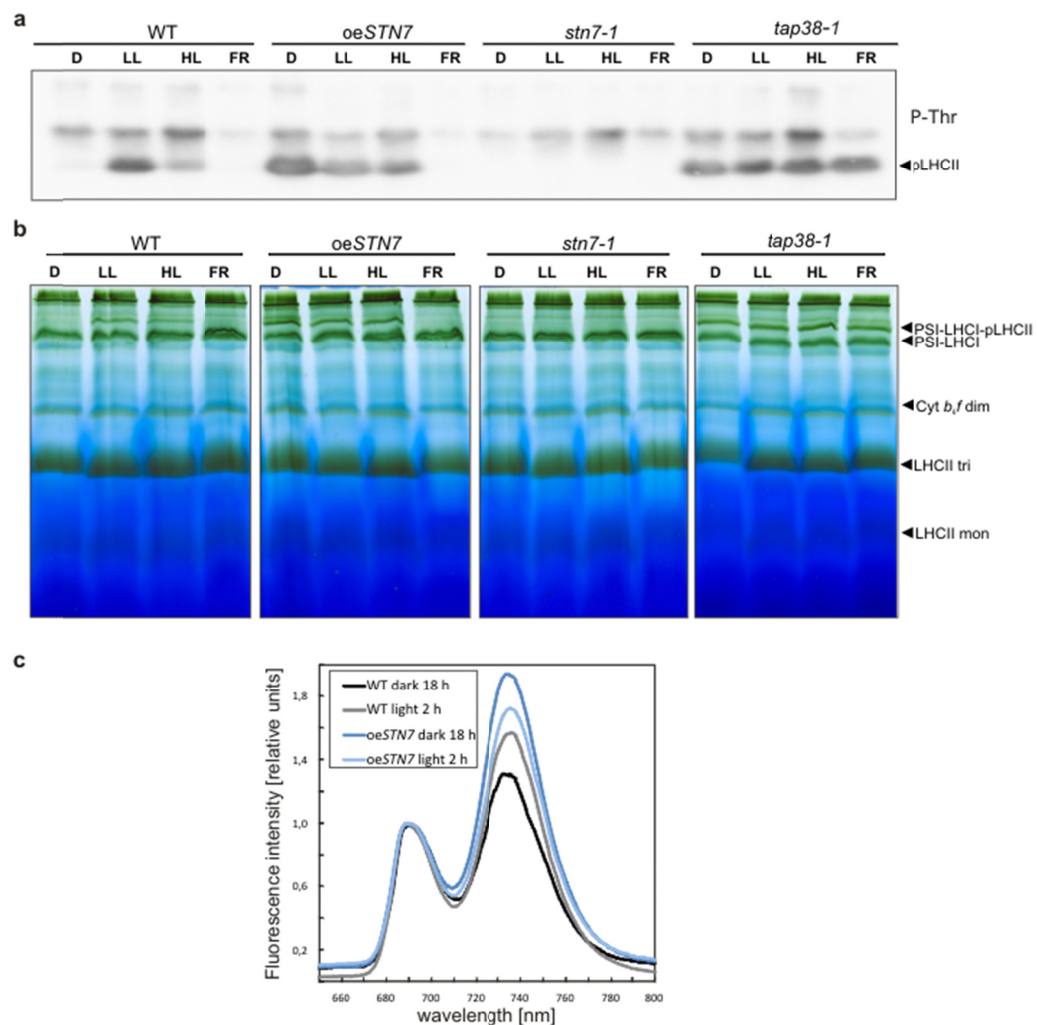


**Figure 16 Effects of increased STN7 levels on LHCII phosphorylation and PSI-LHCI-pLHCII supercomplex formation.**

**a** Thylakoid protein phosphorylation patterns in WT, *stn7-1*, *oeSTN7* and *tap38-1* plants adapted to darkness (D) for 18 h and subsequently transferred for 2 h to LL ( $80 \mu\text{mol photons m}^{-2}\text{s}^{-1}$ ), followed by exposure to 20 min of FR or 60 min of HL ( $800 \mu\text{mol photons m}^{-2}\text{s}^{-1}$ ) exposure. After the light treatments isolated thylakoids were fractionated by SDS-PAGE and transferred to PVDF membranes. Phosphorylated proteins were detected on Western blots using a phosphothreonine-specific antibody (pThr). The position of phosphorylated LHCII (pLHCII) is indicated by a *black arrowhead*. **b** Visualization of the PSI-LHCI-pLHCII complex associated with state-2-adapted plants. Thylakoid membranes ( $50 \mu\text{g}$  of Chl) were solubilized with 1.5 % (w/v) digitonin and fractionated by BN-PAGE. The PSI-LHCI and the PSI-LHCI-pLHCII supercomplexes are indicated by *black arrowheads* as well as dimeric Cyt *b6/f* (Cyt *b6/f* dim), trimeric (LHCII tri) and monomeric (LHCII mon) LHCII. **c** 77 K fluorescence emission spectra of WT (*black/grey lines*) and *oeSTN7* (*blue lines*) thylakoids of plants at the end of the dark or middle of the light period, grown at an 8 h/16 h light/dark cycle. Excitation wavelength was 475 nm. Spectra were normalized at 685 nm. Each spectrum represents the average of at least five individual recordings.

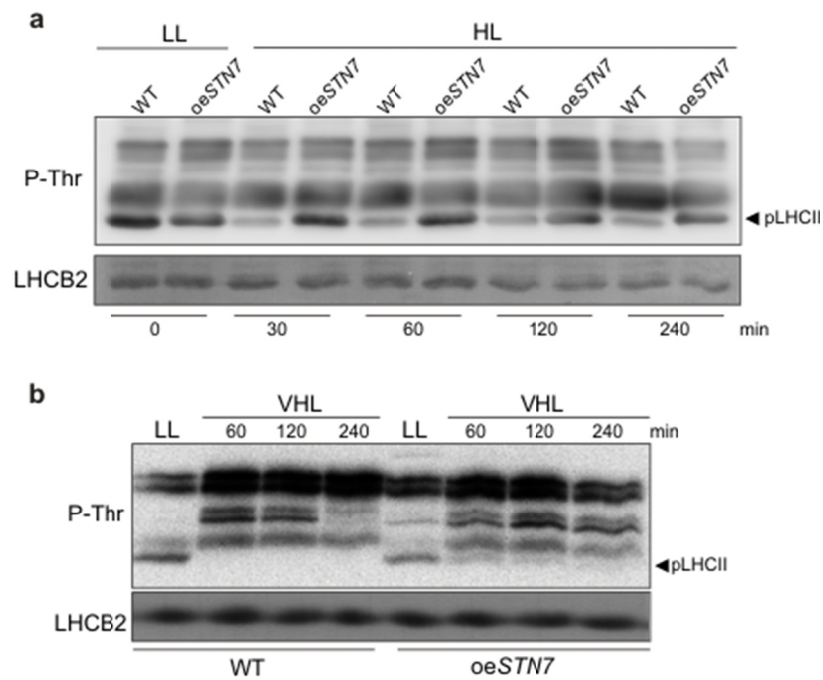


**Figure 17 Response of LHCII phosphorylation in WT and *oeSTN7* plants to high light intensity.**

**a** Time-course of changes in thylakoid phosphorylation in WT and *oeSTN7* plants upon transfer from low light (LL; 80  $\mu\text{mol photons m}^{-2}\text{s}^{-1}$ ) to high light (HL; 800  $\mu\text{mol photons m}^{-2}\text{s}^{-1}$ ). Western blot analysis with phosphothreonine (pThr)- and LHCB2-specific antibodies was performed on the same samples as in **Figure 12 b**. The position of pLHCII is indicated by a *black arrowhead*. **b** Time-course of changes in thylakoid phosphorylation in WT and *oeSTN7* plants upon transfer from low light (LL; 80  $\mu\text{mol photons m}^{-2}\text{s}^{-1}$ ) to very high light (VHL; 1800  $\mu\text{mol photons m}^{-2}\text{s}^{-1}$ ). Analyses were performed as in panel **a**.

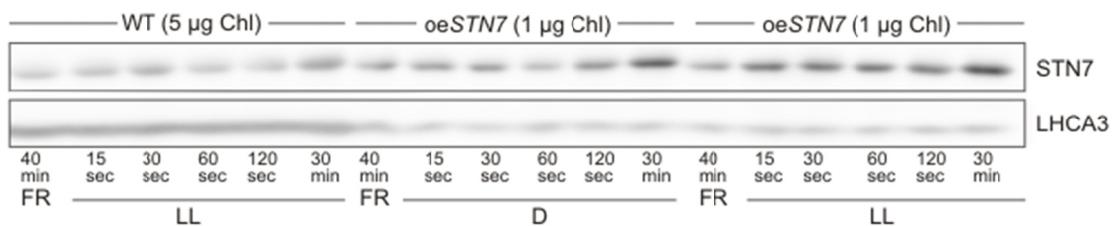


**Figure 18 STN7 protein levels in *oeSTN7* and WT upon a shift from FR to LL or D.**

WT and *oeSTN7* plants were treated for 50 min with FR and subsequently transferred to darkness or, in case of *oeSTN7*, additionally to LL. Leaf material was snap frozen after the indicated exposure times, thylakoids were isolated and Western blot analysis was performed by applying STN7 and LHCA3-specific antibodies. LHCA3 signals served as a loading control. Different amounts of chlorophyll were loaded for WT (5  $\mu\text{g}$ ) and *oeSTN7* (1  $\mu\text{g}$ ).

### 3.4.5 Increased STN7 levels are compatible with state transitions and result in LHCII phosphorylation in the dark

To evaluate the effect of increased levels of STN7 on state transitions, the quenching of chlorophyll (Chl) a fluorescence due to state transitions (measured as qT) was determined in WT and *oeSTN7* plants. To this end, plants were exposed to light conditions that favor either PSI (FR light) or PSII (red light). The *tap38-1* and *stn7-1* mutants served as controls, the first being locked in state 2 (with LHCII constitutively phosphorylated), the other trapped in state 1 (with LHCII constitutively dephosphorylated) (**Figure 19**). The qT values for *oeSTN7* plants were similar to those in WT, while *tap38-1* and *stn7-1* mutants showed strongly decreased qT values (Col-0,  $0.085 \pm 0.003$ ; *tap38-1*,  $-0.001 \pm 0.009$ ; *stn7-1*,  $-0.010 \pm 0.005$ ; *oeSTN7*,  $0.082 \pm 0.019$ ). This indicates that, in contrast to *oeTAP38* lines, which like *stn7-1* mutants are arrested in state 1 (Pribil et al. 2010), *oeSTN7* plants are still capable of undergoing state transitions (**Figure 19**), indicating that they can still regulate the activity of STN7, even though the protein is present in large excess.

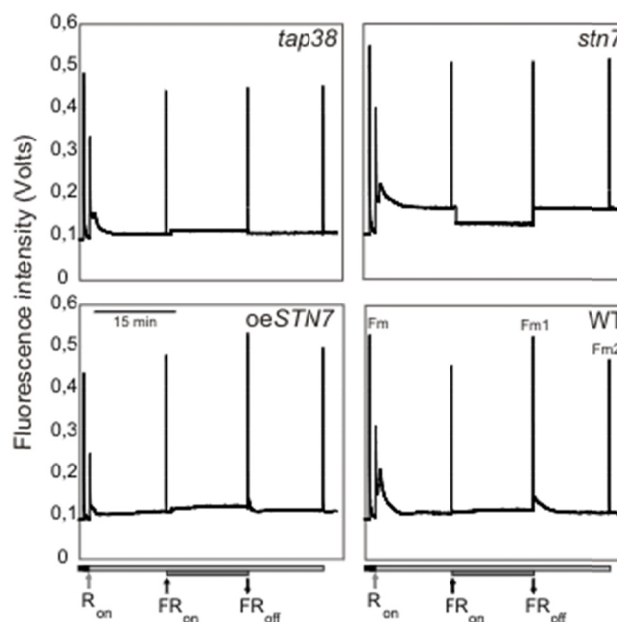


**Figure 19** Measurements of state transitions in *oeSTN7*, *tap38-1*, *stn7-1* and WT plants.

Far-red light (FR) was switched on or off in the presence of actinic red light (R) to induce transitions to state 1 (FR on) or state 2 (FR off). The maximum Chl a fluorescence levels Fm1 and Fm2 were determined after induction of state 1 and state 2, respectively. The duration of illumination is indicated by the bars below the graphs. Fluorescence curves representative of the eight individual measurements performed on each genotype are shown.

However, the kinetics of state transitions do seem to be altered in *oeSTN7* plants. Notably, the switch from FR- to red-light exposure led to a faster fall in steady-state Chl *a* fluorescence in *oeSTN7* plants than was seen in WT plants (**Figure 19**). The lower *F<sub>m</sub>* value observed in *oeSTN7* is likely to result from greater LHCII phosphorylation, and hence increased detachment of LHCII from PSII, even in the dark.

To further investigate differences in the kinetics of state transitions, *oeSTN7* and WT plants were shifted from state 1 to state 2 conditions and *vice versa*, and the timing of LHCII phosphorylation was observed at high resolution (**Figure 20 a, b**). To this end, leaf material was collected at various times, and LHCII phosphorylation was detected by Western blot analysis. Because dark-adapted *oeSTN7* plants, in contrast to WT, are trapped in state 2 (**Figure 16 a, b**), FR treatment had to be employed to drive WT and *oeSTN7* plants into state 1 (with LHCII dephosphorylated). After induction of state 1, plants were exposed to LL for up to 30 min (**Figure 20 a**). Initially (2 min of LL exposure), the rate of LHCII phosphorylation increased slightly faster in *oeSTN7* than in WT. However, after about 6 min of LL, *oeSTN7* and WT plants displayed similar maximum levels of LHCII phosphorylation, and after 30 min similar steady-state pLHCII levels were reached in both genotypes. This implies that, even after the reduction of STN7 amounts by FR treatment (see **Figure 12 a**), the levels still present in WT plants are sufficient to facilitate LHCII phosphorylation. Moreover, the higher level of STN7 available in *oeSTN7* did not markedly enhance LHCII phosphorylation and so accelerate the transition from state 1 to state 2. On the contrary, when the transition from state 2 to state 1 was studied by exposing the two genotypes to LL for state 2 adaptation (LHCII phosphorylated), followed by time-resolved FR light exposure, this transition was found to be markedly delayed in *oeSTN7* plants (**Figure 20 b**). After exposure to FR for 6 min, LHCII was completely dephosphorylated in WT plants, whereas substantial levels of pLHCII were still detectable in *oeSTN7* plants. Only after prolonged FR treatment could *oeSTN7* be quantitatively transferred into state 1.

To further investigate the phosphorylation of LHCII in dark-adapted *oeSTN7* plants (**Figure 16 a**), WT and *oeSTN7* plants were exposed to FR and then placed to darkness (**Figure 20 c**). In WT and *oeSTN7* plants, LHCII was completely dephosphorylated after exposure to FR light for 40 min. But whereas WT plants remained dephosphorylated when transferred to the dark, *oeSTN7* plants showed very strong *de-novo* phosphorylation of LHCII (**Figure 20 c**), which was associated with the formation of the PSI-LHCI-pLHCII complex, as shown by 77 K measurements (**Figure 20 d**).

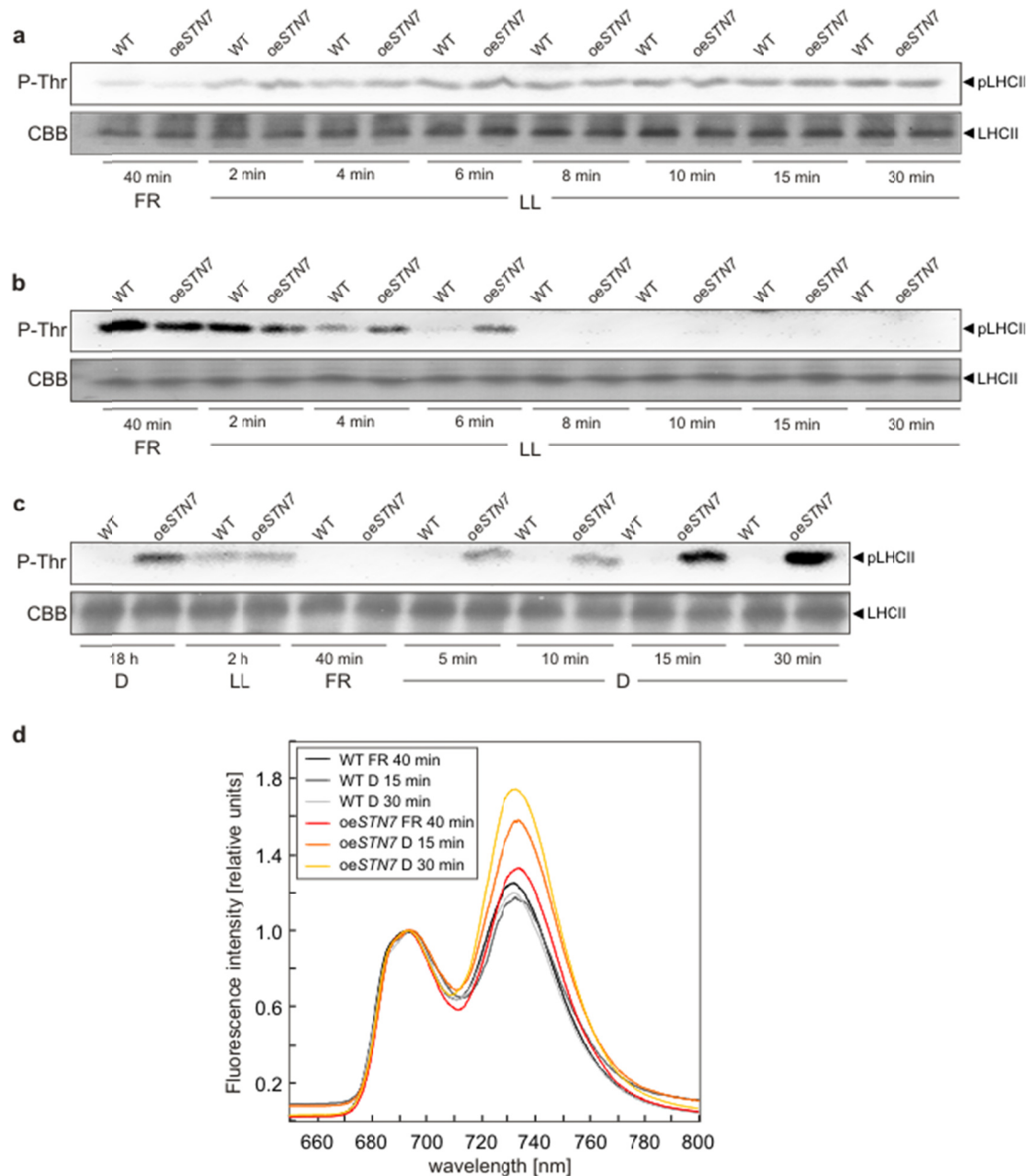


**Figure 20 Time-course of LHCII phosphorylation and 77 K fluorescence emission spectra in different light conditions.**

**a** LHCII phosphorylation of WT and *oeSTN7* after 40 min of exposure to FR and subsequent transfer to LL ( $80 \mu\text{mol photons m}^{-2}\text{s}^{-1}$ ) for up to 30 min. Thylakoids were isolated, fractionated on SDS-PAGE, transferred to PVDF membranes and the filters were probed with a phosphothreonine-specific antibody (pThr). The section of PVDF membranes displaying the LHCII band after staining with Coomassie brilliant blue (CBB) is shown as loading control. **b** As in panel **a**, except that an initial exposure to LL for 40 min was followed by treatment with FR for up to 30 min. **c** As in panel **a**, except that the results of successive treatments with 18 h of D, 2 h of LL ( $80 \mu\text{mol photons m}^{-2}\text{s}^{-1}$ ) and 40 min of FR are shown, directly followed by dark incubation for up to 30 min. **d** 77 K fluorescence

emission spectra of WT (*lines: black to grey*) and *oeSTN7* (*lines: red to yellow*) plants transferred to the dark for 15 min and 30 min, after 40 min of FR treatment. Excitation wavelength was 475 nm. Spectra were normalized with respect to the peak at 685 nm. Each spectrum represents the average of at least five individual recordings.

### 3.4.6 The PQ redox state of *oeSTN7* in the dark is not aberrant from WT

A possibility to explain the strong LHCII phosphorylation of *oeSTN7* in the dark could be the presence of a significantly reduced PQ pool even in the absence of light. To investigate the redox state of the PQ pool in the dark, we performed a non-invasive assay based on the polyphasic fluorescence rise (OJIP-transient) upon the onset of saturating light (**Figure 21**) as described by Toth et al. (2007).

WT and *oeSTN7* plants were dark-adapted and Chl a fluorescence was recorded during a saturation pulse. The  $F_J$  value, defined by the plateau after ~3 ms of illumination, was shown to depend on the availability of oxidized PQ molecules bound to the  $Q_B$  site. This value is close to  $F_m$  if the PQ pool is highly reduced, but much lower in dark-adapted WT plants, which exhibit just a partially reduced PQ pool. Pre-oxidation of the PQ pool by FR illumination just before the saturating light flash provided the minimal  $F_J$  ( $F_{J-ox}$ ) value in a second transient. Based on the equation  $(F_J - F_{J-ox}) / (F_m - F_{J-ox})$  the fraction of reduced PQ can be calculated. Recordings of 20 individual plants identified an average reduced PQ fraction of 15.8 % ( $\pm 2.15$  %) for WT and 14.4 % ( $\pm 2.69$  %) for *oeSTN7*. Therefore, no significant differences of the PQ redox state in the dark could be observed between WT and *oeSTN7*. **Figure 21** depicts representative charts of OJIP-transients of WT and *oeSTN7*.

### 3.4.7 Increased STN7 levels result in a more highly oxidized PQ pool and a higher PSI quantum yield upon light induction

To further define the effects of altered LHCII phosphorylation on photosynthesis, Chl a fluorescence and absorption parameters were determined for WT, *oeSTN7*, *stn7-1* and *tap38-1* plants during dark-light transitions. To this end, dark-adapted plants were exposed to LL for 5 min, followed by 100 s in darkness (**Figure 22 a, b**). After return into the light, the effective quantum yield of PSII ( $\Phi_{II}$ ) in *oeSTN7* and *tap38-1* plants was very similar and clearly higher than in the other genotypes (**Figure 22 a**).

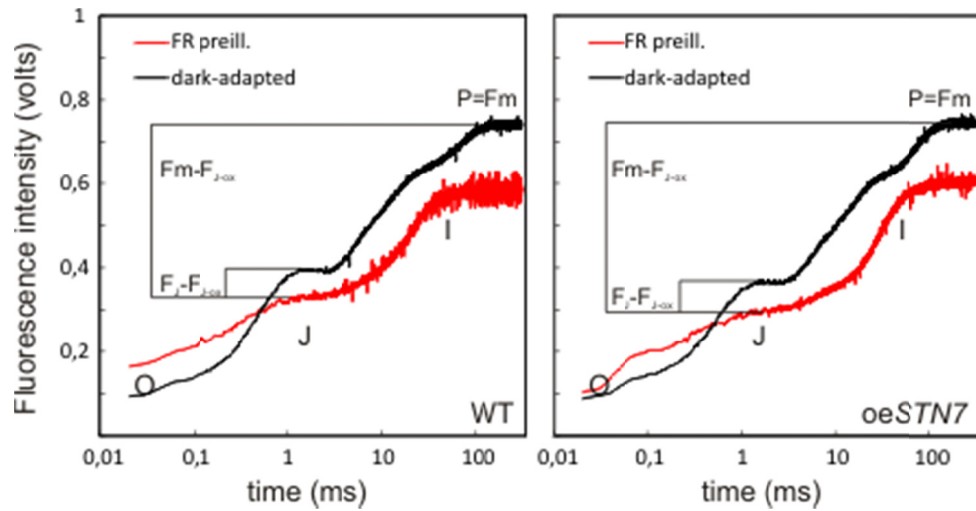


**Figure 21 Determination of the PQ pool redox state in the dark based on OJIP transients.**

Dark-adapted WT (*left panel*) and *oeSTN7* (*right panel*) leaves were instantly flashed by a  $3000 \mu\text{mol photons m}^{-2}\text{s}^{-1}$  red-light pulse (width 300 ms) to obtain the first transient (*black lines*). This transient determines the  $F_m$  (PQ fully reduced) and  $F_J$  (PQ redox state of interest) values necessary for the calculation of the PQ redox state. After additional 5 min of dark incubation and 10 s pre-illumination with FR a second transient was recorded (*red lines*), providing the minimum  $F_J$  ( $F_{J-ox}$ ) value corresponding to a fully oxidized PQ pool. On the basis of 20 likewise obtained transients the fraction of reduced PQ in dark-adapted plants was calculated by the equation  $(F_J - F_{J-ox}) / (F_m - F_{J-ox})$ .  $F_m$ ,  $F_J$ ,  $F_{J-ox}$  values and the OJIP-phases O, J, I, P of the transients are highlighted.

The excitation pressure parameter  $1-q_L$  reflects the size of the reduced fraction of  $Q_A$ , and was lower in *oeSTN7* and *tap38-1* plants than in the other genotypes, although the decline in  $1-q_L$  was more pronounced in *oeSTN7* than in *tap38-1* plants (**Figure 22 b**). The differences in  $\Phi_{II}$  and  $1-q_L$  seen in *oeSTN7* and *tap38-1* plants compared to WT also persisted under stronger light intensities ( $95$  and  $339 \mu\text{mol photons m}^{-2}\text{s}^{-1}$ ) (**Figure 22 c, d**). However, the differences between the genotypes became less pronounced, which agrees with the observations made by Pribil et al. (2010) in lines with altered TAP38 levels. The less reduced PQ pool in *oeSTN7* and *tap38-1* plants in the light is most likely due to their increased PSI antenna size (**Figure 16**).

To assess the performance of PSI, the photochemical quantum yield of PSI ( $\Phi_I$ ), and the quantum yield of non-photochemical energy dissipation in PSI due to donor ( $\Phi_{ND}$ ) or acceptor ( $\Phi_{NA}$ ) side limitation were determined after exposing dark-adapted WT, *oeSTN7*, *stn7-1* and *tap38-1* plants to low light intensities (**Figure 23 a, b, c**).  $\Phi_I$  represents the fraction of reduced P700 centers that are able to transfer their electrons to ferredoxin.

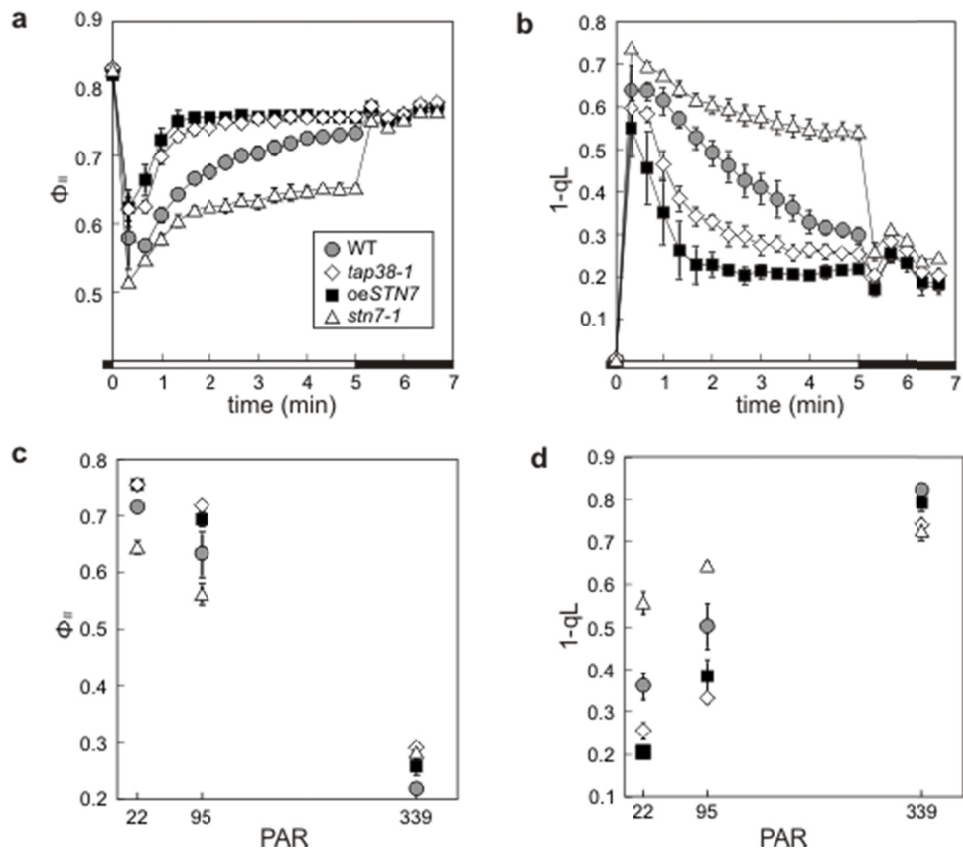


**Figure 22 Kinetics of Chl a fluorescence of WT, *oeSTN7*, *stn7-1* and *tap38-1*.**

Plants were grown under an 8 h/16 h day/night regime at  $100 \mu\text{mol photons m}^{-2}\text{s}^{-1}$ . **a, b** Time-course of effective quantum yield of PSII ( $\Phi_{II}$ ) (**a**) and excitation pressure (1-qL) (**b**) of WT, *oeSTN7*, *stn7-1* and *tap38-1* plants pre-incubated for 10 min in darkness, exposed to actinic red light ( $22 \mu\text{mol photons m}^{-2}\text{s}^{-1}$ ) for 5 min and subsequently exposed again to darkness (100 s). **c, d** Dependence of Chl a fluorescence on light intensity in WT, *oeSTN7*, *stn7-1* and *tap38-1* plants. The effective quantum yield of PSII ( $\Phi_{II}$ ) (**c**) and the excitation pressure (1-qL) (**d**) were recorded at three different fluxes of actinic red light (22, 95 and  $339 \mu\text{mol photons m}^{-2}\text{s}^{-1}$ ) after 5 min of light exposure as in panel **a** and **b**. PAR, photosynthetically active radiation ( $\mu\text{mol photons m}^{-2}\text{s}^{-1}$ ); circles with grey filling, WT; squares with black filling, *oeSTN7*; triangles, *stn7-1*; diamonds, *tap38-1*. Average values ( $\pm$  SD) of five individual plants are shown.

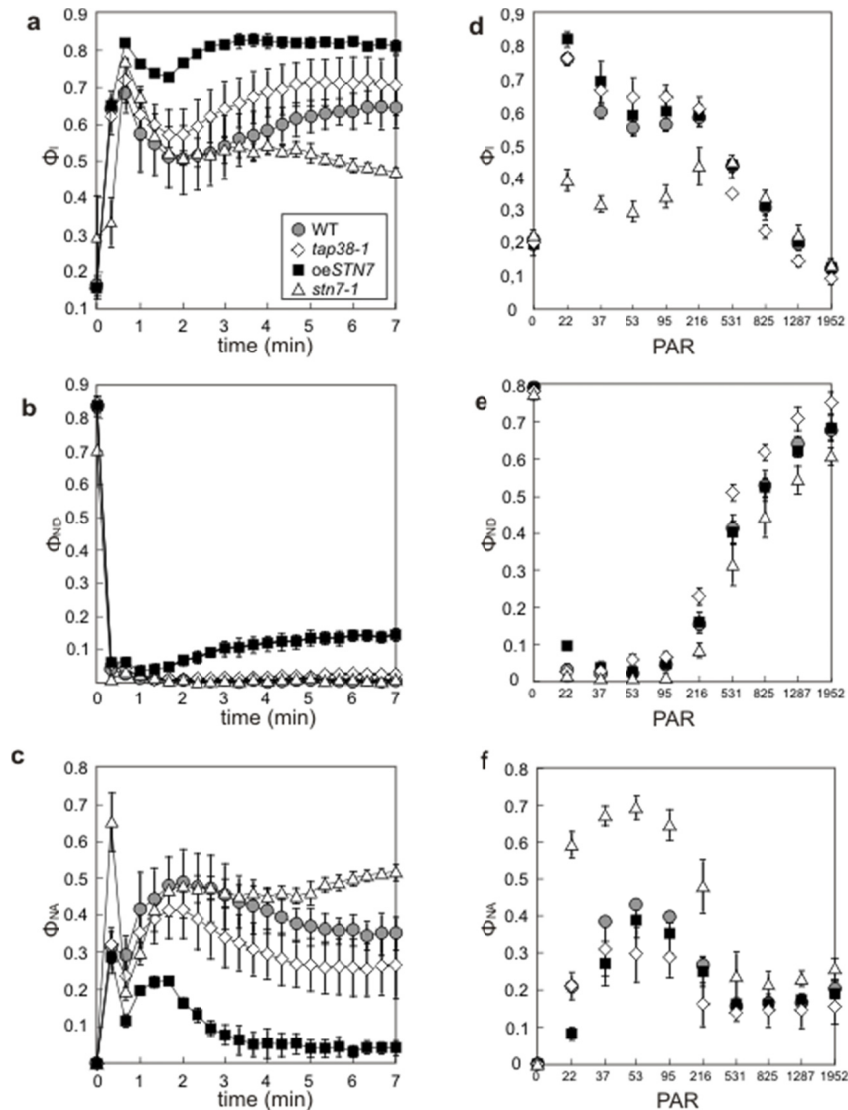


**Figure 23 Kinetics of absorption parameters of WT, *oeSTN7*, *stn7-1* and *tap38-1*.**

Plants were grown under an 8 h/16 h day/night regime at  $100 \mu\text{mol photons m}^{-2}\text{s}^{-1}$ . **a, b, c** Time-course of absorption parameters in WT, *oeSTN7*, *stn7-1* and *tap38-1* plants. Plants adapted for 10 min to darkness were exposed to actinic red light ( $22 \mu\text{mol photons m}^{-2}\text{s}^{-1}$ ) for 7 min to measure the photochemical quantum yield of PSI ( $\Phi_i$ ) (**a**), the quantum yield of non-photochemical energy dissipation in PSI due to donor-side limitation ( $\Phi_{ND}$ ) (**b**) or acceptor-side limitation ( $\Phi_{NA}$ ) (**c**). **d, e, f** Dependence of absorption parameters on light intensity in WT, *oeSTN7*, *stn7-1* and *tap38-1* plants.  $\Phi_i$  (**d**),  $\Phi_{ND}$  (**e**) or  $\Phi_{NA}$  (**f**) were monitored as actinic red light intensity was increased stepwise (22, 37, 53, 95, 216, 513, 825, 1,287 and 1,952  $\mu\text{mol photons m}^{-2}\text{s}^{-1}$ , each lasting for 5 min), following 10 min of dark adaptation. PAR, photosynthetically active radiation ( $\mu\text{mol photons m}^{-2}\text{s}^{-1}$ ); circles with grey filling, WT; squares with black filling, *oeSTN7*; triangles; *stn7-1*; diamonds, *tap38-1*. Average values ( $\pm$  SD) of five individual plants are shown.

In comparison to the other genotypes, *oeSTN7* plants reached a higher steady-state  $\Phi_I$  value faster, whereas  $\Phi_I$  values for *stn7-1* leveled out below those of WT (**Figure 23 a**).  $\Phi_{ND}$  represents the oxidized fraction of P700 centers and becomes relevant upon NPQ induction. Thus, at the LL intensities used in our assay,  $\Phi_{ND}$  plays a rather negligible role for  $\Phi_I$ , as clearly seen in WT, *stn7-1* and *tap38-1* plants (**Figure 23 b**). However, in *oeSTN7* an increased  $\Phi_{ND}$  value was detected, which is compatible with the markedly reduced excitation pressure in this genotype (see **Figure 22 b**).  $\Phi_{NA}$  represents the fraction of reduced but closed P700 centers and, under the LL intensities employed in the assay, it represents the major limitation on  $\Phi_I$  (**Figure 23 c**). In fact, *oeSTN7* and, to a lesser extent, also *tap38-1* plants were less affected by  $\Phi_{NA}$  than the other genotypes. When the PSI parameters were examined under increasing light intensities pronounced differences between the genotypes with respect to  $\Phi_I$  were observed only under light intensities of up to 95  $\mu\text{mol photons m}^{-2}\text{s}^{-1}$  (**Figure 23 d, e, f**).

To rule out that an upregulation of PSI amounts is responsible for the observed increase in PSI activity, the protein levels of PSAC and PSAB were compared between thylakoids of WT and *oeSTN7* plants by immunoblot analysis. **Figure 24** clearly shows that PSI level are not altered between WT and *oeSTN7* and that the observed effects can be ascribed to changes in state transitions.

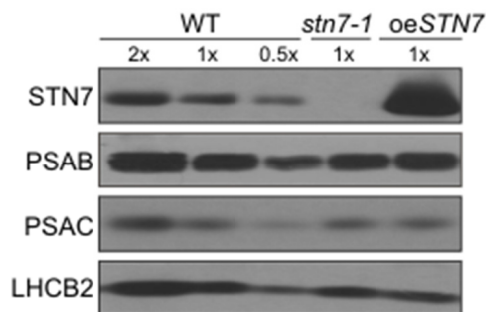


**Figure 24** PSI levels in thylakoids of WT, *stn7-1* and *oeSTN7*.

Thylakoid proteins of dark-adapted WT, *stn7-1* and *oeSTN7* plants were purified for immunoblot analysis, applying antibodies against STN7, PSAC, PSAB and LHCB2. Membrane proteins equivalent to 2.5  $\mu\text{g}$  (1x) of chlorophyll were loaded for each genotype and for WT additional 5  $\mu\text{g}$  (2x) and 1.25  $\mu\text{g}$  (0.5x).

Taken together, the data suggest that in *oeSTN7* plants PSI displays increased quantum efficiency, leading to a shortage of electrons on the donor side of PSI and a more highly oxidized PQ pool. The *tap38-1* mutant exhibits similar behavior - albeit less pronounced, indicating that this effect can be attributed to the increased formation of PSI-LHCI-pLHCII supercomplexes in

the two genotypes. Moreover, this enhanced oxidation of the PQ pool under low and moderate illumination might significantly contribute to the observed lower LHCII-phosphorylation in *oeSTN7* compared to WT.

### 3.4.8 LHCII phosphorylation of *oeSTN7* plants in the dark depends on stromal factors

To assess whether the STN7 activity that persists in *oeSTN7* lines in the dark is, as in WT plants, triggered by the redox state of the PQ pool, in particular by the binding of PQH<sub>2</sub> to the Qo site of the Cyt *b6f* complex (Vener et al. 1997; Zito et al. 1999), experiments were performed with inhibitors of photosynthetic electron flow. Immediately after LHCII dephosphorylation by FR light, DBMIB and DCMU were infiltrated into detached leaves, and the leaves were then exposed to LL or placed in the dark. STN7 activity was analysed by immunodetection of pLHCII. DBMIB competes with PQH<sub>2</sub> for the Qo site of the Cyt *b6f* complex (Vener et al. 1997). The infiltration of leaves with 200 µM DBMIB strongly reduced LHCII phosphorylation in *oeSTN7* in the dark and under LL, but did not completely inhibit *de-novo* LHCII phosphorylation as in WT (**Figure 25 a**). DCMU blocks electron transfer from the PSII acceptor side to PQ, resulting in efficient oxidation of the PQ pool upon illumination (Vener et al. 1997). Infiltration with DCMU resulted in quantitative inhibition of LHCII phosphorylation under LL in both genotypes (**Figure 25 b**).

To eliminate effects of stromal components, an *in-vitro* phosphorylation assay using isolated thylakoids in the presence of phosphorylation-promoting reagents was employed as described previously (Rintamaki et al. 2000) (**Figure 25 c**). Unlike the case in intact leaves, the elevated level of STN7 protein present in isolated thylakoids of *oeSTN7* plants led to greater LHCII phosphorylation under LL conditions than in WT (**Figure 25 c**). Possible explanations for this are the inhibition of TAP38/PPH1-mediated LHCII dephosphorylation activity by the NaF in the *in-vitro* assay, and the absence of stroma-located mechanisms for adjusting STN7 kinase activity. The inhibition of LHCII phosphorylation by DCMU occurred with almost equal efficiency in extracts from *oeSTN7* and WT plants (**Figure 26 a**). However, DBMIB was less effective in inhibiting *in-vitro* LHCII phosphorylation of *oeSTN7* thylakoids and only the addition of high DBMIB concentrations ( $\geq 40$  µM) led to a significant inhibition of LHCII phosphorylation (**Figure 26 b**).

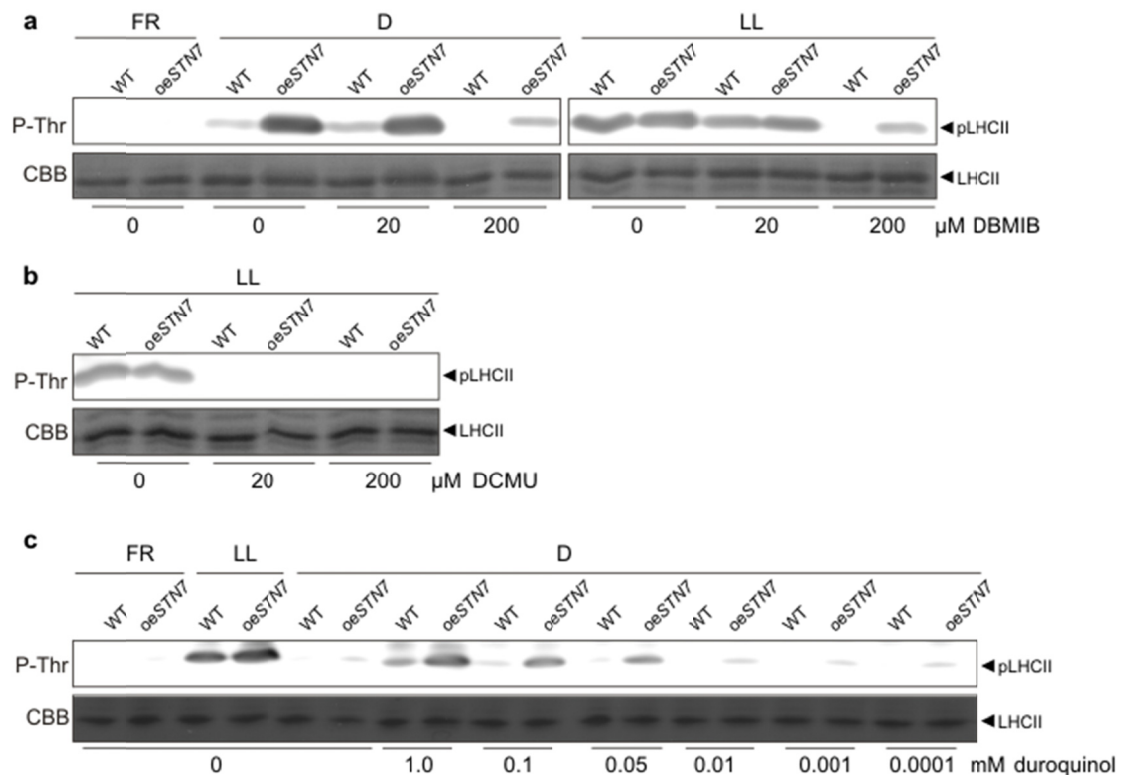


**Figure 25** Effects of chemical modulation of PQ redox state on LHCII phosphorylation in WT and *oeSTN7*.

**a** LHCII phosphorylation after infiltration with DBMIB. Plants were exposed to far-red light for 60 min (FR). Detached leaves were vacuum-infiltrated with 20  $\mu\text{M}$  or 200  $\mu\text{M}$  of DBMIB for 5 min or left untreated (“0”), and then transferred either to low light (LL; 60  $\mu\text{mol photons m}^{-2}\text{s}^{-1}$ ) or darkness (D) for 30 min. Thylakoid membranes were isolated, fractionated by SDS-PAGE, transferred to PVDF membranes and analyzed with phosphothreonine-specific antibodies (pThr). PVDF membranes were stained with Coomassie brilliant blue (CBB) and the section with the LHCII signal is shown as loading control. **b** As in panel **a**, except that DCMU was used instead of DBMIB. **c** *In-vitro* LHCII phosphorylation in the dark following reduction of the PQ pool using duroquinol. After incubating plants for 60 min under FR, thylakoid membranes were isolated and resuspended in phosphorylation buffer containing up to 1.0 mM duroquinol. The *in-vitro* phosphorylation reaction was started by adding 25  $\mu\text{M}$  ATP, and samples were then transferred to the dark for 30 min prior to analysis of LHCII phosphorylation. As a positive control, one sample of each genotype was exposed to LL (60  $\mu\text{mol photons m}^{-2}\text{s}^{-1}$ ). pLHCII and LHCII were detected as in panel **a**.

Given that DBMIB competes with reduced PQ for binding in the Qo pocket of the Cyt *b6f* complex, which in turns leads to the activation of STN7, it can be concluded that an increase of the STN7 concentration might increase the probability of the activation of STN7 molecules. In contrast to the case in intact leaves (see **Figure 16 a** and **20 c**), when LHCII phosphorylation was assayed *in vitro* in thylakoids isolated from FR-pretreated *oeSTN7* plants exposed to 30 min of darkness, it was found to be suppressed. *In-vitro* LHCII phosphorylation in the dark could be

restored by reducing the PQ pool through the addition of duroquinol (**Figure 25 c**), which is able to directly reduce plastoquinone to plastoquinol (White et al. 1978). To this end, *oeSTN7* and WT thylakoids were spiked with increasing amounts of duroquinol, and LHCII phosphorylation was monitored after 20 min of incubation in the dark (**Figure 25 c**). LHCII phosphorylation in *oeSTN7* thylakoids was much more pronounced than in WT and was initiated at lower duroquinol concentrations (0.1  $\mu$ M).

Additionally, the time-course of *de-novo* LHCII phosphorylation in the dark was investigated by *in-vitro* [ $^{33}$ P]-labeling assays. To this end thylakoids were isolated from dark-adapted plants, which still display a partially reduced PQ pool compared to the FR treated plants used during the afore described *in-vitro* assays. *De-novo* thylakoid phosphorylation of WT and *oeSTN7* plants was assessed in the presence of  $^{33}$ P-labeled ATP over a time period of 30 min, while protein dephosphorylation was inhibited by the addition of NaF (**Figure 27**). As expected, the WT LHCII phosphorylation rate under LL conditions was higher than in the dark and further increased when thylakoids were treated with the agent dithionite, which is efficiently reducing the PQ pool in the dark. While LHCII *de-novo* phosphorylation in the dark gradually increased over time, LL led to a rapid reduction of the PQ pool and *de-novo* LHCII phosphorylation showed saturation already after 15 min (**Figure 27**). The addition of dithionite led to a strong increase in LHCII phosphorylation already after 5 min which remained rather constant in the following time-course. For *oeSTN7* thylakoids, all three conditions resulted in stronger *de-novo* LHCII phosphorylation compared to WT, again indicating that an elevated STN7 protein level relatively increases the LHCII phosphorylation efficiency *in vitro*, independent from the reduction level of the PQ pool. Note, that in contrast to afore described non-radioactive assays, here a significant phosphorylation of LHCII was detected in the dark. However, this observation can be explained by the methods increased detection sensitivity and by using dark-adapted plant material, which contained a certain reduced fraction of PQ.

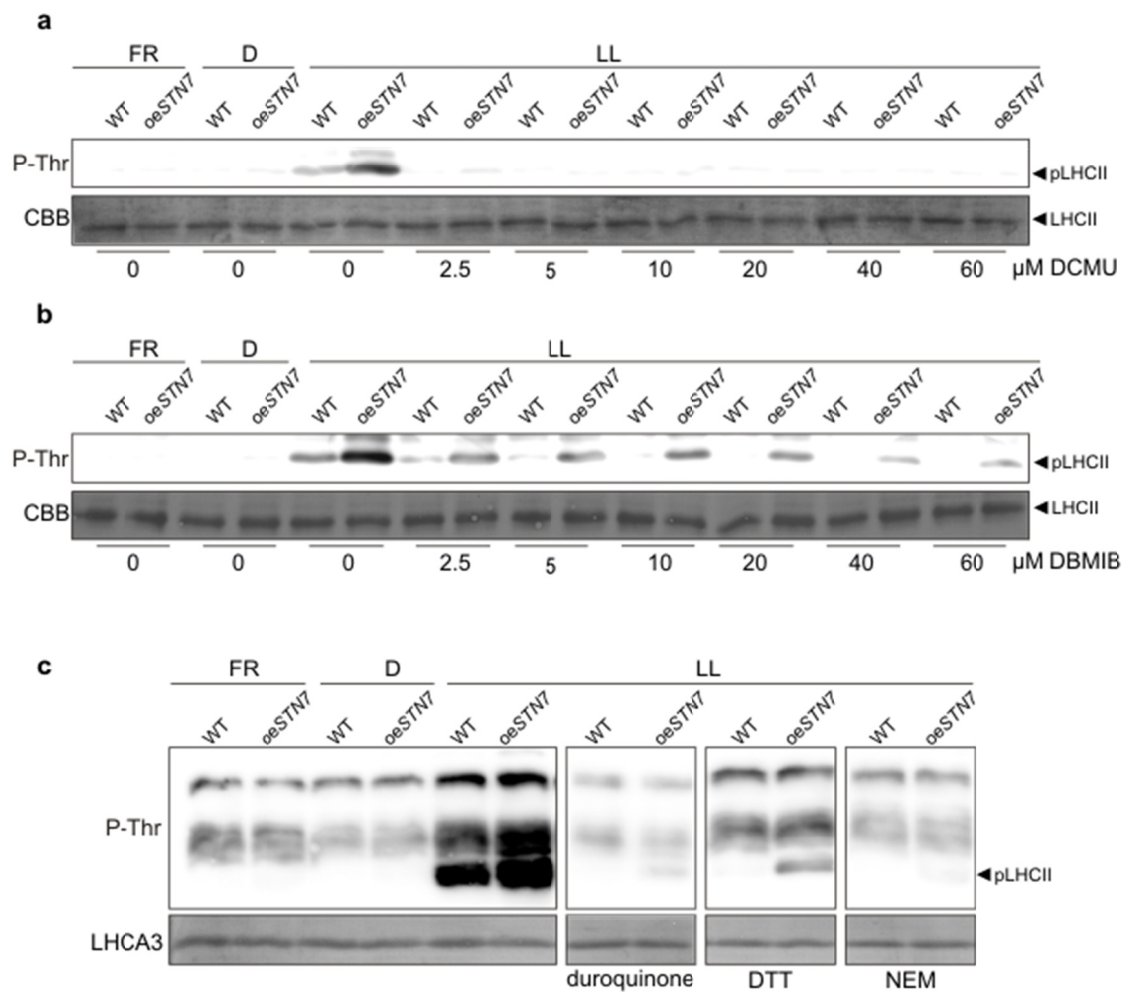


**Figure 26** *In-vitro* LHCII phosphorylation in WT and *oeSTN7* plants after treatment with chemicals that alter the PQ redox state or modify Cys residues.

**a** *In-vitro* LHCII phosphorylation after treatment with DCMU. WT and *oeSTN7* plants were exposed to far-red (FR) light for 60 min. Thylakoid membranes were isolated and resuspended in phosphorylation buffer containing up to 60 μM DCMU. *In-vitro* phosphorylation was initiated by adding 25 μM ATP and transferring the samples to low light (LL; 60 μmol photons m<sup>-2</sup>s<sup>-1</sup>). For each genotype one sample not treated with DCMU was kept in the dark (D). The reactions were stopped after 30 min and thylakoid proteins were fractionated by SDS-PAGE and transferred to PVDF membrane. pLHCII was detected with a phosphothreonine-specific antibody (pThr). The PVDF membrane was stained with Coomassie brilliant blue (CBB) as a loading control, and the section with the LHCII signal is shown. **b** *In-vitro* LHCII phosphorylation after treatment with DBMIB; otherwise the experimental procedure followed was as in panel **a**. **c** *In-vitro* LHCII phosphorylation after treatment with DTT, NEM or duroquinone. The same procedure as described in panel **a** was followed, employing 100 mM DTT, 100 mM NEM or 2 mM duroquinone instead of DCMU. As a loading control, filters were probed with a LHCA3-specific antibody.

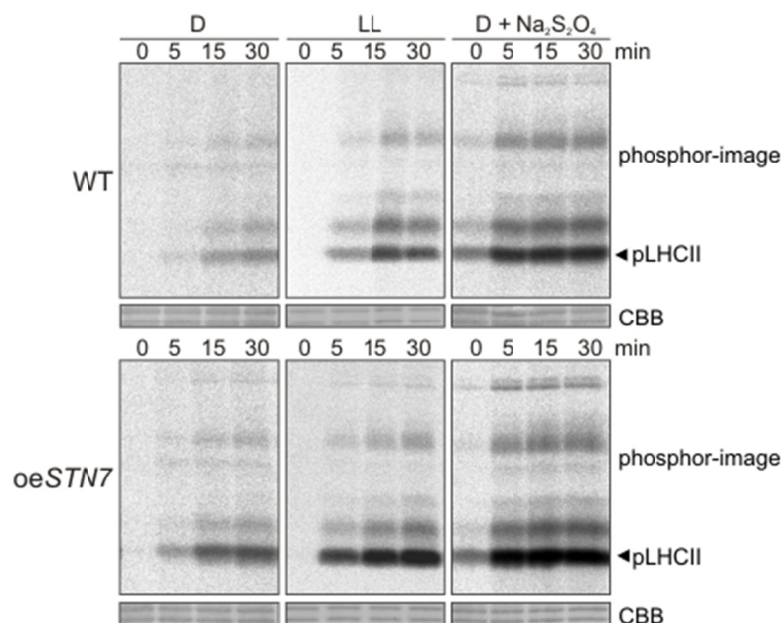


**Figure 27** *In-vitro de-novo* phosphorylation of WT and *oeSTN7* thylakoids using  $^{33}\text{P}$ -ATP.

Thylakoids of WT and *oeSTN7* plants were isolated in the dark. *In-vitro* phosphorylation of thylakoids corresponding to 1  $\mu\text{g}$  chlorophyll was assessed in the presence of  $^{33}\text{P}$ -labeled ATP (10  $\mu\text{Ci}$ ). Dephosphorylation inhibitor NaF was added to the reaction buffer. Samples were taken at time points of 0, 5, 15 and 30 min after addition of  $^{33}\text{P}$ -ATP, supplemented with Laemmli-buffer and separated by SDS-PAGE. Signals were analyzed with a phosphor-imager. *Left panel* (D): thylakoids remained dark-adapted during the course of experiment; *middle panel* (LL): thylakoids were exposed to 20  $\mu\text{mol}$  white light; *right panel* (D +  $\text{Na}_2\text{S}_2\text{O}_4$ ): dithionite (10  $\mu\text{M}$ ) was added in the dark. As loading controls, sectors from the Coomassie-stained gels are shown below each autoradiogram (CBB).

In an additional non-radioactive *in-vitro* phosphorylation assay, the addition of duroquinone, which oxidizes the PQ pool even in the light, led to the inactivation of STN7 in WT and *oeSTN7* thylakoids (**Figure 26 c**), like observed for PQ oxidation by FR or DCMU treatment. These results suggest that, in intact, dark-adapted leaves with a rather oxidized PQ pool, sufficient plastoquinol molecules remain to activate STN7, given that they are present in high amounts as in *oeSTN7* plants. The weak re-reduction of the PQ pool due to electron transport processes acting in the dark (Burrows et al. 1998) seems to effectively activate STN7 in *oeSTN7* plants. However, complete oxidation of the PQ pool abolishes STN7 activity even when the protein is present in excess amounts.

It has been suggested that STN7 kinase activity may be controlled by redox regulation of lumen-located N-terminal cysteine residues (Lemeille and Rochaix 2010). To block the formation

of disulphide bridges, DTT and NEM were applied, which reduce and block cysteine residues respectively. By adding DTT and NEM to WT and *oeSTN7* thylakoids, STN7 activity could be drastically decreased in the two genotypes, although *oeSTN7* thylakoids with their constitutively higher levels of STN7 were more resistant to complete inactivation (**Figure 26 c**).

In summary, these observations suggest that STN7 is activated by the same mechanisms in WT and *oeSTN7* plants. The activity of STN7 that remains in plants kept in the dark appears to depend on the re-reduction of the PQ pool by a stromal electron source. Moreover, dynamic disulphide bridge formation and reduction are required to maintain STN7 kinase activity.

### 3.4.9 The N-terminal cysteine residues of STN7 are essential for its activity

Like STT7, the STN7 kinase contains a potential thioredoxin motif (CxxxxC) at its N-terminus. This motif is thought to represent a regulatory, redox-sensitive domain that is crucial for STN7 kinase activity (Lemeille et al. 2009). To address this issue, cysteine-exchange variants of STN7 were generated, in which one or both N-terminal cysteine residues have been replaced by serine (STN7<sub>C→S:65</sub>, STN7<sub>C→S:70</sub> and STN7<sub>C→S:65+70</sub>), and these were introduced by stable transformation into the *stn7-1* genetic background under control of the 35S promoter. The mutated variants accumulated in the transgenic lines, albeit in lesser amounts than STN7 in WT (**Figure 28**). However, each of the cysteine replacements was associated with an almost complete loss of LHCII kinase activity, and concomitant loss of LHCII phosphorylation and PSI-LHCI-pLHCII supercomplex formation (**Figure 28**). The possibility that the reduction in STN7 protein levels in the transgenic cysteine exchange lines might account for the marked drop in LHCII phosphorylation compared to WT can be excluded, as *leSTN7* plants accumulate similar decreased amounts of STN7 but show substantial LHCII phosphorylation activity (**Figure 30 b**). Compared to *stn7-1*, the Cys-Ser exchange lines retained a slightly higher degree of residual LHCII phosphorylation under LL (**Figure 28 and 30 b**).

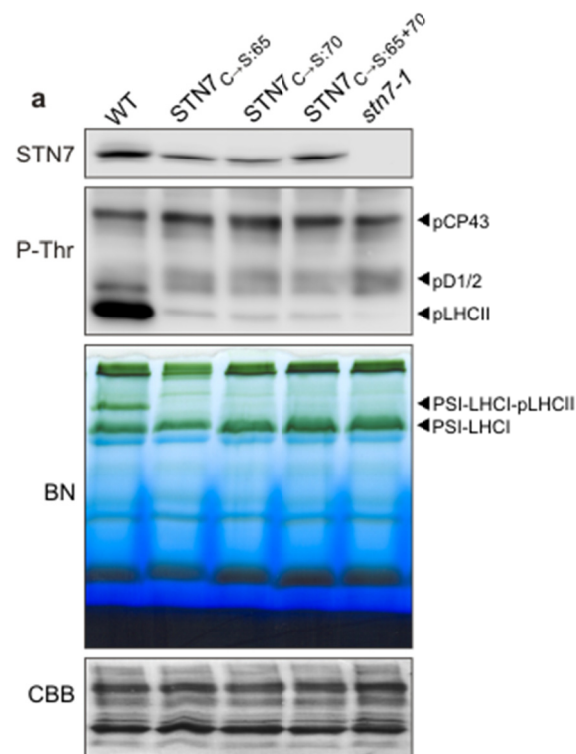


**Figure 28 Activity of Cys/Ser-exchange STN7 variants.**

STN7 protein levels (STN7) and thylakoid phosphorylation patterns (pThr) of WT, *stn7-1* and lines expressing mutated STN7 variants in the *stn7-1* mutant background (STN7<sub>C→S:65</sub>, STN7<sub>C→S:70</sub> and STN7<sub>C→S:65+70</sub>) were determined by Western analysis with an STN7- or pThr-specific antibody, respectively. The positions of phosphoproteins (pLHCII, pCP43 and pD1/2) are indicated by *black arrowheads*. Furthermore, thylakoids (50 µg Chl) solubilized with 1.5 % (w/v) digitonin were subjected to blue native (BN)-PAGE gel analysis. The positions of the PSI-LHCI and the PSI-LHCI-pLHCII supercomplexes are indicated by *black arrowheads*. As a loading control, membranes were stained with Coomassie brilliant blue (CBB).

### 3.4.10 STN7 forms redox-dependent inter- and intramolecular disulphide bridges

To test whether the redox- and Cys residue-dependent STN7 kinase activity is based on the involvement of intra- or intermolecular disulphide bridge formation, potential redox-dependent changes in the migration behavior of STN7 in diagonal-PAGE analysis were assessed (**Figure 29 a**). In this assay, thylakoid proteins are exposed to either reducing or oxidizing conditions before separation in the first dimension, whereas the second-dimension separation occurs under reducing conditions. If the first dimension is run under non-reducing conditions, proteins that do not form inter- or intramolecular disulphide bridges comigrate with large amounts of other proteins on the diagonal of the 2-D gel. However, in case a protein forms intermolecular disulphide bridges it

would migrate left-hand side of the diagonal, or right-hand if undergoing intramolecular disulphide bridge formation (Winger et al. 2007). As a control, thylakoid proteins were reduced with DTT prior to electrophoresis in the first dimension. This resulted in a single signal for STN7 on the respective diagonal (**Figure 29 a**). When thylakoid proteins were treated with the oxidizing agent diamide before separation in the first dimension, STN7 also migrated well left-hand and right-hand side of the diagonal, which indicates the formation of both inter- and intramolecular disulphide bridges by STN7 (**Figure 29 a**).

To possibly visualize these intermolecular interactions of STN7 via non-reducing one-dimensional PAGE, WT plants were afore exposed to different light conditions (FR, LL, HL, or D) or treated with chemicals like DCMU and DBMIB known to inhibit STN7 kinase activity. However, none of these conditions allowed for the identification of a dimeric or multimeric state of STN7 (**Figure 29 b**). Even the addition of diamide to WT thylakoids in order to stabilize potential intermolecular interactions prior to solubilization in loading buffer could not support STN7 dimer formation and/or recognition. Interestingly, a clear negative effect of diamide on STN7 monomer amounts could be observed. One explanation could be that STN7 is dispersed to multiple high molecular interactions if diamide was added (**Figure 29 b**).

Supporting the idea of STN7 dimer formation, a ~110-kDa signal corresponding to the size of a STN7 dimer could be detected in *oeSTN7* plants (**Figure 29 c, 30 b**). In *oeSTN7* plants exposed to FR light the amount of the putative STN7 dimer was lower than that seen under LL conditions, however, the monomer/dimer ratio remained largely constant (**Figure 29 c**).

To reduce the risk of disintegration or degradation of the putative STN7 dimer during thylakoid isolation, the reactivation or inhibition of the kinase was induced after thylakoid isolation right before separation on non-reducing SDS-PAGE (first dimension). To this end, assays similar to the *in-vitro* phosphorylation assays described in **Figure 26** were performed using thylakoids isolated from FR-adapted plants (WT and *oeSTN7*) (**Figure 29 d**). However, none of the applied light conditions (FR, LL, HL, or D) or attempts to chemically manipulate STN7 kinase activity (DCMU or DBMIB) led to a visual formation of STN7 dimers in WT thylakoids (**Figure 29 d**). In thylakoids of *oeSTN7* plants the same conditions did neither significantly alter the abundance of the detectable putative STN7 dimer nor the observed STN7 monomer/dimer ratio (**Figure 29 d**).

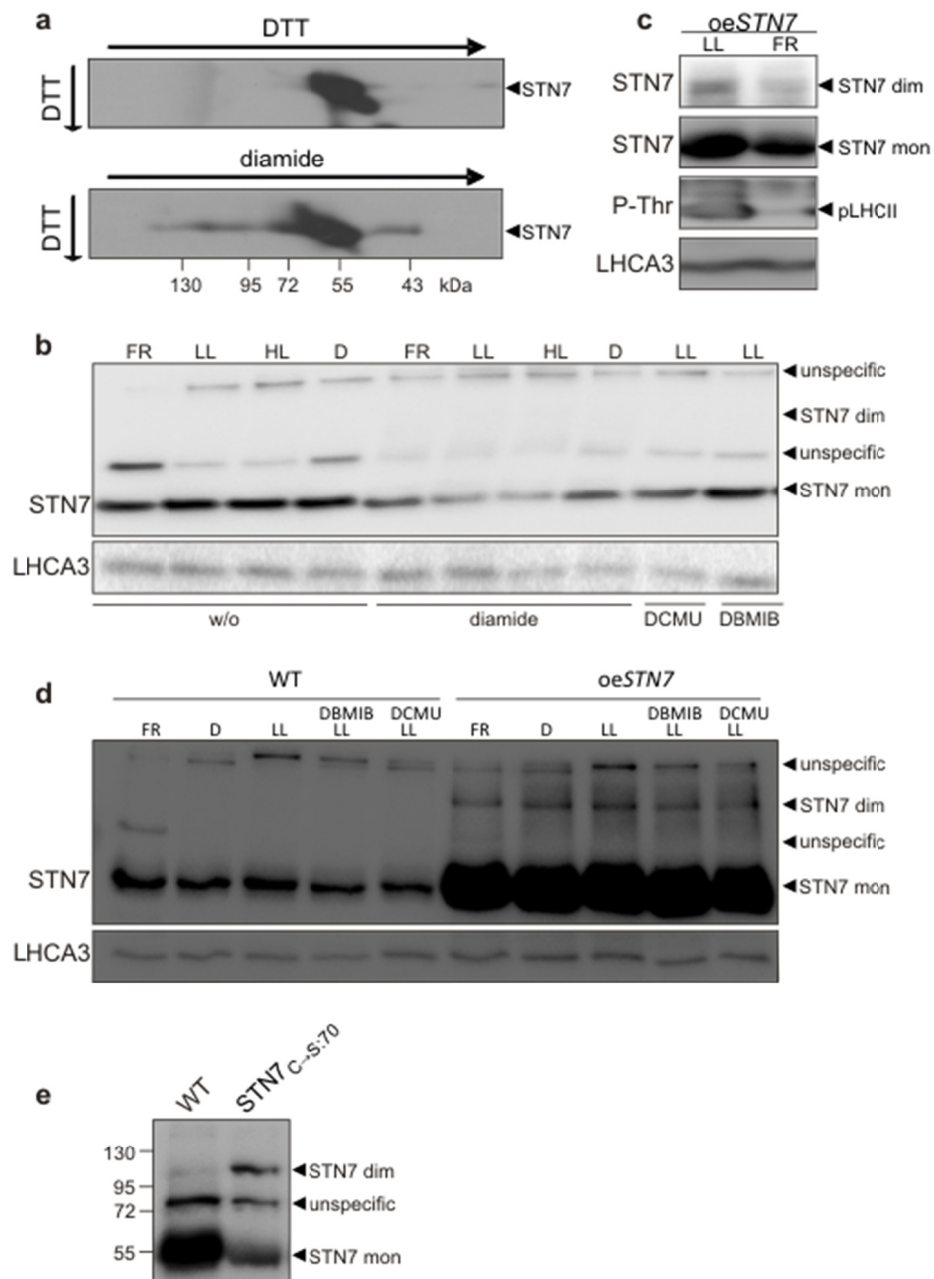


**Figure 29 Elusive formation of a putative STN7 dimer in the WT.**

**a** Diagonal-PAGE of WT thylakoids under reducing or oxidizing conditions. At the top, the results for thylakoid proteins treated with 100 mM DTT before fractionation in the first dimension (reducing conditions) are shown. For the bottom panel, thylakoid proteins were treated with 200 mM diamide prior to separation in the first dimension (oxidizing conditions). For the second dimension reducing conditions (100 mM DTT) were applied in both cases. Proteins were transferred to PVDF membrane and immunolabeled with antibodies specific for STN7. **b** Lack of visible STN7 dimer formation under several various lighting conditions and chemically modulated PQ redox states. WT plants were dark-adapted for 30 min or exposed to LL ( $80 \mu\text{mol photons m}^{-2}\text{s}^{-1}$ ), HL ( $700 \mu\text{mol photons m}^{-2}\text{s}^{-1}$ ) or

FR for 10 min. Furthermore, 20  $\mu\text{M}$  of DCMU or 200  $\mu\text{M}$  of DBMIB solutions were infiltrated into detached leaves prior to LL treatment. Isolated thylakoids were then either treated with 200 mM diamide before separation via non-reducing SDS-PAGE or left untreated (w/o). Proteins were transferred to PVDF membrane and immunodecorated with STN7- or LHCA3-specific antibodies. For STN7 20  $\mu\text{g}$  and for LHCA3 3  $\mu\text{g}$  of chlorophyll were loaded. **c** STN7 dimer formation in *oeSTN7* under low light (LL; 60  $\mu\text{mol photons m}^{-2}\text{s}^{-1}$ ) and FR conditions. *oeSTN7* plants were exposed for 30 min to FR and subsequently transferred to LL for 30 min. Thylakoids were subjected to Western blot analysis using antibodies raised against STN7, as well as phosphothreonine (pThr) or LHCA3 after SDS-PAGE. For STN7 20  $\mu\text{g}$ , for P-Thr 1  $\mu\text{g}$  and for LHCA3 3  $\mu\text{g}$  of chlorophyll were loaded **d** Thylakoids of FR-adapted WT and *oeSTN7* plants were resuspended in phosphorylation buffer and exposed to FR, D, or LL (60  $\mu\text{mol photons m}^{-2}\text{s}^{-1}$ ) for 10 min. Additionally, LL samples were spiked with 50  $\mu\text{M}$  DBMIB or 5  $\mu\text{M}$  DCMU during light exposure. All samples were analyzed by Western blot applying STN7- or LHCA3-specific antibodies. For STN7 20  $\mu\text{g}$  and for LHCA3 3  $\mu\text{g}$  of chlorophyll were loaded. **e** Visualization of STN7 dimers. Isolated thylakoids of LL-adapted WT and STN7<sub>C→S:70</sub> plants corresponding to 20  $\mu\text{g}$  of Chlorophyll were mixed with non-reducing loading buffer and heated for 5 min at 75 °C prior to separation via SDS-PAGE. Proteins were transferred to PVDF membrane and immunodecorated with STN7-specific antibodies.

In the course of this work a method to detect the putative STN7 dimer (110-kDa) in the first dimension, even as a faint band in WT thylakoids, was developed. To this end, thylakoids were solubilized in non-reducing loading buffer, followed by a heating step for 5 min at 75 °C, before performing non-reducing SDS-PAGE (**Figure 29 e**). Possibly, other proteins covering the dimer region undergo conformational changes or become degraded by this heat treatment and thereby lay bare the STN7 dimer. Further analyses applying this method will be subject to future work.

#### 3.4.11 The two N-terminal Cys residues of STN7 are involved in STN7 dimerization

Most attempts to detect STN7 dimers in WT plants by one-dimensional PAGE analysis, even under oxidizing conditions (diamide treatment), failed. However, in the lines expressing STN7 variants with single Cys-Ser exchanges (STN7<sub>C→S:65</sub> and STN7<sub>C→S:70</sub>), the putative STN7 dimers, could be detected (**Figure 30 a**). The STN7 dimers appeared under both normal and oxidizing conditions (diamide treatment), and disappeared under reducing conditions (DTT treatment).

Similar to *oeSTN7* (**Figure 29 c**), STN7<sub>C→S:70</sub> plants exposed to different light conditions showed a significant variation in the total abundance of the mutant STN7, but the STN7 monomer/dimer ratio remained largely constant (**Figure 30 c**).

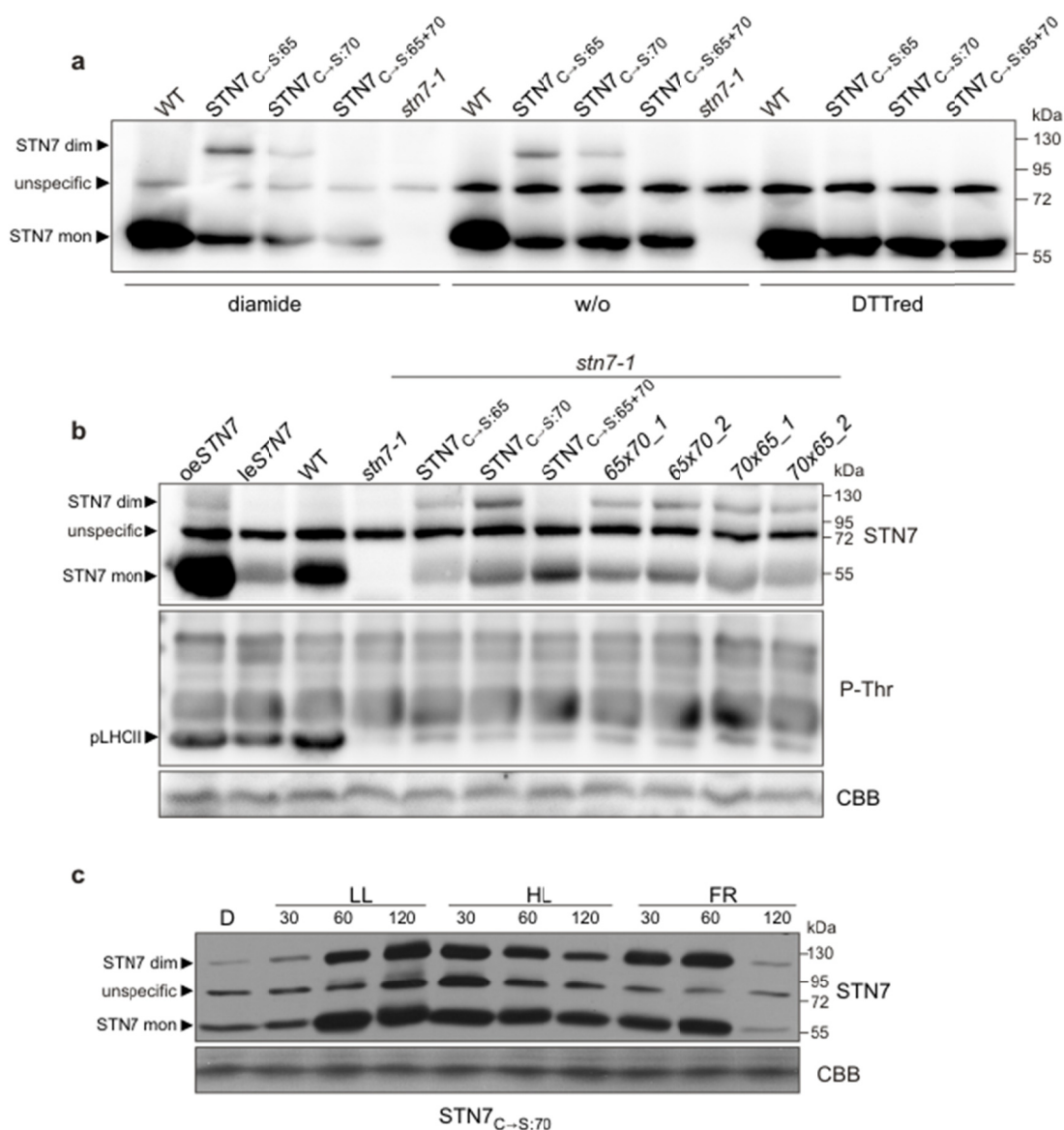


**Figure 30 Dimer formation of STN7 variants.**

**a** Thylakoid proteins were isolated from WT, *stn7-1*, and lines expressing mutated STN7 variants in the *stn7-1* mutant background (STN7<sub>C→S:65</sub>, STN7<sub>C→S:70</sub> and STN7<sub>C→S:65+70</sub>), and were either left untreated (w/o) or were treated with 100 mM DTT or 200 mM diamide before fractionation of 20 µg Chl by non-reducing SDS-PAGE. Proteins were transferred to PVDF membrane and immunolabeled with a STN7-specific antibody. The positions of STN7 dimers (STN7 dim) and monomers (STN7 mon) are indicated by *black arrowheads*. **b** Dimerization and phosphorylation activity of STN7 in *oeSTN7*, *leSTN7*, WT, *stn7-1*, STN7<sub>C→S:65</sub>, STN7<sub>C→S:70</sub>, and STN7<sub>C→S:65+70</sub> lines, as well as in two individuals each from the offspring of the cross STN7<sub>C→S:65</sub> x STN7<sub>C→S:70</sub> (65 x 70), as well as the reciprocal cross (70 x 65). All mutated STN7 variants were expressed in the *stn7-1* background. Thylakoid proteins (20 µg of Chl) were separated on non-reducing SDS-PAGE, transferred to PVDF membrane and immunolabeled with STN7-specific antibodies. Aliquots of the same samples (1 µg of Chl) were fractionated by standard SDS-PAGE and probed with a

phosphothreonine-specific antibody (pThr). The section of the Coomassie brilliant blue-stained (CBB) PVDF membrane displaying the LHCII signal is shown as a loading control. **c** Dimerization of STN7<sub>C→S:70</sub> *in planta* under different light conditions. After 18 h of adaptation to darkness (D), plants were transferred for 120 min to low light (LL, 60 μmol photons m<sup>-2</sup>s<sup>-1</sup>) followed by exposure to high light (HL, 800 μmol photons m<sup>-2</sup>s<sup>-1</sup>) or far-red light (FR) for a further 120 min. STN7 dimers and monomers were detected as in panel **b**, and loading was controlled by staining with Coomassie brilliant blue (CBB). Protein amounts equivalent to 15 μg of Chl were loaded.

In the double Cys-Ser exchange mutant (STN7<sub>C→S:65+70</sub>), formation of the putative STN7 dimers was suppressed, indicating that stable formation of putative STN7 dimers by each of the two STN7 variants with single Cys-Ser exchanges involves Cys-65/Cys-65 and Cys-70/Cys-70 disulphide bridges (**Figure 30 a**). To clarify whether LHCII activity could be restored if cells were given the opportunity to form Cys-65/Cys-70 disulphide bridges, both types of Cys-Ser variants (STN7<sub>C→S:65</sub> and STN7<sub>C→S:70</sub>) were co-expressed *in planta*. However, no recovery of kinase activity was observed (**Figure 30 b**), indicating that the Cys-Ser exchanges *per se* are incompatible with LHCII kinase activity.

To determine whether the ~110-kDa signal truly derives from STN7 dimers, *A. thaliana* lines expressing GFP-tagged STN7 Cys-Ser exchange variants were generated (**Figure 31 a**). In order to demonstrate that the GFP-tag does not interfere with dimerization, lines were analysed in which the GFP-tagged STN7 Cys-Ser exchange variants were expressed in the *stn7-1* mutant background. After exposure to oxidizing or reducing conditions and Western analysis employing a GFP-specific antibody, the lines expressing STN7-GFP, STN7<sub>C→S:65</sub>-GFP, STN7<sub>C→S:70</sub>-GFP and STN7<sub>C→S:65+70</sub>-GFP variants in the *stn7-1* background showed the same STN7 monomer/dimer pattern as the respective STN7 variants without a GFP-tag, and the expected shifts in molecular weight could be observed (compare **Figure 31 a** with **30 a**). In a second step, pull-down assays using the GFP-Trap®™ system (Chromotek) were performed with GFP-tagged STN7 Cys-Ser exchange variants, which were expressed in the WT background. Strikingly, when lines expressing STN7<sub>C→S:65</sub>-GFP or STN7<sub>C→S:70</sub>-GFP in the WT background were used, native STN7 proteins could also be pulled down (**Figure 31 b**). This allowed us to conclude that STN7/STN7<sub>C→S:65</sub>-GFP and STN7/STN7<sub>C→S:70</sub>-GFP heterodimers could be formed. As expected, for lines expressing STN7<sub>C→S:65+70</sub>-GFP in the WT background, only GFP-tagged STN7 was detected after pull down. In the negative controls (WT and *stn7-1*) the pull-down assay failed to yield any signals detectable by the STN7-specific antibody (**Figure 31 b**).

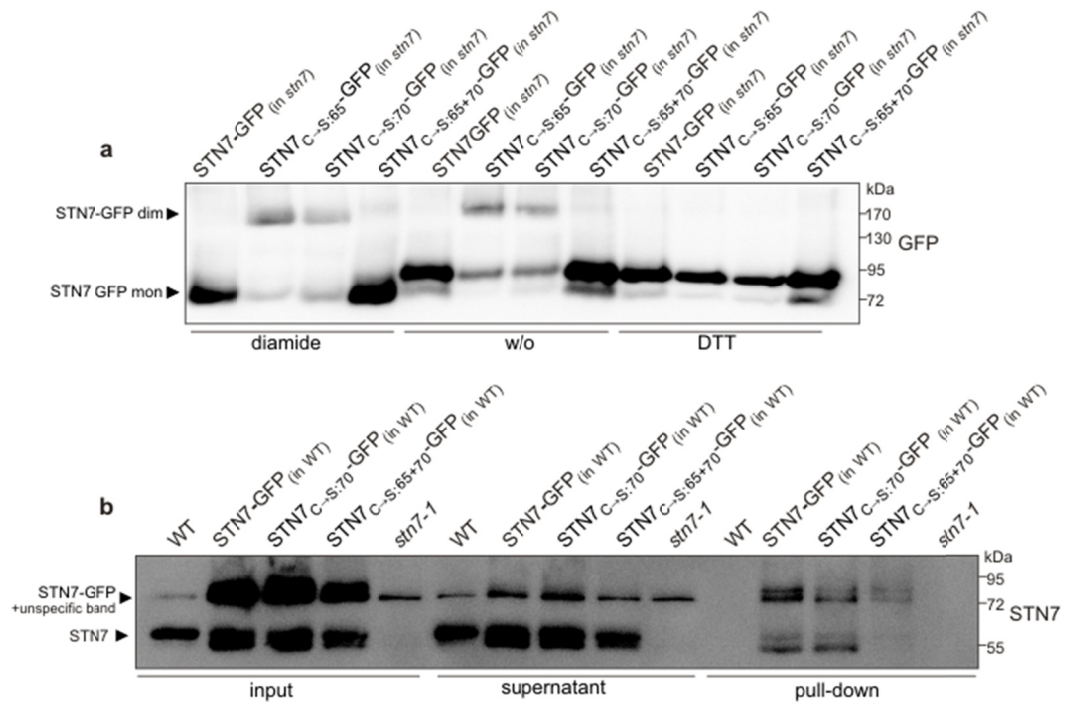


**Figure 31 Confirmation of STN7 homo-dimerization by STN7-GFP-tagged lines.**

**a** STN7-GFP dimer formation, detected by non-reducing SDS-PAGE. Thylakoid proteins were isolated from lines (genetic background *stn7-1*) expressing STN7-GFP, STN7<sub>C→S:65</sub>-GFP, STN7<sub>C→S:70</sub>-GFP or STN7<sub>C→S:65+70</sub>-GFP. Thylakoid proteins remained either untreated (w/o) or were treated with 100 mM DTT or 200 mM diamide, and subsequently separated on a non-reducing SDS-PAGE gel. The GFP fusions were detected by Western analysis using GFP-specific antibodies. **b** Pull-down assay using the GFP-Trap® to identify interactors for GFP fusion proteins. Thylakoids isolated from WT lines expressing STN7-GFP, STN7<sub>C→S:70</sub>-GFP or STN7<sub>C→S:65+70</sub>-GFP, as well as WT and *stn7-1* as controls, were solubilized with  $\beta$ -DM (“input”) and applied to GFP-Trap® beads. After 2 h of incubation the supernatant was removed, and after three successive washing steps proteins were finally eluted (“pull-down”). Aliquots equivalent to 10  $\mu$ g of Chl were fractionated by SDS-PAGE and analyzed on Western blots with STN7-specific antibodies.

### 3.4.12 STN7 single cysteine mutants provide evidence for further intermolecular interaction partners

Interestingly, diagonal-PAGE analyses, conducted with thylakoids of the single cysteine mutant STN7<sub>C→S:70</sub>, revealed an additional intermolecular interaction of STN7 with an unknown protein besides STN7 dimer formation (**Figure 32**). The regularly detected unspecific band of around 80 kDa is overlapping with this signal in immunoblot analyses of first dimension SDS-PAGEs. Regarding its size the interacting protein is about 22 to 26 kDa. Pull-down assays to reveal the identity of this interacting protein were not successful so far. Thus, potential interaction

partners within the respective molecular weight range, like Rieske or LHCII, could not be confirmed.

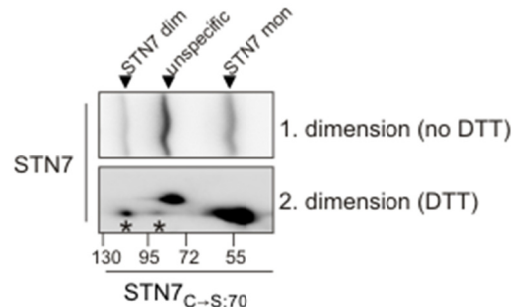


**Figure 32 Diagonal-PAGE of STN7<sub>C→S:70</sub> thylakoids under oxidizing conditions.**

Thylakoids of STN7<sub>C→S:70</sub> were isolated and separated on a non-reducing SDS-PAGE (*upper panel*). Gel stripes were incubated in 100 mM DTT before second dimension separation (*lower panel*). Proteins of first and second dimension gels were transferred to PVDF membrane and immunodecorated with antibodies specific for STN7. Positions of size marker bands are indicated below. STN7 monomer (STN7 mon), STN7 dimer (STN7 dim) and the unspecific band are labeled at the top with *black arrowheads*. STN7 signals originating from the STN7 dimer and an additional intermolecular interaction, which is covered by the unspecific band in the first dimension, are marked with an *asterisk* in the second dimension.

### 3.4.13 Redox sensitivity of STN7 beyond N-terminal cysteines

The STN7 monomer shows a clear size-shift response to redox treatment on non-reducing SDS-PAGE. WT thylakoids were isolated and incubated for 3 h at room temperature in a series of buffers containing ascending ratios of reduced to oxidized DTT. Increasing reducing conditions led to an overall enhanced detection of STN7 protein levels and the appearance of an additional band running below the STN7 monomer representing an apparently 3-4 kDa smaller form of STN7. Under oxidizing conditions this fraction of STN7 is possibly not detectable by immunoblot because of its distribution to various high molecular weight aggregates/complexes. Alternatively, the total amount of STN7 that enters the gel is lower in the absence of DTT. The down-shift of STN7 upon reduction could be explained by the loss of a redox sensitive cofactor (**Figure 33**). Interestingly, thylakoids of STN7<sub>C→S:65+70</sub> plants expressing STN7 without the N-terminal redox sensitive cysteine motif behaved similar to WT in this assay. This indicates that the N-terminal CxxxxC motif is not the only redox sensitive site of the STN7 kinase.

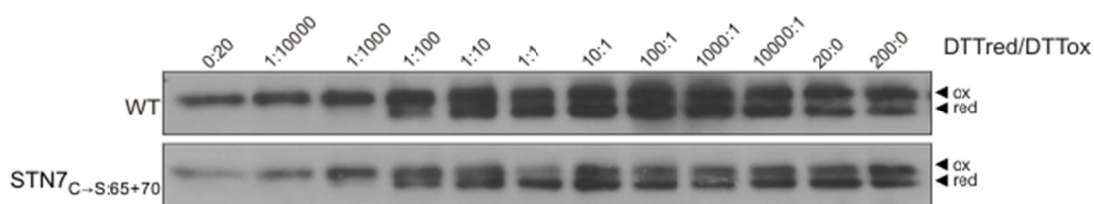


**Figure 33 Redox titration of STN7 variants.**

Isolated thylakoid membranes of WT and STN7<sub>C→S:65+70</sub> were resuspended in 100 mM MOPS pH 7.0, 330 mM sorbitol (pH 7.0) and equilibrated at various redox potentials using the DTTred/DTTox redox couple. After 3 h incubation at RT, samples were separated on non-reducing SDS-PAGE, proteins were transferred to PVDF membrane and antibodies specific for STN7 were applied. DTTred/DTTox ratios are indicated for each lane. Oxidized (ox) and reduced (red) running forms of the STN7 monomer are indicated by *black arrowheads*.

#### 3.4.14 Some indication that STN7 interacts directly with thioredoxin independent of its N-terminal cysteines

Regulation of STN7 and especially its inactivation under HL is supposed to be mediated via stroma located thioredoxins (TRX-f and -m) (Lemeille and Rochaix 2010; Rintamaki et al. 2000). However, until now no such interaction between STN7 and TRXs was shown. To address the question of a potential direct STN7-TRX interaction recombinant TRX-f and TRX-m with single Cys-Ser residue exchanges in the catalytic CGPC-motif (recΔTRX) were immobilized on Ni-NTA resin. Due to this single Cys-Ser residue exchange, the conserved cysteine of the respective motif is able to form stable covalent bonds instead of transient interactions during the disulfide bridge interchange reaction by which TRXs reduce their substrates. In this way, targets of TRXs are trapped as stable dimeric intermediates of the latter process. To covalently bind potential TRX targets, thylakoids of WT were solubilized with 1.5 % (w/v) digitonin and incubated with recΔTRX-coupled resin. After several washing steps potential interaction partners were eluted from the resin by applying DTT-containing buffer and analyzed by western blot. Although shifted in size, a weak STN7 signal could be detected in the elution fraction of the recΔTRX-f resin whereas no STN7 was detectable in the recΔTRX-m elution fraction (**Figure 34 a**). The covalent binding of STN7 to recΔTRX-f was further supported by the significant decrease of STN7 in the flow-through fraction compared to the initial input (**Figure 34 a**).

A TRX mobility shift assay was performed to independently confirm a direct interaction of TRX-f with STN7. To this end, recΔTRX-f was incubated for 30 min with solubilized (0.2 % DOC) thylakoids of WT, *stn7-1* and STN7<sub>C→S:65+70</sub> at room temperature (**Figure 34 b**). A covalent binding of TRX-f to STN7 would lead to a shift of the STN7 signal about the size of

TRX on non-reducing SDS-PAGE gels. However, the expected STN7-TRX-f linkage product could not be detected by Western blot. The STN7 signal seemed to vanish completely upon TRX-f addition (**Figure 34 b**). It remains unclear whether TRX-f treatment led to a precipitation of STN7 or the formation of non-detectable high molecular cross-linked aggregates. Interestingly, also STN7 devoid of the luminal N-terminal cysteines reacted similar, suggesting that a postulated stroma located cysteine motif (Cys 187 and Cys 191) is responsible for this presumable interaction (Puthiyaveetil 2011). A knock-out of this stromal cysteine motif would help to clarify this issue. Nevertheless, both assays independently hint at a possible direct interaction of STN7 and TRX-f.

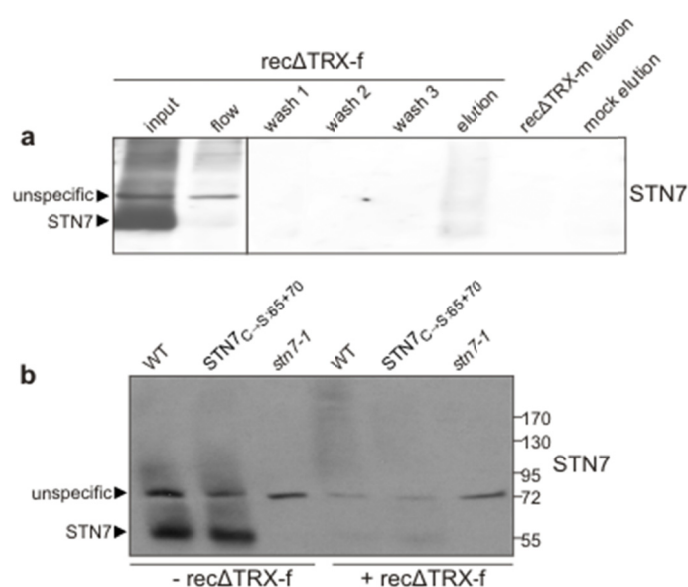


**Figure 34 Affinity chromatography and mobility shift assay indicate STN7-TRX-f interaction.**

**a** Thioredoxin affinity chromatography. His-tagged recTRX-f and -m, with one cysteine exchanged to serine (recΔTRX-f,-m), were expressed in *E. coli* and subsequently purified and bound to Ni-NTA. Thylakoids corresponding to 2 mg of Chl were solubilized with 1.5 % (w/v) digitonin, incubated for 60 min with recΔTRX-resin, washed and eluted with 10 mM DTT. Elutions of recΔTRX-f and -m resins were subjected to Western blot using STN7-specific antibodies. Solubilized WT thylakoids (input; 10 μg Chl), the flow through of the recΔTRX-f resin (flow; equivalent to 10 μg Chl), washes 1-3 of the recΔTRX-f resin and the elution of an equally treated Ni-NTA resin without coupled recΔTRX (mock elution) were loaded as controls. **b** TRX-f mobility shift assay. Thylakoid membranes (10 μg Chl) of WT, STN7<sub>C→S:65+70</sub> and *stn7-1* mutants were solubilized with 0.2 % DOC and incubated with 25 μg recΔTRX-f for 30 min in 100 mM MOPS pH 7.0 and 330 mM sorbitol at room temperature. Proteins were separated by non-reducing SDS-PAGE, blotted to PVDF membrane and antibodies specific for STN7 were applied.

### 3.5 In-depth analysis of the chloroplast protein kinase STN8

#### 3.5.1 STN8 protein levels do not respond to light treatments

Similar to STN7, also STN8 activity is regulated by changes in light quality and quantity (Bonardi et al. 2005; Tikkanen et al. 2010). Especially FR-light and HL lead to a decrease respectively increase in PSII core protein phosphorylation (Tikkanen et al. 2010; Tikkanen et al. 2008a). To investigate whether STN8 activity and protein amounts are similarly regulated in a light-dependent manner as shown for STN7, WT plants were exposed to LL for 2 h after 18 h of darkness and subsequently transferred for 4 h to FR or HL ( $800 \mu\text{mol photons m}^{-2}\text{s}^{-1}$ ). In contrast to STN7, STN8 protein levels did not markedly changed upon the performed light-shift treatments (**Figure 35**). Moreover, plants exposed to LL for up to 9 h, basically showed no significant variations in STN8 protein levels during a full day time-course (**Figure 35**).

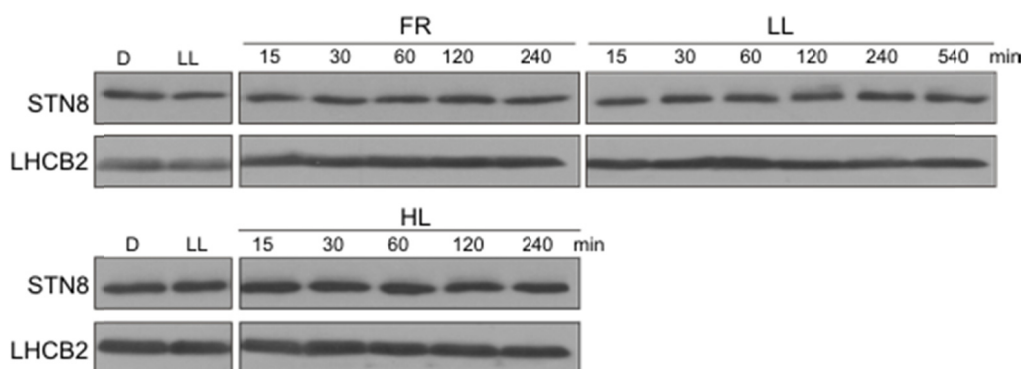


**Figure 35** Variation of STN8 protein levels upon D, LL, FR and HL exposure.

WT plants were dark-adapted for 18 h, transferred to LL ( $80 \mu\text{mol photons m}^{-2}\text{s}^{-1}$ ) for 2 h and then to FR or HL ( $800 \mu\text{mol photons m}^{-2}\text{s}^{-1}$ ) for additional 4 h. Leaf material was collected after each light treatment and thylakoids were isolated, fractionated by SDS-PAGE and analyzed by Western blot using antibodies specific for STN7 and LHCB2 (loading control).

#### 3.5.2 STN8 overexpression increases PSII phosphorylation and decreases PSII-supercomplex formation

To determine the effect of elevated STN8 accumulation on thylakoid phosphorylation, WT, *stn8-1*, *stn7 stn8* and *oeSTN8* plants were exposed for 2 h to LL ( $80 \mu\text{mol photons m}^{-2}\text{s}^{-1}$ ) after 18 h dark-adaptation followed by either 4 h of HL ( $1000 \mu\text{mol photons m}^{-2}\text{s}^{-1}$ ) or 2 h of FR. Isolated thylakoid membranes were then fractionated by SDS-PAGE and thylakoid protein phosphorylation was monitored by Western blot using phosphothreonine-specific antibodies

(**Figure 36 a**). *oeSTN8* plants exhibited a significant increase in PSII core protein phosphorylation under all investigated light conditions. While PSII phosphorylation in WT plants is decreased in the dark compared to LL, it remains on LL levels in *oeSTN8* lines. Even after FR treatment residual PSII phosphorylation is exclusively detected in *oeSTN8* thylakoids. Under LL solely the pCP43 levels are significantly increased compared to WT. However, under STN8 activity inducing HL conditions the strongest increase in PSII core protein phosphorylation in *oeSTN8* compared to WT was observed. It is worth mentioning that pLHCII level behaved similar to WT throughout the experiment (**Figure 36 a**).

Based on experiments with *stn8-1* mutant plants, the phosphorylation of thylakoid membrane proteins, in particular of the PSII core proteins, was suggested to affect the formation of PSII supercomplexes or more precisely the degradation of the latter under HL (Tikkanen et al. 2008a). To validate these observations, BN-PAGEs of *oeSTN8* thylakoids were performed to determine the effects of increased PSII phosphorylation on PSII-supercomplex formation after exposure to 18 h D, 2 h LL ( $80 \mu\text{mol photons m}^{-2}\text{s}^{-1}$ ) or 2 h HL ( $1200 \mu\text{mol photons m}^{-2}\text{s}^{-1}$ ). Although BN-PAGEs after solubilization with 1.5 % digitonin did not reveal significant differences between WT and *stn8-1*, a minor decrease in the amount of PSII supercomplexes in *oeSTN8* was detected (**Figure 36 b left**). More pronounced differences in PSII-supercomplex accumulation were obtained for the respective lines after solubilization with 1.5 %  $\beta$ -DM. Here, WT plants showed again more PSII supercomplexes than *oeSTN8* but also fewer PSII supercomplexes than *stn8-1*, which is in accordance to recent findings (**Figure 36 b right**) (Tikkanen et al. 2008a). However, in contrast to Tikkanen et al. (2008a) these differences were observed under all three applied light conditions not only under HL.

Additionally 2D BN/SDS-PAGEs were performed on the HL treated samples to check for the distribution of the PSII core proteins between PSII supercomplexes, dimers and monomers. In *stn8-1* more D1 (PSBA) accumulation was observed in the very high molecular PSII-complexes compared to WT, whereas the opposite was the case for *oeSTN8* (**Figure 36 c**). These results are in accordance with those obtained by Tikkanen et al. (2008a) for *stn7 stn8* mutants. However, it has to be noted that under the conditions used in this work the specificity was much less pronounced.

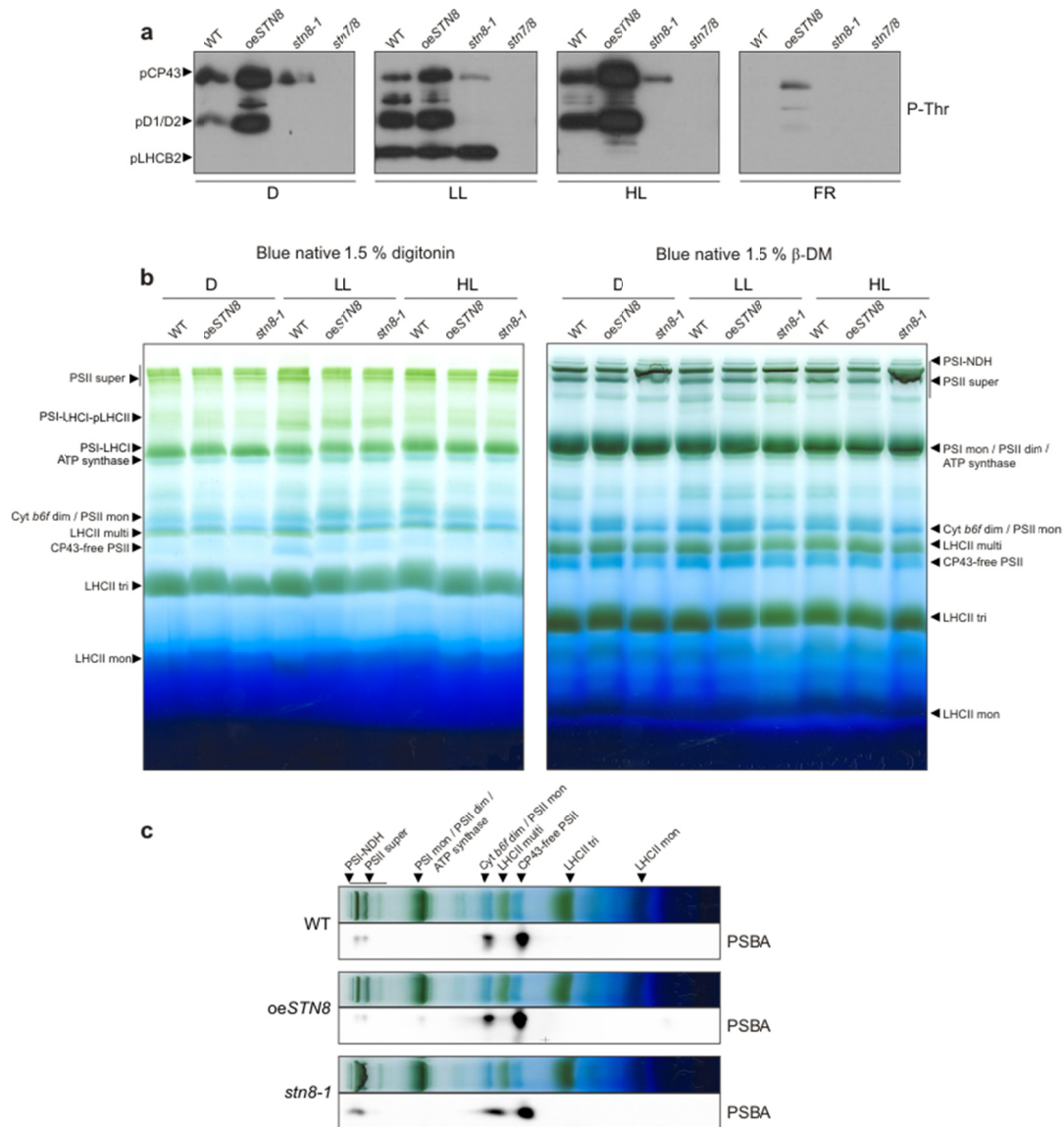


**Figure 36 STN8 dosage effects on thylakoid phosphorylation and PSII supercomplex formation.**

**a** Thylakoid protein phosphorylation patterns of WT, *oeSTN8*, *stn8-1* and *stn7 stn8* (*stn7/8*) plants dark-adapted for 18 h (D), subsequently transferred to LL ( $80 \mu\text{mol photons m}^{-2}\text{s}^{-1}$ ) for 2 h and for additional 2 h to FR or 4 h to HL ( $1000 \mu\text{mol photons m}^{-2}\text{s}^{-1}$ ). After exposure, isolated thylakoids were analyzed by SDS-PAGE and immunoblot applying phosphothreonine-specific antibodies (pThr). The positions of phosphorylated LHCII (pLHCII), CP43 (pCP43) and D1/2 (pD1/2) are indicated by *black arrowheads*. **b** Supercomplex pattern of WT, *oeSTN8* and *stn8-1* on BN-PAGE. Thylakoid membranes of WT, *oeSTN8* and *stn8-1* plants, either exposed to LL ( $80 \mu\text{mol photons m}^{-2}\text{s}^{-1}$ ) for 2 h, HL ( $1200 \mu\text{mol photons m}^{-2}\text{s}^{-1}$ ) for 2 h or kept in the dark for 18 h, were solubilized with 1.5 % digitonin (*left panel*) or 1.5 %  $\beta$ -DM (*right panel*) and separated by BN-PAGE. **c** BN-PAGE lanes of HL treated samples (shown in **b**) were subjected to second dimension SDS-PAGE, blotted to PVDF membrane and analyzed by D1 (PSBA) - specific antibodies. Protein chlorophyll complexes are indicated by *black arrowheads* as in **Figure 8 a** and **16 b**.

### 3.5.3 *oeSTN8* is slightly less susceptible to PSII photoinhibition

Even though based on two different theories, Fristedt et al. (2009) and Tikkanen et al. (2008a) claimed a slowed down D1 repair in *stn7 stn8* and *stn8-1*. Accordingly, this would result in increased sensitivity towards photoinhibition, which translates into lower Fv/Fm values compared to WT during HL kinetics. These results are in conflict with Bonardi et al. (2005), where for *stn8-1* only a slight susceptibility to HL was observed. Moreover, all experiments performed in this work, using various light intensities in order to detect a photoinhibition phenotype for *stn8-1* failed. Interestingly, *oeSTN8* showed a certain tendency to significant differences in most of the experiments. One representative experiment is shown in **Figure 37**. Here plants were exposed to fluctuating light intensities switching every 3 min from LL (10  $\mu\text{mol photons m}^{-2}\text{s}^{-1}$ ) to HL (1250  $\mu\text{mol photons m}^{-2}\text{s}^{-1}$ ). While *stn8-1* and WT plants did not differ significantly in their Fv/Fm values, *oeSTN8* constantly showed above WT levels. Possibly, light fluctuations enhance the positive effect of elevated STN8 levels at the onset of HL exposure, by allowing a faster response to sudden light stress.

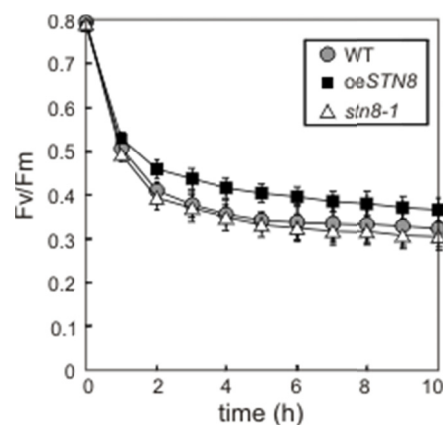


**Figure 37** PSII photoinhibition time-course of WT, *stn8-1* and *oeSTN8* plants.

WT, *stn8-1* and *oeSTN8* plants were exposed to fluctuating blue light intensities for 10 h by switching every 3 min from HL (1250  $\mu\text{mol photons m}^{-2}\text{s}^{-1}$ ) to LL (10  $\mu\text{mol photons m}^{-2}\text{s}^{-1}$ ). The maximal quantum yield of PSII, Fv/Fm, was measured every 60 min after the LL phase and additional 5 min dark adaptation. HL exposure and PAM measurements were performed by the aid of the Imaging PAM (Heinz Walz GmbH). Average values ( $\pm$  SD) of eight individual plants are shown.

### 3.5.4 Increased STN8 protein levels result in a tendency for larger grana stacks

Fristedt et al. (2009) claimed that PSII phosphorylation mediated by STN8 affects macroscopic folding of the thylakoid membrane, supposing that the negative charges of the

phosphorylated thylakoid proteins repulse the single membrane layers, which leads to a looser stacking and therewith allows for a faster lateral protein movement. Furthermore, it was shown that upon *STN8* knock-out the shape of grana stacks is shifted towards an increased length/diameter (Fristedt et al. 2009). Such differences in the thylakoid ultrastructure can be made visible by transmission electron microscopy (TEM). To this end, WT, *oeSTN8* and *stn8-1* plants were adapted to LL for 1.5 h after 12 h of darkness and chloroplasts were analyzed by TEM. Grana stacks of WT exhibited an average length/width ratio of 0.47/0.11 ( $\pm$  SD 0.07/0.04), *stn8-1* of 0.58/0.06 ( $\pm$  SD 0.10/0.01) and *oeSTN8* of 0.54/0.15 ( $\pm$  SD 0.10/0.06) (**Figure 38**).

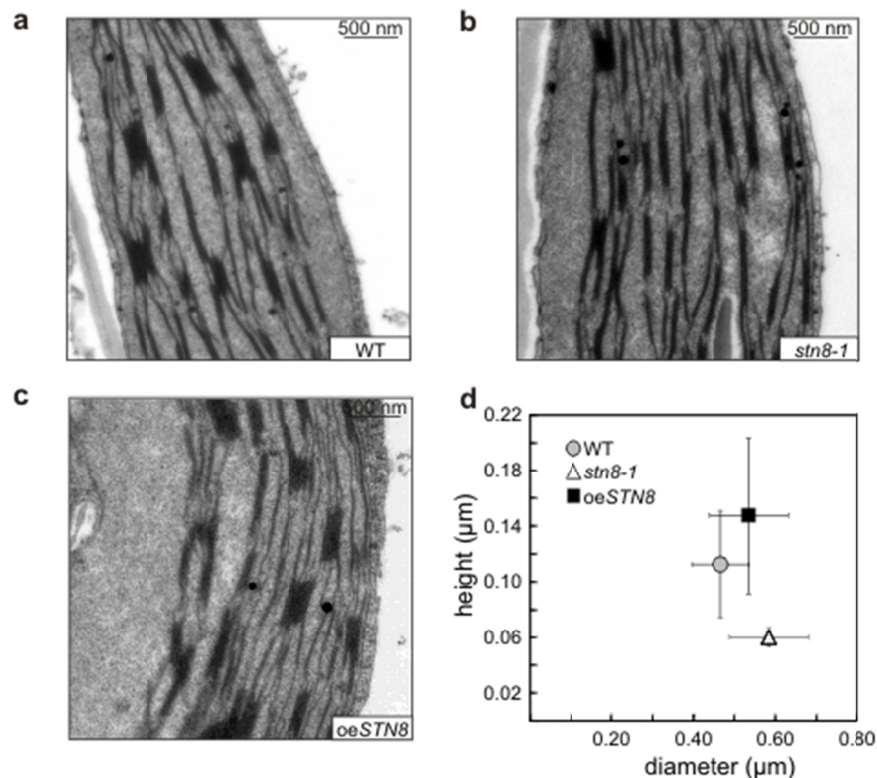


**Figure 38 Analysis of thylakoid ultrastructure of WT, *stn8-1* and *oeSTN8* plants by transmission electron microscopy (TEM).**

Leaves (6<sup>th</sup> leave) of 4-week-old WT, *stn8-1* and *oeSTN8* plants grown under 12 /12 h night/day regime were fixed 1.5 h after onset of light and processed for TEM. Representative cross-sections of chloroplasts are shown in **a**, **b** and **c** for WT, *oeSTN8* and *stn8-1*, respectively. Depicted bars represent 500 nm. Panel **d** shows the quantification of the length and width of grana stacks by means of 8 TEM cross sections of 3 independent leaves.

Thus, the tendency of *stn8-1* to form longer grana stacks (Fristedt et al. 2009) was confirmed. However, the observed decrease in the amount of grana stack layers was not described

before. Consequently, for mutants with increased PSII core protein phosphorylation, one would expect a higher amount of grana stack layers but in return a shorter diameter of grana stacks. Interestingly, *oeSTN8* differed from WT (within the standard deviation) by forming longer and higher grana stacks. Eventually, these results demonstrate a clear effect of increased STN8 levels on the thylakoid ultrastructure.

Summing up, it can be stated that STN8 levels have an effect on PSII-supercomplex formation and thylakoid ultrastructure. However, a clear dosage-dependent correlation cannot be deduced.

### 3.5.5 Increased STN8 levels result in a slightly higher oxidized PQ pool

To determine the effects of altered PSII core phosphorylation on photosynthesis, Chl *a* fluorescence and absorption parameters were recorded for WT, *oeSTN8*, *stn8-1* and *stn7 stn8* plants during dark-light transitions (**Figure 39, 40**). When dark-adapted plants were exposed to LL (22  $\mu\text{mol photons m}^{-2}\text{s}^{-1}$ ) for 6 min, no significant differences in the effective quantum yield of PSII ( $\Phi_{\text{II}}$ ) were detected between WT and *stn8-1*, while in *oeSTN8* plants  $\Phi_{\text{II}}$  was initially higher but eventually converged to WT levels in the course of the measurement (**Figure 39 a**). The parameter 1-qL indicating the excitation pressure of PSII was somewhat lower in *oeSTN8* compared to WT and *stn8-1*, which corresponds to a more oxidized PQ pool (**Figure 39 b**). As expected, the *stn7 stn8* mutant showed higher 1-qL and lower  $\Phi_{\text{II}}$  values than the WT. As *oeSTN8* showed an increased resistance to photoinhibition (**Figure 37**), one might expect detectable aberration in photosynthetic performance under high light intensities already in short-term experiments. However, performing  $\Phi_{\text{II}}$  and 1-qL measurements under increasing light intensities (5 min intervals) no significant differences could be observed (**Figure 39 c, d**). Solely the non-photochemical quenching (NPQ), a photoprotective mechanism (Ruban et al. 2012), showed tendencies to be higher for *oeSTN8* but also for *stn7 stn8* (**Figure 39 c**).

To measure the performance of PSI, the photochemical quantum yield of PSI ( $\Phi_{\text{I}}$ ), and the quantum yield of non-photochemical energy dissipation in PSI due to donor ( $\Phi_{\text{ND}}$ ) or acceptor ( $\Phi_{\text{NA}}$ ) side limitation of WT, *oeSTN8*, *stn7 stn8* and *stn8-1* plants were determined by performing a light curve with increasing light intensities in 5 min intervals (**Figure 40 a, b, c**). All three determined PSI values of the mutant lines except for *stn7 stn8* lay within the standard deviations of the WT (**Figure 40 a, b, c**). However, at lower light intensities up to 216  $\mu\text{mol photons m}^{-2}\text{s}^{-1}$ , *oeSTN8* showed a tendency for higher and *stn8-1* for lower  $\Phi_{\text{I}}$  values.

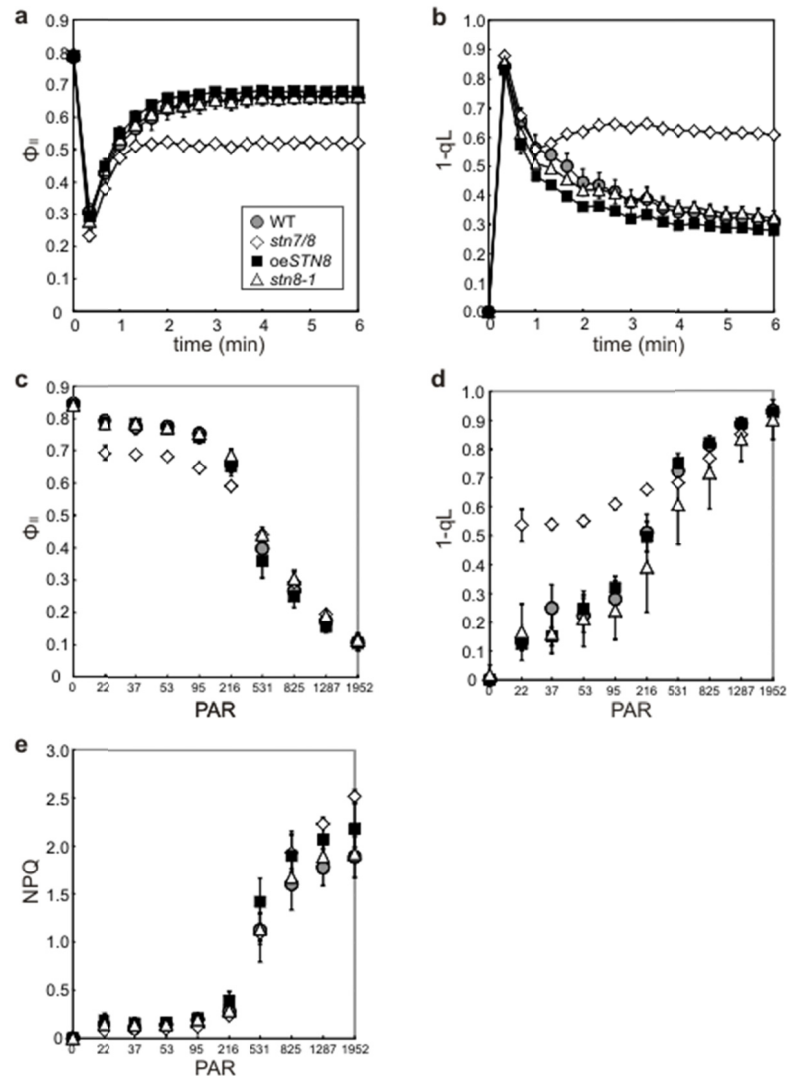


**Figure 39** Kinetics of Chl a fluorescence parameters of WT, *oeSTN8*, *stn8-1* and *stn7 stn8*.

WT, *oeSTN8*, *stn8-1* and *stn7 stn8* plants were grown under an 8 h/16 h day/night regime at  $100 \mu\text{mol photons m}^{-2}\text{s}^{-1}$ .

**a, b** Time-course of effective quantum yield of PSII ( $\Phi_{II}$ ) (**a**) and excitation pressure ( $1-qL$ ) (**b**) of plants pre-incubated for 10 min in darkness, exposed to actinic red light ( $22 \mu\text{mol photons m}^{-2}\text{s}^{-1}$ ) for 6 min. **c, d, e** Light-intensity dependence of Chl a fluorescence.  $\Phi_{II}$  (**c**),  $1-qL$  (**d**) and the non-photochemical quenching of chlorophyll fluorescence (NPQ) (**e**) were monitored during stepwise increasing actinic red light intensities (22, 37, 53, 95, 216, 513, 825, 1,287 and 1,952  $\mu\text{mol photons m}^{-2}\text{s}^{-1}$ , each lasting for 5 min) after 10 min of dark adaptation. PAR, photosynthetically active radiation ( $\mu\text{mol photons m}^{-2}\text{s}^{-1}$ ); circles with grey filling, WT; squares with black filling, *oeSTN8*; triangles; *stn8-1*; diamonds, *stn7 stn8*. Average values ( $\pm$  SD) of five individual plants are shown.

For higher light intensities this tendency was reversed and vanished (**Figure 40 a**). Regarding *oeSTN8*, the higher  $\Phi_{ND}$  caused the lower  $\Phi_I$  at higher light intensities (**Figure 40 a, b**), whereas the lower  $\Phi_{NA}$  was responsible for the higher  $\Phi_I$  at lower light intensities (**Figure 40 a, c**).

Altogether, differences in STN8 protein levels did not significantly affect the photosynthetic performance, except for a slightly increased oxidation of the PQ pool during the transition from dark to LL in *oeSTN8* compared to WT.

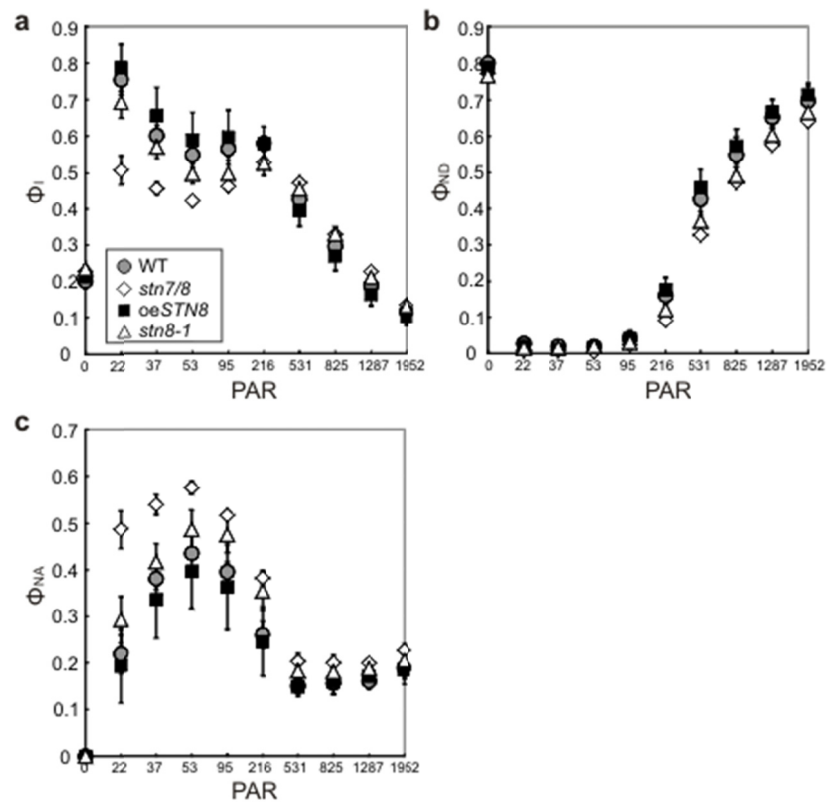


**Figure 40** Light-intensity dependence of absorption parameters of WT, *oeSTN8*, *stn8-1* and *stn7 stn8*.

Plants were grown under an 8 h/16 h day/night regime at 100  $\mu\text{mol photons m}^{-2}\text{s}^{-1}$ . **a, b, c** The photochemical quantum yield of PSI ( $\Phi_I$ ) (**a**), the quantum yield of non-photochemical energy dissipation in PSI due to donor side limitation ( $\Phi_{ND}$ ) (**b**), or due to acceptor side limitation ( $\Phi_{NA}$ ) (**c**) were monitored during stepwise increasing actinic red light intensities (22, 37, 53, 95, 216, 513, 825, 1,287 and 1,952  $\mu\text{mol photons m}^{-2}\text{s}^{-1}$ , each lasting for 5 min) after 10 min of dark adaptation. PAR, photosynthetically active radiation ( $\mu\text{mol photons m}^{-2}\text{s}^{-1}$ ); *circles with grey filling*, WT; *squares with black filling*, *oeSTN8*; *triangles*, *stn8-1*; *diamonds*, *stn7 stn8*. Average values ( $\pm$  SD) of five individual plants are shown.

### 3.6 Interdependence of STN kinase levels

In previous studies a certain substrate overlap of STN7 and STN8 was suggested (Bonardi et al. 2005), which could be ascribed to mutual influence of STN7 and STN8 on protein level. To elucidate such a potential interdependence, thylakoids of LL-acclimated WT, *oeSTN8*, *oeSTN7* and *stn8-1* plants were analyzed by comparative Western blots. The levels of STN7 in WT and *stn8-1* were basically equal and at the most slightly increased in the STN8 overexpressing line (**Figure 41 a.**) *Vice versa* also the STN8 protein level in *oeSTN7* was the same as in WT (**Figure 41 b.**) Thus, increased levels of one STN kinase do not cause a compensatory down-regulation of the other.

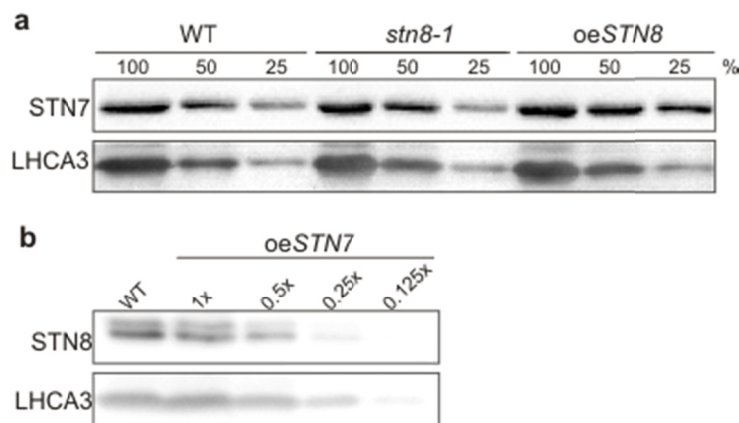


**Figure 41 Interdependence of STN kinase accumulation.**

**a** Accumulation of the STN7 protein in thylakoids of WT, *oeSTN8* and *stn8-1* mutant plants. Thylakoid proteins of each genotype corresponding to 8 µg (100 %), 4 µg (50 %) and 2 µg (25 %) of Chl were loaded on SDS-Gel and detected by immune blot applying specific antibodies against STN7 and LHCA3 (as loading control). **b** Accumulation of STN8 protein in thylakoids of WT and *oeSTN7*. Thylakoid membranes of WT corresponding to 5 µg of Chl and decreasing amounts of *oeSTN7* thylakoids proteins were separated by SDS-PAGE, and STN8 protein levels were estimated by Western blot analysis applying antibodies specific for STN8 and, as loading control, for LHCA3.

## 4 Discussion

### 4.1 STN7 and STN8 are associated with high molecular weight supercomplexes of the thylakoid membrane

With the aid of newly generated STN7 and STN8 specific antibodies, the localization and topology of both kinases in the thylakoid membrane could be further resolved. A single transmembrane domain of STN8 was predicted for the sequence enclosing the amino acids 32 to 62. The kinase domain is supposed to face the stroma and a short N-terminal sequence the lumen (Vainonen et al. 2005). However, there are ambiguous predictions regarding the potential transmembrane helix since several algorithms for TM prediction rather propose a soluble character for STN8 (i.e. TMHMM and SOSUI). The analysis of soluble and membrane fractions of chloroplasts clarified that STN8 appears solely in the thylakoid membrane fraction (**Figure 7 a**). Salt washes of thylakoid membranes further demonstrated a strong membrane integral character for both kinases predominantly based on electrostatic interactions (**Figure 7 b**). Tryptic thylakoid digests in combination with STN8 full-length and peptide-specific antibodies supported a stromal localization of its C-terminal part. (**Figure 11**) (Vainonen et al. 2005). By similar means a STT7-like topology could be confirmed for STN7 with its C-terminal ATP pocket facing the stroma. Regarding the location of the essential N-terminal cysteine motif, a luminal localization could not unambiguously be verified within the scope of this work but a situation similar to STT7 is likely (Lemeille et al. 2009). A way to address this issue could be the generation of STN7 full-length specific antibodies with increased specificity (**Figure 6 b**) or transgenic lines with N-terminal tagged STN7.

In *C. reinhardtii*, STT7 is associated under state 1 and state 2 conditions with a high molecular weight complex, overlapping with fractions of PSI and Cyt *b6f* complex in sucrose density gradients (Lemeille et al. 2009). In this study the question whether STN7 and STN8 act as monomeric enzymes or are associated with other proteins in higher molecular weight complexes was addressed by proteolytic assays, 2D BN-/SDS-PAGE and sucrose density gradient centrifugation. The presented results on protease treatments suggest that both kinases are embedded in a large molecular complex. Thereby, the stroma-exposed C-termini of STN7 and STN8 comprising the respective kinase domains seemed to be partially protected by interacting proteins (**Figure 10, 11**). In 2D BN-/SDS-PAGE analyses immune-specific signals of both kinases were distributed throughout the gel, suggesting multiple assembly states and association

with high molecular weight supercomplexes (**Figure 8 a**). The presence of multiple assembly states of high molecular weight were further supported by data obtained from sucrose density gradient centrifugation (**Figure 8 b**). Thus, there is comprehensive evidence that both STN7 and STN8 are not operating as single enzymes but are embedded in complex-structures.

Interestingly, STN8 does not accumulate in plants lacking PSII complexes (*hcf136*) (**Figure 9**). This PSII-dependent accumulation of STN8 probably reflects the necessity of its close contact with the PSII core proteins which at the same time represent the main substrate. In line with these findings, STN8 was mainly detected in the grana stacks or grana margins, the same thylakoid fractions where PSII accumulates (**Figure 8 c**). These observations suggest a direct phosphorylation of PSII subunits by STN8. Alternatively, a kinase cascade residing in close proximity to the PSII complex is conceivable.

Hou et al. (2003) demonstrated that washing of thylakoids with 2 M NaBr leads to a loss of PSII core protein phosphorylation capacity. Contrarily, **Figure 7 b** shows that after similar treatment most of the STN8 protein remains bound to the membrane. Therefore, it is tempting to speculate that washes with NaBr do not directly affect STN8 activity, but rather remove kinases that are part of a putative PSII core phosphorylation cascade. To obtain more reliable evidence for the latter, salt washed thylakoid fractions should be tested in parallel for STN8 activity and protein accumulation.

The inability of mutants devoid of a functional Cyt *b6f* complex to accumulate STN7 (**Figure 15 c**) is in line with studies that detected LHCII phosphorylation activity in purified Cyt *b6f* complexes (Gal et al. 1990). Furthermore, in differential fractionated thylakoids STN7 and the Rieske protein (PETC) were both enriched in the stroma lamellae fraction independent of state 1 or 2 conditions. In *C. reinhardtii* also STT7 was shown to tightly interact with the Rieske protein (Lemeille et al. 2009). The prevailing idea of STN7 activity being dependent on the physical interaction between STN7 and the Cyt *b6f* complex is further supported by the here presented results (**Figure 8 c**). The LHCII phosphatase TAP38/PPH1, sharing the same substrate with STN7, was similarly found to be enriched in the stroma lamellae (Shapiguzov et al. 2010). As state transitions are believed to predominantly occur in the grana margins (Tikkanen et al. 2008b), the tendency for a spatial separation of STN7 from PSII-LHCII would give hints for an involvement of a kinase cascade in LHCII phosphorylation. However, differential centrifugation is certainly not the ideal method to isolate grana margins in a sufficiently pure manner. Therefore, a direct phosphorylation of LHCII by STN7 is still one of the most likely options. Especially

under PSII light, when the interplay between TAP38 and STN7 activity leads to a balanced LHCII phosphorylation, a localization of both enzymes in close proximity to the phosphorylation sites of pLHCII bound to PSI outside the grana stacks is to be expected. Moreover, two running forms of STN7 can be detected (**Figure 8 c**). While the presumably larger one seems to be evenly distributed throughout the thylakoid membrane, the lower migrating band accumulates mainly in the stroma lamellae and could represent a fraction of STN7 that is involved in its own turnover (Willig et al. 2011).

## **4.2 Control of *STN7* transcript abundance and transient STN7 dimerization are involved in the regulation of STN7 activity**

### **4.2.1 At what level is STN7 abundance regulated?**

In *A. thaliana*, STN7 protein abundance is regulated in a light-quality dependent manner (Willig et al. 2011). Furthermore STT7, the STN7 orthologue in *C. reinhardtii*, is subject to proteolytic degradation after prolonged exposure to high light levels (Lemeille et al. 2009). Here, we have demonstrated that, in addition to concomitant decreases in *STN7* mRNA and protein levels in *A. thaliana* plants exposed to either HL or FR (**Figure 12 a-d**), several mutant lines (*hcf136*, *psad1-1 psad2-1*, *petc-1*; **Figure 15 c, d**) exhibit alterations in STN7 protein abundance and corresponding changes in *STN7* mRNA levels, relative to WT. This raises the question whether or not STN7 protein amounts change primarily as a consequence of alterations in the abundance of *STN7* mRNA - i.e. via regulation of STN7 abundance at the transcript level. Alternatively, they might be mainly due to post-translational control of protein accumulation, as suggested previously for STT7/STN7 (Lemeille et al. 2009; Willig et al. 2011), with changes in *STN7* transcript levels arising from a secondary effect, e.g. being mediated by plastid retrograde signalling. Some lines of evidence suggest that the latter scenario applies. Thus, in the Cys-Ser exchange line STN7<sub>C→S.70</sub>, the mutant protein seems to be subject to increased degradation despite the fact that *STN7* transcript levels increase, possibly as a compensatory response (**Figure 13 a, b**). Moreover, it seems also very likely that in mutants without PSII (*hcf136*) or a functional Cyt *b6f* complex (*petc-1*), down-regulation of the STN7 protein occurs primarily at the protein level, whereas the drop in *STN7* transcripts in these genotypes might be mediated by retrograde signalling. In this context it is interesting to note that STN7 itself has also been implicated in retrograde signalling, as a component of a signal transduction pathway that relays information on the redox state of the PQ pool to the nucleus (Bonardi et al. 2005; Pesaresi et al. 2009). It

therefore appears possible that STN7 can regulate its own expression at the transcriptional level when altered STN7 levels result in changes in retrograde signalling. In the case of the down-regulation of STN7 transcript and protein levels induced by HL and FR, it cannot be excluded that regulation at the transcript level is the driving force behind the observed changes in STN7 protein abundance. However, for the *oeSTN7* and *leSTN7* lines (**Figure 13 a, b**), it is clear that the altered transcript levels are responsible for the alterations in STN7 protein level. In summary, it was not only confirmed that STN7 amounts can be regulated at the post-translational level, but also shown that modes of regulation at the transcript level are utilized. In other cases, where STN7 protein and transcript levels change in a concerted way, it remains to be clarified which is the cause and which the consequence.

#### 4.2.2 At what level is STN7 activity regulated?

It is clear that the level of LHCII phosphorylation depends on the redox state of the PQ pool and, under HL, also on the stromal redox state, i.e. that of the ferredoxin-thioredoxin system. But does this allow us to conclude that the activity of the STN7 kinase itself is under redox control? No straightforward answer can be given because the abundance of STN7 is also redox dependent (**Figure 15 a, 12 a, b, 14**). Thus, on exposure to HL and FR, both the abundance of STN7 and the level of LHCII phosphorylation decrease. The *oeSTN7* plants with more STN7 also display, in general, more LHCII phosphorylation (**Figure 16 a**). Moreover, in PSI mutants like *psad1-1* and *psae1-3*, both LHCII phosphorylation (Ihnatowicz et al. 2008) and STN7 levels (**Figure 15 a**) are increased. Therefore, it seems possible that under these conditions the intrinsic activity of STN7 is not changed, and that the rise in the total activity simply reflects the increase in the number of molecules present. Conversely, taking the autophosphorylation of STN7, and its increased stability in the phosphorylated state, into account (Willig et al. 2011), it is tempting to speculate that the activity of STN7 itself might regulate STN7 protein levels. This hypothesis is supported by the behavior of the *STN7<sub>C→S:70</sub>* line, in which levels of the mutant STN7 are low, despite an increase in the amount of the corresponding transcript (**Figure 13**). This could be directly related to the lack of LHCII phosphorylation and autophosphorylation activity (**Figure 28, 30 b**). Similarly, *leSTN7* expressing very low amounts of *STN7* might not reach a certain protein threshold level, which is required for efficient self stabilization (**Figure 13**).

The results of this work also clearly show that even when the STN7 kinase is present in excess amounts, it is still subject to redox control and can be inactivated when the PQ pool

becomes oxidized (**Figure 20 b, 25 b, 26 a**). The inhibitor experiments suggest that STN7 is activated by the same mechanisms in WT and *oeSTN7* plants. However, whereas under standard lighting conditions WT and *oeSTN7* plants exhibited very similar levels of LHCII phosphorylation (**Figure 16 a, b, 20 a**), *in-vitro* phosphorylation studies of isolated thylakoids showed that *oeSTN7* accumulated more pLHCII than WT (**Figure 25 c, 26**). This discrepancy between the STN7 activity measured *in vitro* and in *oeSTN7* plants can be explained by assuming that, in intact cells, LHCII phosphorylation is modulated by mechanisms that no longer operate in our *in-vitro* assay. Possible modulatory influences might include a compensatory increase in TAP38/PPH1 activity, a more highly oxidized PQ pool under illumination (**Figure 22 b**) or enhanced inactivation of STN7 via stromal components in *oeSTN7* plants (Rintamaki et al. 2000).

Based on experiments with HL treated *oeSTN7* and WT plants (**Figure 16, 17**), a deactivation of STN7 via the ferredoxin-thioredoxin pathway was suggested to be STN7 dosage dependent. Both, the amount of active STN7 kinase and the accumulation of reduced thioredoxin in the stroma upon HL exposure, significantly affected the efficiency of STN7 inhibition. The increased amounts of activated STN7 in *oeSTN7* required stronger light intensities for a quantitative deactivation of the same (**Figure 16, 17**). These results strengthen the hypothesis that HL inhibition of STN7 is mediated via a redox-dependent reaction independent of its activation via the Cyt *b6f* complex (Rintamaki et al. 2000). Thus, in contrast to studies of Willig et al. (2011) and Lemeille et al. (2009) (Lemeille et al. 2009; Willig et al. 2011), which present equal levels of LHCII phosphorylation regardless of the amount of accumulated LHCII kinase, a clear STN7 abundance effect becomes evident in this study. However, these dosage-effects of STN7 are overridden by the redox-dependent adjustment of STN7 activity.

#### **4.2.3 Why is LHCII phosphorylation in dark-adapted *oeSTN7* lines higher than in light-adapted ones?**

Owing to their increased LHCII phosphorylation and the larger PSI antenna size (**Figure 20**), thylakoid electron flow is more efficient in *oeSTN7* plants than in either WT or the *tap38-1* mutant, especially at the onset of illumination (**Figure 22, 23**). Remarkably, in *oeSTN7* plants, levels of LHCII phosphorylation and PSI-LHCI-pLHCII complex formation reach their maxima after incubation in the dark (**Figure 16 b, 20 c, d**). This raises the question of why STN7 is active in the dark. Electron transport processes across the thylakoid membrane, e.g. chlororespiration, still occur in the dark (Bondarava et al. 2003; Casano et al. 2000; Pospisil 2011; Rumeau et al.

2007; Schwenkert et al. 2006; Shinopoulos and Brudvig 2012). These processes depend on the presence of reducing equivalents in the stroma, and lead to light-independent reduction of PQ (Rumeau et al. 2007; Shinopoulos and Brudvig 2012) even after complete oxidation of the PQ pool by FR treatment. Therefore, the low PQH<sub>2</sub>/PQ ratio in the dark, which still allows for some binding of PQH<sub>2</sub> to the Qo site of the Cyt *b6f* complex, is sufficient to activate STN7 in WT plants (**Figure 25 a**). This is even more true when the kinase is present in high concentrations, as given in *oeSTN7* plants (**Figure 25 a**). Among the factors that might account for the enhanced LHCII phosphorylation in dark-adapted *oeSTN7* plants are the following: an increased amount of STN7 leads to (i) a higher reduction rate of PQ, (ii) a lower luminal pH, or (iii) more activated STN7 molecules even if the occupancy of the Qo site by PQH<sub>2</sub> is not changed compared to WT.

With regard to the first possibility (i), increased reduction of the PQ pool in the dark (with enhanced LHCII phosphorylation) has been achieved by feeding with glucose and NADPH (Hou et al. 2003; Rintamaki et al. 2000; Tikkanen et al. 2010) and by application of heat stress (Sazanov et al. 1998), suggesting that changing the metabolic state of the chloroplast might allow for an altered PQ redox state. Furthermore, the activity of the NDH complex was reported to be controlled by reversible phosphorylation of the NDH-F subunit, mediated by a so far unknown kinase (Lascano et al. 2003). In this respect, changes in gene expression and thylakoid composition due to altered STN7 expression and retrograde signalling (Pesaresi et al. 2009; Tikkanen et al. 2006) that could lead to a more reduced PQ pool in the dark were considered. However, with the OJIP transient based method to determine the PQ pool redox state in the dark, *oeSTN7* and WT plants showed no significant differences in the fraction of PQH<sub>2</sub> (**Figure 21**). Even though this explanation does not hold for *oeSTN7* plants, it is interesting to note that, like *oeSTN7*, a mutant defective in the E subunit of PSI exhibits increased levels of STN7 (**Figure 15 a**) and of LHCII phosphorylation (Ihnatowicz et al. 2008) even in the dark (Pesaresi et al. 2002), and also shows a marked increase in the reduction state of the PQ pool at least under illumination (Varotto et al. 2000). Furthermore, a *PSBI* knock-out was discussed to disturb the cytochrome b559 pathway by preventing the discharging of PQ in the dark (Bondarava et al. 2003; Schwenkert et al. 2006). Yet, another explanation could be that the *psbi* mutant simply accumulates more STN7 protein.

Regarding the second possible factor (ii) mentioned above, a low luminal pH may act to stabilize PQH<sub>2</sub> in the Qo site, keeping the Cyt *b6f* complex in an STN7-activating mode in the dark, even under conditions where the overall PQ pool is in a relatively more oxidized state

(Vener et al. 1997; Zito et al. 1999). In this scenario, the Qo site in *oeSTN7* might exhibit a higher affinity for the residual PQH<sub>2</sub> than in WT, keeping the Cyt *b6f* complex in a kinase activating mode even at a low PQH<sub>2</sub>/PQ ratio and thereby increasing STN7 activity. Further experiments will be needed to clarify whether the luminal pH is actually decreased in *oeSTN7* plants and whether this contributes to the increase in dark LHCII phosphorylation. In this respect, the significantly lower Fm value of dark-adapted *oeSTN7* plants relative to Fm2 determined after illumination with actinic red light (**Figure 19**) could be a consequence of NPQ induction in the dark due to an increased acidification of the lumen. This correlation between STN7 levels and qE is conceivable, since the amount of PSBS, the key enzyme for NPQ (qE) was shown to be altered in *stn7* mutant plants (Tikkanen et al. 2006).

Taking the experiments with chemical additives into account, the third possibility (iii) seems feasible. *In-vitro* experiments with duroquinol and dithionite (**Figure 25 c, 27**) revealed that an equal PQH<sub>2</sub> reduction by defined amounts of artificial electron donors leads to a significantly stronger increase in LHCII phosphorylation in *oeSTN7* plants. While the *in-vitro* (**Figure 26 b**) and *in-planta* (**Figure 25 a**) application of DBMIB should equally inhibit the Qo sites of the Cyt *b6f* complex in WT and *oeSTN7* plants, LHCII phosphorylation was anyway higher in *oeSTN7*. The same was true for thylakoids of FR-pretreated WT and *oeSTN7* plants which should both reach a maximal PQH<sub>2</sub>/PQ ratio upon LL illumination, since stromal electron acceptors are missing. However, also here thylakoids of *oeSTN7* showed an enhanced *de-novo* LHCII phosphorylation capacity (**Figure 26**). A straightforward explanation of these findings might be the low abundance of the kinase in comparison to Cyt *b6f* (Gal et al. 1997; Lemeille et al. 2009; Wollman 2001). The LHCII Kinase/Cyt *b6f* ratio was estimated to be around 1:60 (in higher plants) (Gal et al. 1997) or 1:20 (in *C. reinhardtii*) (Lemeille et al. 2009). Thus, an excess of STN7 protein compared to WT could lead to a higher occupancy of free STN7-binding sites at the Cyt *b6f* complexes that now contribute to kinase activation in *oeSTN7* plants. The Qo site at the Cyt *b6f* complex still seems to be of overriding importance and ultimately decides on the activation of STN7 depending on the PQ redox state. The five fold excess of STN7 in *oeSTN7* compared to WT seems to elevate its activation probability, which appears to be high enough to outcompete TAP38 activity (**Figure 21**). The increased STN7 levels also speak in favor of STN7 dimer formation being potentially required for kinase activation (**Figure 29, 30**).

But why is the level of LHCII phosphorylation in *oeSTN7* plants decreased in LL compared to D (**Figure 16 a, 20 c, 25 a**) although STN7 protein levels are similar to those found under low

light conditions (**Figure 18**)? An explanation could be seen in the bigger amount of reduced stromal components that were shown to inhibit STN7 activity. Upon light exposure state transitions seems to be under permanent feedback control by the state of the stromal metabolism. Also an enhanced oxidation of the PQ pool under low and moderate illumination (**Figure 22 b, d**) due to an increased formation of PSI-LHCI-pLHCII supercomplexes might account for it. Further unknown factors that influence LHCII phosphorylation in the light could be modulated in the dark, including TAP38/PPH1 activity, even if the latter was claimed not to be affected by light (Elich et al. 1997). The observation that LHCII phosphorylation in the dark seems not to be under the same strict regulation as under LL could be an indication for different regulatory mechanisms acting on STN7 in land plants and *C. reinhardtii*. For the latter state transitions play a role in the switch between LEF and CEF (Finazzi et al. 1999). Here, the *stt7* mutant only shows a phenotype in combination with defects in respiration, suggesting a crucial role for state transitions in the regulation of the ATP status (Cardol et al. 2009; Fleischmann et al. 1999).

#### 4.2.4 What is the physiological significance of STN7 dimerization?

Redox active chemicals like NEM and DTT disturbing any free thiol interaction such as cysteine-mediated dimerization prevented STN7 activity (**Figure 26 c**). An involvement of a dimeric state of STN7 in its own regulation in *C. reinhardtii* was previously mentioned (Lemeille and Rochaix 2010). However, in *A. thaliana* the STN7 dimer in WT plants is very elusive regarding its detection by Western blot. Possibly, the dimeric form of STN7 accumulates to a substantial amount *in planta* but gets lost during purification and electrophoresis due to its weak stability. Alternatively, the dimer conformation is a transient, short lived state of STN7. In *oeSTN7* plants, and lines expressing single Cys-Ser exchanges in STN7, dimers are unambiguously detectable. When the total level of STN7 changes with variant light conditions, the ratio of monomer to dimer forms remains essentially unchanged (**Figure 29 c, 30 c**). Moreover, like for STT7, (Lemeille et al. 2009) replacement of single N-terminal cysteines of STN7 virtually abolished kinase activity, and lines expressing STN7<sub>C→S:65+70</sub> accumulated only STN7 monomers but had equally diminished kinase activity (**Figure 28, 30 a, b**). Thus, neither the dimer nor monomer can be referred to as the active form. Possibly, under normal conditions the two Cys residues might predominantly form an intramolecular disulfide bridge and if one Cys residue is removed by mutation, an intermolecular bond is enforced and the STN7 dimer is formed. However, also in WT the N-terminal Cys residues of STN7 seem to be directly involved

in the formation of redox-sensitive disulfide bridges between two STN7 molecules (**Figure 29 a, e, 30 a**), which might be a prerequisite for its activity, assuming that the Cys residues are not essential for the activity of the kinase domain *per se*. Possibly STN7 dimers normally have a short life time, as suggested by the problems to detect them in WT plants. In fact, the transition from monomer to dimer and *vice versa* might represent the hub at which the redox state of PQ pool and the total amount of STN7 proteins exert their effects on STN7 activation and activity. Thus, the increased STN7 amounts in *oeSTN7* might shift the equilibrium between monomers and dimers, thereby resulting in the unusually high kinase activity in the dark. It was assumed that an interaction of STN7 in *C. reinhardtii* with the Rieske protein of the Cyt *b6f* complex is essential for kinase activation and involves its N-terminal cysteines (Lemeille et al. 2009). Coming back to the kinase activation model via the Cyt *b6f* complex depicted in **Figure 4** (Finazzi et al. 2001), it is tempting to speculate that STN7 is activated as a dimer that then monomerizes upon release from the Cyt *b6f* complex. In this respect, mutation of both N-terminal cysteines would in the first place prevent the interaction with the Rieske protein, which is necessary for activating the kinase. On the contrary, the stable dimers in the single cysteine exchange mutants might get stuck at the kinase binding sites of the Cyt *b6f* complex. The potential interaction of STN7 with an unknown protein around the size of the Rieske protein, which was particularly visible in STN7 single cysteine mutants, supports this idea (**Figure 32**).

#### 4.2.5 Is STN7 regulated by thioredoxins?

The inhibition of STN7 in land plants via the stromal ferredoxin-thioredoxin pathway is generally accepted. However, the precise inactivation-site is still subject to speculation. Thioredoxins could either directly target the stromal cysteines (Cys 187 and Cys 191) in the ATP binding pocket (Puthiyaveetil 2011) (**Figure 3**) or the redox signal is transferred to the lumen by the putative Ccda/Hcf164 pathway addressing the lumen located cysteines Cys 65 and Cys 70 (Lemeille and Rochaix 2010). So far, physical interaction between STN7 and thioredoxins was not experimentally shown. In this study indication for an interaction of STN7 with recombinant mutated thioredoxin-f (*recΔTRX-f*) was presented, independently from the presence of cysteines Cys 65 and Cys 70 in the STN7 molecule (**Figure 34**). This observation supports the idea of a STN7 kinase that is targeted at the stromal side by thioredoxins. Further experiments are required to obtain a better idea about the involved processes. In this respect the generation of a transgenic line expressing STN7 without the stromal Cxxx motif represents the next logical step. It would

be interesting to see whether the mutated STN7 variant is less susceptible to HL inhibition. The fact that this stromal cysteine motif is not conserved in STT7, and so far no HL-induced inhibition was shown for *C. reinhardtii* (Puthiyaveetil 2011), speaks in favor of this scenario. Surprisingly, even though a decrease in STT7 levels was observed upon HL treatment by Lemeille et al. (2009) (Lemeille et al. 2009), the same study did not provide any evidence for its HL deactivation but refers to older studies about land plants (Rintamaki et al. 2000). Further indirect evidence for the formation of an additional cysteine bridge is provided by the redox titration experiment performed with both WT and STN7<sub>C→S:65+70</sub> thylakoids. DTT reduction of STN7 resulted in a second STN7 monomer signal on SDS-PA gels, even when the N-terminal cysteine motif was removed (**Figure 33**). This suggests the presence of another redox sensitive motif beside the established N-terminal one, which could be regulated by thioredoxins. Usually cleavage of a disulfide bond results in a slower migration of the reduced protein inside the gel. The fact, that the observed reduced STN7 signal is rather down- and not up-shifted is uncommon and might be ascribed to the release of a yet unknown STN7-bound cofactor.

### **4.3 Which physiological effects do variable STN8 protein levels bring about?**

#### **4.3.1 STN8 activity is not regulated via modulation of STN8 protein levels**

STN8 kinase activity was shown to be light-dependent since phosphorylation of Thr-4 of PSBH occurs only under illumination (Vener et al. 2001). Even if STN8 activity and as a consequence also PSII core phosphorylation is persistent in the dark, it becomes significantly increased upon HL treatment (Bonardi et al. 2005; Tikkanen et al. 2010; Vainonen et al. 2005). The conserved STN7 cysteine motives that are thought to be involved in thioredoxin-mediated down-regulation of STN7 protein levels under HL (Lemeille et al. 2009; Puthiyaveetil 2011; Rintamaki et al. 2000) are absent in STN8. Only one of the stromal CxxxC motif cysteines (Cys 191) is actually conserved in the *C. reinhardtii* homolog STL1. Thus, in contrast to STN7 which is deactivated under HL, STN8 activity is retained or even increased under these lighting conditions (Bonardi et al. 2005; Tikkanen et al. 2008a). It is assumed, that similar to STN7, the redox state of the PQ pool promotes STN8 activity. However, compared to STN7, the signal sensing and regulation of STN8 activity is completely unknown. Since STN8 does not contain any obvious redox-sensitive cysteine motives that would allow for a redox-dependent control of its activity (Depege et al. 2003), a regulation on the level of protein amounts seemed plausible. However, in contrast to STN7 the protein levels of STN8 are not susceptible to light treatments.

STN8 protein accumulation was neither changed by light conditions promoting its activity (e.g. HL) nor by light conditions leading to STN8 inactivation (e.g. FR) (**Figure 35**). A further possibility to regulate STN8 activity would be via reversible phosphorylation. STL1, the putative STN8 homolog in *C. reinhardtii* was shown to be phosphorylated under state 2 conditions in a STT7-dependent manner (Lemeille et al. 2010). However, no significant size-shift of STN8 due to changes in its phosphorylation state could be observed on Western blot under any of the investigated conditions.

#### **4.3.2 STN8 protein levels affect PSII core phosphorylation, supercomplex formation and thylakoid ultrastructure**

The elevated amounts of STN8 kinase in *oeSTN8* result in a significantly increased phosphorylation of CP43, D1 and D2 under all applied light conditions (**Figure 36 a**). Similar to *oeSTN7* the phosphorylation pattern of WT and *oeSTN8* is most equal under LL, suggesting that under these conditions a well-balanced phosphorylation of thylakoid proteins is crucial for an efficient electron flow through the photosynthetic complexes. The clear decrease in phosphorylation under FR illustrates that STN8 activity correlates with the PQ redox state even when STN8 is present in excess amounts (**Figure 36 a**). This dephosphorylation of PSII core proteins was suggested to be relevant for the formation of the most efficient form of PSII, the PSII supercomplexes (Tikkanen and Aro 2012; Tikkanen et al. 2008a), which as a consequence would be strongly promoted under PSI light. In contrast, this effect would be harmful under HL intensities when the organism pursues a down-regulation of both photosystems. Thus, under HL conditions dephosphorylated LHCII preferentially participates in heat dissipation instead of binding to the photosystems and the number of PSII supercomplexes was reported to become decreased (Tikkanen et al. 2010; Tikkanen et al. 2008a). These mechanisms play an important role in the protection of the photosynthetic machinery from photodamage under HL and are accompanied by an increase of PSII core protein phosphorylation, which in turn is supposed to facilitate PSII repair (Baena-Gonzalez et al. 1999). However, for *stn8* and *stn7 stn8* mutants, reports of a defect or delay in D1 turnover were contradictory (Bonardi et al. 2005; Fristedt et al. 2009; Tikkanen et al. 2008a). Here, the question arises whether the higher maximum PSII core phosphorylation in *oeSTN8* plants (**Figure 36 a**) could increase the resistance to photoinhibition under high light intensities. Indeed, *oeSTN8* maintained a slightly higher PSII efficiency after long-term exposure to fluctuating HL (**Figure 37**). This implies that the increased PSII

phosphorylation under HL allows for a faster D1 turnover and therewith functional PSII complexes. These observations can be explained by two current theories, based either on (i) modulation of thylakoid membrane stacking (Fristedt et al. 2009) or (ii) supercomplex formation (Tikkanen et al. 2008a).

(i) The slightly higher resistance of *oeSTN8* to photoinhibition could be ascribed to a partial destacking of the thylakoid grana due to an increase in negative phosphate groups, which lead to a charge-dependent repulsion of the thylakoid membranes. As a consequence, lateral movement of damaged and repaired PSII cores and of the involved proteases is facilitated like proposed by Fristedt et al. (2009). In fact, compared to WT, slight changes in macroscopic thylakoid membrane folding could be observed in *oeSTN8* under low light intensities (**Figure 38**), where differences in PSII phosphorylation between *oeSTN8* and WT are only marginal (**Figure 36 a**). However, both height and length of the grana stacks was slightly increased (**Figure 38**), which would not favor a faster movement of membrane proteins between grana and stroma thylakoids (Fristedt et al. 2009). Interestingly, Fristedt et al. (2009) as well observed a slight increase in grana stacking for WT plants exposed to HL compared to LL by TEM analyses. The HL-induced PSII phosphorylation might just coincide with grana stacking while actually other HL-induced processes are decisive for increased grana stacking that do not require STN8-dependent protein phosphorylation. However, the fact that increased PSII core protein phosphorylation in *oeSTN8* already increases grana stacking in the absence of HL (**Figure 38**) provides evidence that elevated PSII phosphorylation mediated by STN8 is indeed responsible for the observed changes in thylakoid folding. Recently, Herbstova et al. (2012) could observe a lateral shrinkage of grana length and an increased protein mobility in grana stacks in HL treated plants by performing confocal laser scanning microscopy (CLSM) and diffusion measurements by the FRAP (fluorescence recovery after photobleaching) technique, respectively. These changes in the thylakoid network would both be advantageously for the repair of damaged PSII (Herbstova et al. 2012). Comparative TEM, CLSM and FRAP analyses of D and HL exposed WT and *oeSTN8* plants would help to clarify these partly conflicting results by making use of the strongly enhanced phosphorylation phenotype of *oeSTN8* under those light conditions (**Figure 36 a**). Furthermore, an increase in grana stack length in STN8-deficient lines, as detected by Fristedt et al. (2009), could be confirmed (**Figure 38**) (Fristedt et al. 2009). Interestingly, in addition to the latter study, also a decrease of the grana stack height was observed. However, for none of the

*STN8* knock-out mutants (neither *stn8* nor *stn7 stn8*) significant differences in photoinhibition compared to wild type could be detected within this study (**Figure 37**).

Ultimately, it remains unclear whether STN8-dependent phosphorylation directly affects membrane stacking or whether it changes the abundance or functionality of so far unknown proteins responsible for thylakoid folding.

(ii) Tikkanen et al. (2008a) also observed a delayed D1 degradation in *STN8* knock-out mutants, which in turn was explained by a retarded disassembly of PSII supercomplexes under HL (Tikkanen et al. 2008a). As a consequence, the migration of damaged PSII cores from grana to stroma lamellae would be hindered by a lack of PSII core phosphorylation. These differences in the ratio between PSII complexes and PSII monomers could not be detected by Fristedt et al. (2009) after 3 h of HL treatment. Furthermore, in the absence of lincomycin, differences in the PSII monomer/dimer ratio became only evident after prolonged HL-treatment (Tikkanen et al. 2008a). Interestingly, in this study the direct comparison of supercomplex formation in WT, *oeSTN8* and *stn8-1* revealed an obvious discrepancy between the genotypes already under D and LL conditions (**Figure 36 b**). The high levels of STN8 in *oeSTN8* slightly promoted the disassembly of PSII complexes, whereas *stn8-1* clearly accumulated PSII supercomplexes. Thus, prolonged HL treatment or lincomycin infiltration combined with HL seems not to be a prerequisite for retarded supercomplex disassembly in *stn8-1* plants as claimed by Tikkanen et al. (2008a). However, this phenotype was enhanced under HL (**Figure 36 b**). These observations are not sufficient to explain the altered resistance to photoinhibition observed for *oeSTN8* but not for *stn8-1* (**Figure 37**) as both genotypes exhibit aberrant supercomplex formation. Whether the differences in supercomplex formation are a secondary effect due to the modulation of macroscopic thylakoid membrane folding remains to be elucidated. Mutant lines with aberrant thylakoid ultrastructure but WT-like PSII protein phosphorylation could help to answer this question.

#### **4.3.3 STN8 protein levels and PSII core phosphorylation have minor effects on photosynthetic performance**

The aberrant phosphorylation of PSII core proteins in *oeSTN8* and *stn8-1* plants only results in minor effects on photosynthetic performance as shown in **Figure 39** and **40**. A slightly more oxidized PQ pool at the beginning of illumination tends to result in higher efficiency of PSII

(**Figure 39 a, b**). This significant difference could be due to the higher PSII core pre-phosphorylation of *oeSTN8* in the dark (**Figure 36 a**) as it disappears after some minutes of light exposure (**Figure 39 a, b**), like differences in PSII phosphorylation between WT and *oeSTN8* are as well diminished in the LL (**Figure 36 a**) (Tikkanen and Aro 2012; Tikkanen et al. 2010). Possibly, the enhanced core protein phosphorylation slightly decreases PQ reduction by destabilizing PSII supercomplexes (**Figure 36 b**) (Tikkanen and Aro 2012; Tikkanen et al. 2010). An alternative explanation could be that not PSII core protein phosphorylation leads to minor changes in photosynthetic performance but the previously reported substrate overlap between STN8 and STN7. STN8 seems to support STN7 in LHCII phosphorylation shifting the PAM phenotype into the direction of *oeSTN7* lines, which possess a more oxidized PQ pool (**Figure 22 b**). This as a consequence could lower the reduction pressure of the PQ pool (**Figure 39 b**). In summary, differences in PSII core phosphorylation do not result in significant changes of photosynthesis besides affecting its fine tuning.

#### **4.4 An overlap in substrate specificity of STN7 and STN8 does not correlate with a mutual influence on each other's protein levels**

It was shown that the STN8 homolog named STL1 in *C. reinhardtii* becomes STT7-dependently phosphorylated (Lemeille et al. 2010), which supports the idea that STN7 and STN8 might be part of a kinase cascade (Lemeille and Rochaix 2010). At least a partial substrate overlap between the two kinases was demonstrated (Bonardi et al. 2005; Tikkanen et al. 2010; Tikkanen et al. 2008a). Even the activity of the LHCII phosphatase TAP38/PPH1 comprises STN8 substrates (Pribil et al. 2010; Vainonen et al. 2008) while PBCP overexpression affects state transitions (Samol et al. 2012). However, despite this complex interplay the knock-out or overexpression of one kinase seems not to obviously affect the activity or protein levels of the other one (**Figure 41 a, b**).

## 5 References

- Adam Z, Rudella A, van Wijk KJ (2006) Recent advances in the study of Clp, FtsH and other proteases located in chloroplasts. *Curr Opin Plant Biol* 9: 234-240
- Allen JF (1992) Protein phosphorylation in regulation of photosynthesis. *Biochim Biophys Acta* 1098: 275-335
- Allen JF (1995) Thylakoid protein phosphorylation, state 1 - state 2 transitions, and photosystem stoichiometry adjustment: redox control at multiple levels of gene expression. *Physiol Plant* 93: 196-205
- Allen JF, Pfannschmidt T (2000) Balancing the two photosystems: photosynthetic electron transfer governs transcription of reaction centre genes in chloroplasts. *Philos Trans R Soc Lond B Biol Sci* 355: 1351-1359
- Anderson JM (1989) The grana margins of plant thylakoid membranes. *Physiol Plant* 76: 243-248,
- Aro EM, Suorsa M, Rokka A, Allahverdiyeva Y, Paakkarinen V, Saleem A, Battchikova N, Rintamaki E (2005) Dynamics of photosystem II: a proteomic approach to thylakoid protein complexes. *J Exp Bot* 56: 347-356
- Aronsson H, Jarvis P (2002) A simple method for isolating import-competent *Arabidopsis* chloroplasts. *FEBS Lett* 529: 215-220
- Baena-Gonzalez E, Barbato R, Aro EM (1999) Role of phosphorylation in the repair cycle and oligomeric structure of photosystem II. *Planta* 208: 196--204
- Baginsky S, Tiller K, Link G (1997) Transcription factor phosphorylation by a protein kinase associated with chloroplast RNA polymerase from mustard (*Sinapis alba*). *Plant Mol Biol* 34: 181-189
- Bassi R, Marquardt J, Lavergne J (1995) Biochemical and functional properties of photosystem II in agranal membranes from maize mesophyll and bundle sheath chloroplasts. *Eur J Biochem* 233: 709-719
- Bellafiore S, Barneche F, Peltier G, Rochaix JD (2005) State transitions and light adaptation require chloroplast thylakoid protein kinase STN7. *Nature* 433: 892-895
- Bennett J, Shaw EK, Michel H (1988) Cytochrome b6f complex is required for phosphorylation of light-harvesting chlorophyll a/b complex II in chloroplast photosynthetic membranes. *Eur J Biochem* 171: 95-100
- Bonardi V, Pesaresi P, Becker T, Schleiff E, Wagner R, Pfannschmidt T, Jahns P, Leister D (2005) Photosystem II core phosphorylation and photosynthetic acclimation require two different protein kinases. *Nature* 437: 1179-1182
- Bondarava N, De Pascalis L, Al-Babili S, Goussias C, Golecki JR, Beyer P, Bock R, Krieger-Liszka A (2003) Evidence that cytochrome b559 mediates the oxidation of reduced plastoquinone in the dark. *J Biol Chem* 278: 13554-13560
- Breyton C (2000) Conformational changes in the cytochrome b6f complex induced by inhibitor binding. *J Biol Chem* 275: 13195-13201
- Breyton C, Nandha B, Johnson GN, Joliot P, Finazzi G (2006) Redox modulation of cyclic electron flow around photosystem I in C3 plants. *Biochemistry* 45: 13465-13475
- Buchanan BB, Balmer Y (2005) Redox regulation: a broadening horizon. *Annu Rev Plant Biol* 56: 187-220
- Buchanan BB, Gruissem W, Jones R (2002) *Biochemistry & Molecular Biology of Plants*. John Wiley & Sons
- Bulté L, Gans P, Rebéillé F, Wollman FA (1990) ATP control on state transitions in vivo in *Chlamydomonas reinhardtii*. *Biochim Biophys Acta - Bioenergetics* 1020: 72-80
- Burrows PA, Sazanov LA, Svab Z, Maliga P, Nixon PJ (1998) Identification of a functional respiratory complex in chloroplasts through analysis of tobacco mutants containing disrupted plastid *ndh* genes. *EMBO J* 17: 868-876
- Caffarri S, Croce R, Cattivelli L, Bassi R (2004) A look within LHCI: differential analysis of the Lhcb1-3 complexes building the major trimeric antenna complex of higher-plant photosynthesis. *Biochemistry* 43: 9467-9476
- Cain P, Hall M, Schroder WP, Kieselbach T, Robinson C (2009) A novel extended family of stromal thioredoxins. *Plant Mol Biol* 70: 273-281

- Cardol P, Alric J, Girard-Bascou J, Franck F, Wollman FA, Finazzi G (2009) Impaired respiration discloses the physiological significance of state transitions in *Chlamydomonas*. *Proc Natl Acad Sci U S A* 106: 15979-15984
- Casano LM, Zapata JM, Martin M, Sabater B (2000) Chlororespiration and poisoning of cyclic electron transport. Plastoquinone as electron transporter between thylakoid NADH dehydrogenase and peroxidase. *J Biol Chem* 275: 942-948
- Chuartzman SG, Nevo R, Shimoni E, Charuvi D, Kiss V, Ohad I, Brumfeld V, Reich Z (2008) Thylakoid membrane remodeling during state transitions in *Arabidopsis*. *Plant Cell* 20: 1029-1039
- Clough SJ, Bent AF (1998) Floral dip: a simplified method for *Agrobacterium*-mediated transformation of *Arabidopsis thaliana*. *Plant J* 16: 735-743
- Coughlan SJ (1988) Chloroplast thylakoid protein phosphorylation is influenced by mutations in the cytochrome b6f complex. *Biochim Biophys Acta* 933: 413-422
- DalCorso G, Pesaresi P, Masiero S, Aseeva E, Schunemann D, Finazzi G, Joliot P, Barbato R, Leister D (2008) A complex containing PGRL1 and PGR5 is involved in the switch between linear and cyclic electron flow in *Arabidopsis*. *Cell* 132: 273-285
- de Lacroix de Lavalette A, Finazzi G, Zito F (2008) b6f-Associated chlorophyll: structural and dynamic contribution to the different cytochrome functions. *Biochemistry* 47: 5259-5265
- de Vitry C, Ouyang Y, Finazzi G, Wollman FA, Kallas T (2004) The chloroplast Rieske iron-sulfur protein. At the crossroad of electron transport and signal transduction. *J Biol Chem* 279: 44621-44627
- Dekker JP, Boekema EJ (2005) Supramolecular organization of thylakoid membrane proteins in green plants. *Biochim Biophys Acta* 1706: 12-39
- Delosme R, Beal D, Joliot P (1994) Photoacoustic detection of flash-induced charge separation in photosynthetic systems - spectral dependence of the quantum yield. *Biochim Biophys Acta* 1185: 56-64
- Delosme R, Olive J, Wollman FA (1996) Changes in light energy distribution upon state transitions: an in vivo photoacoustic study of the wild type and photosynthesis mutants from *Chlamydomonas reinhardtii* *Biochim Biophys Acta* 1273: 150-158
- Depege N, Bellaifiore S, Rochaix JD (2003) Role of chloroplast protein kinase Stt7 in LHCII phosphorylation and state transition in *Chlamydomonas*. *Science* 299: 1572-1575
- Dietzel L, Brautigam K, Pfannschmidt T (2008) Photosynthetic acclimation: state transitions and adjustment of photosystem stoichiometry--functional relationships between short-term and long-term light quality acclimation in plants. *FEBS J* 275: 1080-1088
- Droux M, Jacquot JP, Migina-Maslow M, Gadal P, Huet JC, Crawford NA, Yee BC, Buchanan BB (1987) Ferredoxin-thioredoxin reductase, an iron-sulfur enzyme linking light to enzyme regulation in oxygenic photosynthesis: purification and properties of the enzyme from C3, C4, and cyanobacterial species. *Arch Biochem Biophys* 252: 426-439
- Eberhard S, Finazzi G, Wollman FA (2008) The dynamics of photosynthesis. *Annu Rev Genet* 42: 463-515
- Elich TD, Edelman M, Mattoo AK (1997) Evidence for light-dependent and light-independent protein dephosphorylation in chloroplasts. *FEBS Lett* 411: 236-238
- Endo T, Shikanai T, Takabayashi A, Asada K, Sato F (1999) The role of chloroplastic NAD(P)H dehydrogenase in photoprotection. *FEBS Lett* 457: 5-8
- Fey V, Wagner R, Brautigam K, Pfannschmidt T (2005) Photosynthetic redox control of nuclear gene expression. *J Exp Bot* 56: 1491-1498
- Finazzi G, Furia A, Barbagallo RP, Forti G (1999) State transitions, cyclic and linear electron transport and photophosphorylation in *Chlamydomonas reinhardtii*. *Biochim Biophys Acta* 1413: 117-129
- Finazzi G, Rappaport F, Furia A, Fleischmann M, Rochaix JD, Zito F, Forti G (2002) Involvement of state transitions in the switch between linear and cyclic electron flow in *Chlamydomonas reinhardtii*. *EMBO Rep* 3: 280-285

- Finazzi G, Zito F, Barbagallo RP, Wollman FA (2001) Contrasted effects of inhibitors of cytochrome b6/f complex on state transitions in *Chlamydomonas reinhardtii*: the role of Qo site occupancy in LHCII kinase activation. *J Biol Chem* 276: 9770-9774
- Fleischmann MM, Ravanel S, Delosme R, Olive J, Zito F, Wollman FA, Rochaix JD (1999) Isolation and characterization of photoautotrophic mutants of *Chlamydomonas reinhardtii* deficient in state transition. *J Biol Chem* 274: 30987-30994
- Frauer C, Rottach A, Meilinger D, Bultmann S, Fellingner K, Hasenoder S, Wang M, Qin W, Soding J, Spada F, Leonhardt H (2011) Different binding properties and function of CXXC zinc finger domains in Dnmt1 and Tet1. *PLoS one* 6: e16627
- Frenkel M, Bellaïf S, Rochaix JD, Jansson S (2007) Hierarchy amongst photosynthetic acclimation responses for plant fitness. *Physiol Plant* 129: 455-459
- Fristedt R, Willig A, Granath P, Crevecoeur M, Rochaix JD, Vener AV (2009) Phosphorylation of photosystem II controls functional macroscopic folding of photosynthetic membranes in *Arabidopsis*. *Plant Cell* 21: 3950-3964
- Fujita Y (1997) A study on the dynamic features of photosystem stoichiometry: Accomplishments and problems for future studies. *Photosynth Res* 53: 83-93
- Fulgosi H, Vener AV, Altschmied L, Herrmann RG, Andersson B (1998) A novel multi-functional chloroplast protein: identification of a 40 kDa immunophilin-like protein located in the thylakoid lumen. *EMBO J* 17: 1577-1587
- Gal A, Hauska G, Herrmann R, Ohad I (1990) Interaction between light harvesting chlorophyll-a/b protein (LHCII) kinase and cytochrome b6/f complex. In vitro control of kinase activity. *J Biol Chem* 265: 19742-19749
- Gal A, Shahak Y, Schuster G, Ohad I (1987) Specific loss of LHCII phosphorylation in *Lemna* mutant 1073 lacking the cytochrome b6/f complex. *FEBS Lett* 221: 205-210
- Gal A, Zer H, Ohad I (1997) Redox-controlled thylakoid protein phosphorylation. News and views. *Physiol Plant* 100: 869-885
- Grieco M, Tikkanen M, Paakkari V, Kangasjarvi S, Aro EM (2012) Steady-state phosphorylation of light-harvesting complex II proteins preserves Photosystem I under fluctuating white light. *Plant Physiol* 160: 1896-1910
- Haldrup A, Naver H, Scheller HV (1999) The interaction between plastocyanin and photosystem I is inefficient in transgenic *Arabidopsis* plants lacking the PSI-N subunit of photosystem I. *Plant J* 17: 689-698
- Hamel P, Olive J, Pierre Y, Wollman FA, de Vitry C (2000) A new subunit of cytochrome b6/f complex undergoes reversible phosphorylation upon state transition. *J Biol Chem* 275: 17072-17079
- Hammer MF, Sarath G, Osterman JC, Markwell J (1995) Assessing modulations of stromal and thylakoid light-harvesting complex-II phosphatase activities with phosphopeptide substrates. *Photosynth Res* 44: 107-115
- Heinemeyer J, Eubel H, Wehmhoner D, Jansch L, Braun HP (2004) Proteomic approach to characterize the supramolecular organization of photosystems in higher plants. *Phytochemistry* 65: 1683-1692
- Herbstova M, Tietz S, Kinzel C, Turkina MV, Kirchhoff H (2012) Architectural switch in plant photosynthetic membranes induced by light stress. *Proc Natl Acad Sci U S A*
- Hohmann-Marriott MF, Blankenship RE (2011) Evolution of photosynthesis. *Annu Rev Plant Biol* 62: 515-548
- Hou CX, Rintamaki E, Aro EM (2003) Ascorbate-mediated LHCII protein phosphorylation--LHCII kinase regulation in light and in darkness. *Biochemistry* 42: 5828-5836
- Ihnatowicz A, Pesaresi P, Leister D (2007) The E subunit of photosystem I is not essential for linear electron flow and photoautotrophic growth in *Arabidopsis thaliana*. *Planta* 226: 889-895
- Ihnatowicz A, Pesaresi P, Lohrig K, Wolters D, Muller B, Leister D (2008) Impaired photosystem I oxidation induces STN7-dependent phosphorylation of the light-harvesting complex I protein Lhca4 in *Arabidopsis thaliana*. *Planta* 227: 717-722

- Ihnatowicz A, Pesaresi P, Varotto C, Richly E, Schneider A, Jahns P, Salamini F, Leister D (2004) Mutants for photosystem I subunit D of *Arabidopsis thaliana*: effects on photosynthesis, photosystem I stability and expression of nuclear genes for chloroplast functions. *Plant J* 37: 839-852
- Iwai M, Yokono M, Inada N, Minagawa J (2010) Live-cell imaging of photosystem II antenna dissociation during state transitions. *Proc Natl Acad Sci U S A* 107: 2337-2342
- Izawa S, Pan RL (1978) Photosystem I electron transport and phosphorylation supported by electron donation to the plastoquinone region. *Biochem Biophys Res Commun* 83: 1171-1177
- Jagannathan B, Golbeck JH (2009) Understanding of the binding interface between PsaC and the PsaA/PsaB heterodimer in photosystem I. *Biochemistry* 48: 5405-5416
- Jensen PE, Gilpin M, Knoetzel J, Scheller HV (2000) The PSI-K subunit of photosystem I is involved in the interaction between light-harvesting complex I and the photosystem I reaction center core. *J Biol Chem* 275: 24701-24708
- Joliot P, Joliot A (2005) Quantification of cyclic and linear flows in plants. *Proc Natl Acad Sci U S A* 102: 4913-4918
- Kanervo E, Suorsa M, Aro EM (2005) Functional flexibility and acclimation of the thylakoid membrane. *Photochem Photobiol Sci* 4: 1072-1080
- Karnauchov I, Herrmann RG, Klosgen RB (1997) Transmembrane topology of the Rieske Fe/S protein of the cytochrome b6/f complex from spinach chloroplasts. *FEBS Lett* 408: 206-210
- Kleffmann T, von Zychlinski A, Russenberger D, Hirsch-Hoffmann M, Gehrig P, Gruissem W, Baginsky S (2007) Proteome dynamics during plastid differentiation in rice. *Plant Physiol* 143: 912-923
- Klughammer C, Ulrich Schreiber U (2008) Saturation Pulse method for assessment of energy conversion in PS I Heinz Walz GmbH, Effeltrich, Germany PAM Application Notes: 11 - 14
- Kohzuma K, Dal Bosco C, Kanazawa A, Dhingra A, Nitschke W, Meurer J, Kramer DM (2012) Thioredoxin-insensitive plastid ATP synthase that performs moonlighting functions. *Proc Natl Acad Sci U S A* 109: 3293-3298
- Koivuniemi A, Aro EM, Andersson B (1995) Degradation of the D1- and D2-proteins of photosystem II in higher plants is regulated by reversible phosphorylation. *Biochemistry* 34: 16022-16029
- Kruk J, Karpinski S (2006) An HPLC-based method of estimation of the total redox state of plastoquinone in chloroplasts, the size of the photochemically active plastoquinone-pool and its redox state in thylakoids of *Arabidopsis*. *Biochim Biophys Acta* 1757: 1669-1675
- Laemmli UK (1970) Cleavage of structural proteins during the assembly of the head of bacteriophage T4. *Nature* 227: 680-685
- Lascano HR, Casano LM, Martin M, Sabater B (2003) The activity of the chloroplastic Ndh complex is regulated by phosphorylation of the NDH-F subunit. *Plant Physiol* 132: 256-262
- Laugesen S, Bergoin A, Rossignol M (2004) Deciphering the plant phosphoproteome: tools and strategies for a challenging task. *Plant Physiol Biochem* 42: 929-936
- Lemaire C, Girard-Bascou J, Wollman FA (1986) Characterization of the b6/f complex subunits and studies on the LHC-kinase in *Chlamydomonas reinhardtii* using mutants strains altered in the b6/f. *Progress in Photosyn Res*: 10-15
- Lemaire SD, Michelet L, Zaffagnini M, Massot V, Issakidis-Bourguet E (2007) Thioredoxins in chloroplasts. *Curr Genet* 51: 343-365
- Lemeille S, Rochaix JD (2010) State transitions at the crossroad of thylakoid signalling pathways. *Photosyn Res* 106: 33-46
- Lemeille S, Turkina MV, Vener AV, Rochaix JD (2010) Stt7-dependent phosphorylation during state transitions in the green alga *Chlamydomonas reinhardtii*. *Mol Cell Proteomics* 9: 1281-1295
- Lemeille S, Willig A, Depege-Fargeix N, Delessert C, Bassi R, Rochaix JD (2009) Analysis of the chloroplast protein kinase Stt7 during state transitions. *PLoS Biol* 7: e45

- Lennartz K, Plucken H, Seidler A, Westhoff P, Bechtold N, Meierhoff K (2001) HCF164 encodes a thioredoxin-like protein involved in the biogenesis of the cytochrome b(6)f complex in Arabidopsis. *The Plant cell* 13: 2539-2551
- Leon S, Touraine B, Ribot C, Briat JF, Lobreaux S (2003) Iron-sulphur cluster assembly in plants: distinct NFU proteins in mitochondria and plastids from Arabidopsis thaliana. *Biochem J* 371: 823-830
- Lodish H, Berk A, Zipursky SL, Matsudaira P, Baltimore D, Darnell JE (2000) Molecular cell biology. S. Tenney, ed (New York: W.H. Freeman and Company)
- Lunde C, Jensen PE, Haldrup A, Knoetzel J, Scheller HV (2000) The PSI-H subunit of photosystem I is essential for state transitions in plant photosynthesis. *Nature* 408: 613-615
- Maiwald D, Dietzmann A, Jahns P, Pesaresi P, Joliet P, Joliet A, Levin JZ, Salamini F, Leister D (2003) Knock-out of the genes coding for the Rieske protein and the ATP-synthase delta-subunit of Arabidopsis. Effects on photosynthesis, thylakoid protein composition, and nuclear chloroplast gene expression. *Plant Physiol* 133: 191-202
- Marri L, Zaffagnini M, Collin V, Issakidis-Bourguet E, Lemaire SD, Pupillo P, Sparla F, Miginiac-Maslow M, Trost P (2009) Prompt and easy activation by specific thioredoxins of calvin cycle enzymes of Arabidopsis thaliana associated in the GAPDH/CP12/PRK supramolecular complex. *Mol Plant* 2: 259-269
- Martinsuo P, Pursiheimo S, Aro EM, Rintamaki E (2003) Dithiol oxidant and disulfide reductant dynamically regulate the phosphorylation of light-harvesting complex II proteins in thylakoid membranes. *Plant Physiol* 133: 37-46
- Melis A (1991) Dynamics of photosynthetic membrane composition and function. *Biochim Biophys Acta* 1058: 87-106
- Meurer J, Plucken H, Kowallik KV, Westhoff P (1998) A nuclear-encoded protein of prokaryotic origin is essential for the stability of photosystem II in Arabidopsis thaliana. *EMBO J* 17: 5286-5297
- Motohashi K, Hisabori T (2006) HCF164 receives reducing equivalents from stromal thioredoxin across the thylakoid membrane and mediates reduction of target proteins in the thylakoid lumen. *J Biol Chem* 281: 35039-35047
- Motohashi K, Kondoh A, Stumpp MT, Hisabori T (2001) Comprehensive survey of proteins targeted by chloroplast thioredoxin. *Proc Natl Acad Sci U S A* 98: 11224-11229
- Munekage Y, Hojo M, Meurer J, Endo T, Tasaka M, Shikanai T (2002) PGR5 is involved in cyclic electron flow around photosystem I and is essential for photoprotection in Arabidopsis. *Cell* 110: 361-371
- Nath K, Mishra S, Zulfugarov, Raffi S, An G, Lee C (2007) Characterization of a T-DNA inserted STN8 kinase mutant of Oryza sativa L. *Photosyn Res* 91: 289
- Nellaepalli S, Kodru S, Subramanyam R (2012) Effect of cold temperature on regulation of state transitions in Arabidopsis thaliana. *J Photochem Photobiol B* 112: 23-30
- Nellaepalli S, Mekala NR, Zsiros O, Mohanty P, Subramanyam R (2011) Moderate heat stress induces state transitions in Arabidopsis thaliana. *Biochim Biophys Acta* 1807: 1177-1184
- Nixon PJ, Barker M, Boehm M, de Vries R, Komenda J (2005) FtsH-mediated repair of the photosystem II complex in response to light stress. *J Exp Bot* 56: 357-363
- Olsen JV, Blagoev B, Gnad F, Macek B, Kumar C, Mortensen P, Mann M (2006) Global, in vivo, and site-specific phosphorylation dynamics in signaling networks. *Cell* 127: 635-648
- Page ML, Hamel PP, Gabilly ST, Zegzouti H, Perea JV, Alonso JM, Ecker JR, Theg SM, Christensen SK, Merchant S (2004) A homolog of prokaryotic thiol disulfide transporter CcdA is required for the assembly of the cytochrome b6f complex in Arabidopsis chloroplasts. *J Biol Chem* 279: 32474-32482
- Garrett LK (2006) Get Ready for Biology. Pearson Education Inc., publishing as Benjamin Cummings.
- Pesaresi P, Hertle A, Pribil M, Kleine T, Wagner R, Strissel H, Ihnатовicz A, Bonardi V, Scharfenberg M, Schneider A, Pfannschmidt T, Leister D (2009) Arabidopsis STN7 kinase provides a link between short- and long-term photosynthetic acclimation. *Plant Cell* 21: 2402-2423

- Pesaresi P, Lunde C, Jahns P, Tarantino D, Meurer J, Varotto C, Hirtz RD, Soave C, Scheller HV, Salamini F, Leister D (2002) A stable LHCII-PSI aggregate and suppression of photosynthetic state transitions in the *psae1-1* mutant of *Arabidopsis thaliana*. *Planta* 215: 940-948
- Pesaresi P, Varotto C, Meurer J, Jahns P, Salamini F, Leister D (2001) Knock-out of the plastid ribosomal protein L11 in *Arabidopsis*: effects on mRNA translation and photosynthesis. *Plant J* 27: 179-189
- Pfannschmidt T, Schutze K, Brost M, Oelmuller R (2001) A novel mechanism of nuclear photosynthesis gene regulation by redox signals from the chloroplast during photosystem stoichiometry adjustment. *J Biol Chem* 276: 36125-36130
- Pfannschmidt T, Schutze K, Fey V, Sherameti I, Oelmuller R (2003) Chloroplast redox control of nuclear gene expression--a new class of plastid signals in interorganellar communication. *Antioxid Redox Signal* 5: 95-101
- Pfeiffer S, Krupinska K (2005) New Insights in Thylakoid Membrane Organization. *Plant Cell Physiol* 46(9): 1443-1451
- Porra RJ (2002) The chequered history of the development and use of simultaneous equations for the accurate determination of chlorophylls a and b. *Photosyn Res* 73: 149-156
- Pospisił P (2011) Enzymatic function of cytochrome b559 in photosystem II. *J Photochem Photobiol B* 104: 341-347
- Pribil M, Pesaresi P, Hertle A, Barbato R, Leister D (2010) Role of plastid protein phosphatase TAP38 in LHCII dephosphorylation and thylakoid electron flow. *PLoS Biol* 8: e1000288
- Pursiheimo S, Mulo P, Rintamaki E, Aro EM (2001) Coregulation of light-harvesting complex II phosphorylation and *lhcb* mRNA accumulation in winter rye. *Plant J* 26: 317-327
- Puthiyaveetil S (2011) A mechanism for regulation of chloroplast LHC II kinase by plastoquinol and thioredoxin. *FEBS Lett* 585: 1717-1721
- Puthiyaveetil S, Ibrahim IM, Allen JF (2012) Oxidation-reduction signalling components in regulatory pathways of state transitions and photosystem stoichiometry adjustment in chloroplasts. *Plant Cell Environ* 35: 347-359
- Reiland S, Finazzi G, Endler A, Willig A, Baerenfaller K, Grossmann J, Gerrits B, Rutishauser D, Grusissem W, Rochaix JD, Baginsky S (2011) Comparative phosphoproteome profiling reveals a function of the STN8 kinase in fine-tuning of cyclic electron flow (CEF). *Proc Natl Acad Sci U S A* 108: 12955-12960
- Rintamaki E, Kettunen R, Aro EM (1996) Differential D1 dephosphorylation in functional and photodamaged photosystem II centers. Dephosphorylation is a prerequisite for degradation of damaged D1. *J Biol Chem* 271: 14870-14875
- Rintamaki E, Martinsuo P, Pursiheimo S, Aro EM (2000) Cooperative regulation of light-harvesting complex II phosphorylation via the plastoquinol and ferredoxin-thioredoxin system in chloroplasts. *Proc Natl Acad Sci U S A* 97: 11644-11649
- Rochaix JD (2007) Role of thylakoid protein kinases in photosynthetic acclimation. *FEBS Lett* 581: 2768-2775
- Ruban AV, Johnson MP (2009) Dynamics of higher plant photosystem cross-section associated with state transitions. *Photosyn Res* 99: 173-183
- Ruban AV, Johnson MP, Duffy CD (2012) The photoprotective molecular switch in the photosystem II antenna. *Biochim Biophys Acta* 1817: 167-181
- Rumeau D, Peltier G, Cournac L (2007) Chlororespiration and cyclic electron flow around PSI during photosynthesis and plant stress response. *Plant Cell Environ* 30: 1041-1051
- Saito H (2001) Histidine phosphorylation and two-component signaling in eukaryotic cells. *Chem Rev* 101: 2497-2509
- Samol I, Shapiguzov A, Ingelsson B, Fucile G, Crevecoeur M, Vener AV, Rochaix JD, Goldschmidt-Clermont M (2012) Identification of a photosystem II phosphatase involved in light acclimation in *Arabidopsis*. *Plant Cell* 24: 2596-2609
- Sazanov LA, Burrows PA, Nixon PJ (1998) The chloroplast Ndh complex mediates the dark reduction of the plastoquinone pool in response to heat stress in tobacco leaves. *FEBS Lett* 429: 115-118

- Schaffner W, Weissmann C (1973) A rapid, sensitive, and specific method for the determination of protein in dilute solution. *Anal Biochem* 56: 502-514
- Schottkowski M, Gkalypoudis S, Tzekova N, Stelljes C, Schunemann D, Ankele E, Nickelsen J (2009a) Interaction of the periplasmic PrtA factor and the PsbA (D1) protein during biogenesis of photosystem II in *Synechocystis* sp. PCC 6803. *J Biol Chem* 284: 1813-1819
- Schottkowski M, Ratke J, Oster U, Nowaczyk M, Nickelsen J (2009b) PrtA, a novel tetra-tricopeptide repeat protein involved in light-dependent chlorophyll biosynthesis and thylakoid membrane biogenesis in *Synechocystis* sp. PCC 6803. *Mol Plant* 2: 1289-1297
- Schreiber U (2004) Pulse-Amplitude-Modulation (PAM) Fluorometry and Saturation Pulse Method: An Overview. In: Papageorgiou GC, Govindjee (eds.) *Chlorophyll a Fluorescence: A Signature of Photosynthesis*: 279-319
- Schwenkert S, Umate P, Dal Bosco C, Volz S, Mlcochova L, Zoryan M, Eichacker LA, Ohad I, Herrmann RG, Meurer J (2006) PsbI affects the stability, function, and phosphorylation patterns of photosystem II assemblies in tobacco. *J Biol Chem* 281: 34227-34238
- Shapiguzov A, Ingelsson B, Samol I, Andres C, Kessler F, Rochaix JD, Vener AV, Goldschmidt-Clermont M (2010) The PPH1 phosphatase is specifically involved in LHCII dephosphorylation and state transitions in *Arabidopsis*. *Proc Natl Acad Sci U S A* 107: 4782-4787
- Shikanai T (2007) Cyclic electron transport around photosystem I: genetic approaches. *Annu Rev Plant Biol* 58: 199-217
- Shinopoulos KE, Brudvig GW (2012) Cytochrome b(5)(5)(9) and cyclic electron transfer within photosystem II. *Biochim Biophys Acta* 1817: 66-75
- Silverstein T, Cheng L, Allen JF (1993) Chloroplast thylakoid protein phosphatase reactions are redox-independent and kinetically heterogeneous. *FEBS Lett* 334: 101-105
- Tetlow IJ, Wait R, Lu Z, Akkasaeng R, Bowsher CG, Esposito S, Kosar-Hashemi B, Morell MK, Emes MJ (2004) Protein phosphorylation in amyloplasts regulates starch branching enzyme activity and protein-protein interactions. *Plant Cell* 16: 694-708
- Tikkanen M, Aro EM (2012) Thylakoid protein phosphorylation in dynamic regulation of photosystem II in higher plants. *Biochim Biophys Acta* 1817: 232-238
- Tikkanen M, Grieco M, Aro EM (2011) Novel insights into plant light-harvesting complex II phosphorylation and 'state transitions'. *Trends Plant Sci* 16: 126-131
- Tikkanen M, Grieco M, Kangasjarvi S, Aro EM (2010) Thylakoid protein phosphorylation in higher plant chloroplasts optimizes electron transfer under fluctuating light. *Plant Physiol* 152: 723-735
- Tikkanen M, Nurmi M, Kangasjarvi S, Aro EM (2008a) Core protein phosphorylation facilitates the repair of photodamaged photosystem II at high light. *Biochim Biophys Acta* 1777: 1432-1437
- Tikkanen M, Nurmi M, Suorsa M, Danielsson R, Mamedov F, Styring S, Aro EM (2008b) Phosphorylation-dependent regulation of excitation energy distribution between the two photosystems in higher plants. *Biochim Biophys Acta* 1777: 425-432
- Tikkanen M, Piippo M, Suorsa M, Sirpio S, Mulo P, Vainonen J, Vener AV, Allahverdiyeva Y, Aro EM (2006) State transitions revisited—a buffering system for dynamic low light acclimation of *Arabidopsis*. *Plant Mol Biol* 62: 779-793
- Tokutsu R, Iwai M, Minagawa J (2009) CP29, a monomeric light-harvesting complex II protein, is essential for state transitions in *Chlamydomonas reinhardtii*. *J Biol Chem* 284: 7777-7782
- Toth SZ, Schansker G, Strasser RJ (2007) A non-invasive assay of the plastoquinone pool redox state based on the OJIP-transient. *Photosyn Res* 93: 193-203
- Vainonen JP, Hansson M, Vener AV (2005) STN8 protein kinase in *Arabidopsis thaliana* is specific in phosphorylation of photosystem II core proteins. *J Biol Chem* 280: 33679-33686

- Vainonen JP, Sakuragi Y, Stael S, Tikkanen M, Allahverdiyeva Y, Paakkarinen V, Aro E, Suorsa M, Scheller HV, Vener AV, Aro EM (2008) Light regulation of CaS, a novel phosphoprotein in the thylakoid membrane of *Arabidopsis thaliana*. *FEBS J* 275: 1767-1777
- van Oort B, Alberts M, de Bianchi S, Dall'Osto L, Bassi R, Trinkunas G, Croce R, van Amerongen H (2010) Effect of antenna-depletion in Photosystem II on excitation energy transfer in *Arabidopsis thaliana*. *Biophys J* 98: 922-931
- Varotto C, Pesaresi P, Meurer J, Oelmuller R, Steiner-Lange S, Salamini F, Leister D (2000) Disruption of the *Arabidopsis* photosystem I gene *psaE1* affects photosynthesis and impairs growth. *Plant J* 22: 115-124
- Vener AV, Harms A, Sussman MR, Vierstra RD (2001) Mass spectrometric resolution of reversible protein phosphorylation in photosynthetic membranes of *Arabidopsis thaliana*. *J Biol Chem* 276: 6959-6966
- Vener AV, Ohad I, Andersson B (1998) Protein phosphorylation and redox sensing in chloroplast thylakoids. *Curr Opin Plant Biol* 1: 217-223
- Vener AV, van Kan PJ, Rich PR, Ohad I, Andersson B (1997) Plastoquinol at the quinol oxidation site of reduced cytochrome *b<sub>f</sub>* mediates signal transduction between light and protein phosphorylation: thylakoid protein kinase deactivation by a single-turnover flash. *Proc Natl Acad Sci U S A* 94: 1585-1590
- Wagner R, Dietzel L, Brautigam K, Fischer W, Pfannschmidt T (2008) The long-term response to fluctuating light quality is an important and distinct light acclimation mechanism that supports survival of *Arabidopsis thaliana* under low light conditions. *Planta* 228: 573-587
- Walters RG (2005) Towards an understanding of photosynthetic acclimation. *J Exp Bot* 56: 435-447
- White CC, Chain RK, Malkin R (1978) Duroquinol as an electron donor for chloroplast electron transfer reactions. *Biochim Biophys Acta* 502: 127-137
- Willig A, Shapiguzov A, Goldschmidt-Clermont M, Rochaix JD (2011) The phosphorylation status of the chloroplast protein kinase STN7 of *Arabidopsis* affects its turnover. *Plant Physiol* 157: 2102-2107
- Winger AM, Taylor NL, Heazlewood JL, Day DA, Millar AH (2007) Identification of intra- and intermolecular disulphide bonding in the plant mitochondrial proteome by diagonal gel electrophoresis. *Proteomics* 7: 4158-4170
- Wollman FA (2001) State transitions reveal the dynamics and flexibility of the photosynthetic apparatus. *EMBO J* 20: 3623-3630
- Wollman FA, Lemaire C (1988) Studies on kinase-controlled state transitions in photosystem II and *b<sub>6</sub>f* mutants from *Chlamydomonas reinhardtii* which lack quinone-binding proteins. *Biochim Biophys Acta* 85: 85-94
- Wunder T, Liu Q, Aseeva E, Bonardi V, Leister D, Pribil M (2012) Control of STN7 transcript abundance and transient STN7 dimerisation are involved in the regulation of STN7 activity. *Planta* 1-18
- Yakushevskaya AE, Keegstra W, Boekema EJ, Dekker JP, Andersson J, Jansson S, Ruban AV, Horton P (2003) The structure of photosystem II in *Arabidopsis*: localization of the CP26 and CP29 antenna complexes. *Biochemistry* 42: 608-613
- Yan J, Cramer WA (2003) Functional insensitivity of the cytochrome *b<sub>6</sub>f* complex to structure changes in the hinge region of the Rieske iron-sulfur protein. *J Biol Chem* 278: 20925-20933
- Yang WC, Li H, Wang F, Zhu XL, Yang GF (2012) Rieske iron-sulfur protein of the cytochrome *bc<sub>1</sub>* complex: a potential target for fungicide discovery. *Chembiochem* 13: 1542-1551
- Zhang N, Schurmann P, Portis AR, Jr. (2001) Characterization of the regulatory function of the 46-kDa isoform of Rubisco activase from *Arabidopsis*. *Photosyn Res* 68: 29-37
- Zito F, Finazzi G, Delosme R, Nitschke W, Picot D, Wollman FA (1999) The Qo site of cytochrome *b<sub>6</sub>f* complexes controls the activation of the LHCII kinase. *EMBO J* 18: 2961-2969

## Acknowledgements

I am deeply grateful to Prof. Dr. Dario Leister for funding, supervising and supporting my work, and for his trust in me throughout my PhD.

I would like to thank Prof. Dr. Peter Geigenberger for taking over the “Zweitgutachten”.

I would like to thank Dr. Elena Aseeva for introducing me into the project and supervising me during the first months of my PhD.

I would like to thank Prof. Dr. Roberto Barbato and Dr. Paolo Pesaresi for the generation of antibodies and Prof. Dr. Wanner and his group for the TEM analyses.

I would like to thank my colleagues Liu Qiuping, Thomas Blunder, Dr. Alexander Hertle and Dr. Paolo Pesaresi for enjoyably cooperation and Dr. Vera Bonardi for providing a proper basis for my project.

I dearly want to thank my supervisor Dr. Mathias Pribil for being a seemingly inexhaustible source of motivation and encouraging words. I appreciated the fruitful discussions we had, his guidance with a clear sense of the essential, his endless patience and his valuable personal commitment towards the success of this work. I count myself more than lucky that I have been a part of his team. Thank you!

I would like to thank Dr. Alexander Hertle for supporting me with his inexhaustible knowledge, enthusiasm for science and sense of entertainment.

I am most thankful to the whole AG Leister including active and former members like Wenteng, Michi, Angie etc., to the gardeners, and to all other colleagues of the department, like Dr. Fatima Chigri, who all made the time period of my thesis such an interesting and pleasant time. Although I cannot mention every single one of you, you all can be sure that I was happy and thankful for having you around and supporting me!

I'm deeply thankful to my parents and family, who followed and supported me without reserve through the whole period of my studies and beyond. Along with all my friends, like Flo and my band mate Christian, I have to thank them for creating a life outside the lab with me.

I would also like to heartily thank my “second” family, which cordially welcomed me and supported me from Munich and Bosnia. Puno Hvala!

Most of all, I would like to thank Alma, moj mali melek i blijesta zvijezda, whose importance for this work and my whole life cannot be phrased. Volim te!

## Publications

- Hertle AP, Blunder T, **Wunder T**, Pesaresi P, Pribil M, Armbruster U, Leister D (2013) PGRL1 is the elusive ferredoxin-plastoquinone reductase in photosynthetic cyclic electron flow. *Mol Cell* 49(3): 511-523
- # **Wunder T**, Liu Q, Aseeva E, Bonardi V, Leister D, Pribil M (2013) Control of STN7 transcript abundance and transient STN7 dimerisation are involved in the regulation of STN7 activity. *Planta* 237(2): 541-558
- Pesaresi P, Pribil M, **Wunder T**, Leister D (2011) Dynamics of reversible protein phosphorylation in thylakoids of flowering plants: the roles of STN7, STN8 and TAP38. *Biochim Biophys Acta* 1807: 887-896
- Wunder T**, Bredemeier R, Ruprecht M & Schleiff E (2009) The Omp85 proteins of *Anabaena* sp. PCC 7120 and *E. coli* are functionally distinct. *Endocytobiosis Cell Res* 19: 20–30
- Wunder T**, Martin R, Loffelhardt W, Schleiff E, Steiner JM (2007) The invariant phenylalanine of precursor proteins discloses the importance of Omp85 for protein translocation into cyanelles. *BMC Evol Biol* 7: 236

# publications related to this thesis

## **Eidesstattliche Erklärung**

Ich versichere hiermit an Eides statt, dass die vorgelegte Dissertation von mir selbständig und ohne unerlaubte Hilfe angefertigt ist. Der Autor hat zuvor nicht versucht, anderweitig eine Dissertation einzureichen oder sich einer Doktorprüfung zu unterziehen. Die Dissertation wurde keiner weiteren Prüfungskommission weder in Teilen noch als Ganzes vorgelegt.

München, 16. Dezember 2012

.....

Tobias Wunder